THE IONIC MASS TRANSFER COEFFICIENTS OF
CATION AND ANION EXCHANGE RESINS
AT VARIOUS FLOW RATES AND
INFLUENT CONCENTRATIONS
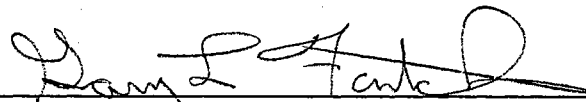IN SINGLE AND MIXED BEDS

By

GANG-CHOON LEE

Bachelor of Science
Sungkyunkwan University
Seoul, Korea
1986

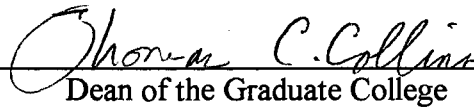Master of Science
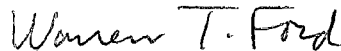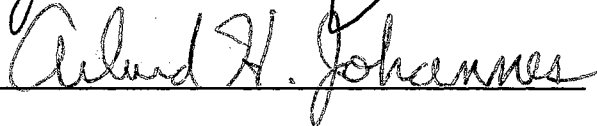Sungkyunkwan University
Seoul, Korea
1988
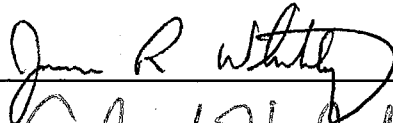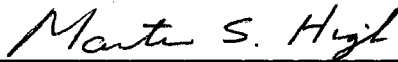
Submitted to the Faculty of the
Graduate College of the
Oklahoma State University
in partial fulfillment of
the requirements for
the Degree of
DOCTOR OF PHILOSOPHY
May, 1994

THE IONIC MASS TRANSFER COEFFICIENTS OF

CATION AND ANION EXCHANGE RESINS

AT VARIOUS FLOW RATES AND

INFLUENT CONCENTRATIONS

IN SINGLE AND MIXED BEDS

Thesis Approved:

_____
Thesis Adviser

_____
Martin S. High

_____
James R. Whiteley

_____
Arland H. Johannes

_____
Warren T. Ford

_____
Thomas C. Collins
Dean of the Graduate College

ACKNOWLEDGMENTS

TABLE OF CONTENTS

LIST OF TABLES

LIST OF FIGURES

NOMENCLATURE

A   cross sectional area of a column, cm^2

a_s specific surface area of cation or anion resin, cm^2/cm^3 resin

C_i concentration of species i, ppb or meq/cm^3

C_t total counterion concentration, meq/cm^3

d_p particle diameter of cation or anion resin, cm

D_i diffusion coefficient of species i, cm^2/s

D_e effective liquid-phase diffusivity, cm^2/s

D_{mp} effective diffusivity in resin pore, cm^2/s

F   Faraday's constant, coulombs/mole

J_i ionic flux of species i, $meq/(s \times cm^2)$

k_H mass transfer coefficient estimated by Equation (20), cm/s or m/s

k_l film mass transfer coefficient, cm/s or m/s

k_m effective mass transfer coefficient, cm/s or m/s

k_{model} mass transfer coefficient estimated by the model, cm/s or m/s

K_A^B selectivity coefficient for ion B in the solution replacing ion A in resin phase

k_o overall mass transfer coefficient, cm/s or m/s

k_p particle mass transfer coefficient, cm/s or m/s

q_i mean resin phase concentration of species i, meq/cm^3

Q_i total resin exchange capacity of resin i, meq/ml

R   universal gas constant

R_i (i) volume fraction of cation or anion resin in mixed bed
(ii) ratio of electrolyte to nonelectrolyte mass transfer coefficient in Equation (8)

Re   particle Reynold number

S   specific surface area, $S = a_s(1-\varepsilon)$, cm^2/cm^3 resin

Sc   Schmidt number

T   temperature, K

u_f superficial linear velocity, cm/s

V   volumetric flow rate, ml/min

x_i equivalent fraction of species i in solution

y   distance normal to solid-liquid interface, cm

y_i equivalent fraction of species i in resin phase

z   distance from column inlet, cm

Z   bed depth, cm

Greek Letters

δ liquid film thickness, cm

ε bed void fraction

φ electric potential, ergs/coulomb

ρ solution density, g/cm^3

ρ_p resin particle density, g/cm^3

Superscripts

*   interfacial equilibrium condition

eff   column effluent condition

f   feed condition

o   bulk solution condition

CHAPTER I

INTRODUCTION

Ion exchange is the reversible stoichiometric exchange of ions between a resin particle and a liquid, without substantial change in the solid structure. Ion exchange has been used frequently as an economical and convenient separation method for producing high purity water. Thus, ion exchange is used commercially where high purity water is needed: rinse water for microchip production, ammonia and hydrogen production, steam reformation, condensate polishing and makeup water purification, and closed-loop water reclamation for space missions (Foutch, 1991).

Ion exchange resin is made of insoluble solid material which has exchangeable cations or anions, 'counterions,' and its structure is a cross-linked polyelectrolyte hydrocarbon matrix. The matrix holds counterions and is elastic. Therefore, a liquid diffuses into the matrix and ions in the liquid are exchanged with counterions which are attached in the matrix (Dowex, 1958). Polymeric resins of both bead and powder type are used.

Kunin and McGarvey (1951) investigated the advantages of mixed bed ion exchange resins compared with a series of cation and anion single beds. The typical mixed bed is prepared by intimate mixing of strong-acid cation resins in the hydrogen form and strong-base anion resins in the hydroxide form. These ions exchange cations and anions in the liquid phase, respectively, and the exchanged hydrogen and hydroxide produce water by neutralization.

1

Haub and Foutch (1986a, b) developed a mixed bed ion exchange model appropriate for hydrogen cycle operation at ultra-low solution concentrations. Divekar et al. (1987) added temperature effects to Haub and Foutch's model, and Zecchini (1990) extended Haub and Foutch's model to be suitable to multicomponent systems. Yoon (1990), King (1991) and Noh (1992) obtained experimental breakthrough curves for mixed beds at different operating conditions and compared the curves with the model prediction.

Haub and Foutch used Carberry's (1960) and Kataoka's (1973) correlations as non-ionic mass transfer coefficients depending on the flow regime. Yoon (1990), however, showed that Haub and Foutch's model did not accurately predict his breakthrough curves and proposed a new non-ioic mass transfer coefficient correlation which made the model fit experimental data well. He insisted that Carberry's and Kataoka's correlations were not appropriate for ultra-low solution concentrations. Yoon (1990) performed his experiments at a superficial linear velocity of 1.48 cm/min. This flow rate, however, is lower than industrial operating conditions.

Harries and Ray (1984) and Harries (1986, 1987) presented a method to measure mass transfer coefficients for new and used resins. They used dimensionally balanced Frisch and Kunin's (1960) mass transfer equation based on film diffusion control, and estimated the mass transfer coefficients for chloride and sulphate. They concluded that the mass transfer coefficients of new resins depended only on flow rate and those of the used resins depended on influent concentration as well as flow rate. In addition, they claimed that the kinetics of used resins cannot be explained only by a film diffusion mechanism and concluded that other factors, like reaction or particle diffusion, also affects the overall exchange rate. However, the influent concentrations used in their experiments were higher than typical feed concentrations used in industry. Their equation

cannot explain the effects of the existence of coions, the diffusivities of single ions, and concentration changes in the bulk and at the interface between the resin and liquid-phase to exchange rate. Haub and Foutch's (1986a, b) model can account for those effects.

Harries and Ray's (1984) mass transfer coefficient measurement method is the simplest and most valuable method if mass transfer coefficients are a critical parameter for ion exchange plant design and model development. The resins used in this study are still used by industry, but there are no mass transfer data for the resins.

The objectives of this study, therefore, are:

1) to estimate mass transfer coefficients of new and used resins for sodium and chloride in a wider influent concentration range than used by Harries and Ray at operating conditions in industry.

2) to determine mass transfer coefficients to match experimental effluent concentrations with Haub and Foutch's mixed ion exchange model in order to figure out the effects of the existence of coions, the diffusivities of single ions, and the concentration changes in bulk and at the interface between resin and liquid-phase to mass transfer coefficients.

3) to compare mass transfer coefficients estimated by Harries and Ray's equation and the model. The comparison will be a criterion for eligibility of Harries and Ray's measurement method.

4) to approximate particle mass transfer coefficients for used resins with overall coefficients calculated by Harries and Ray's equation and Haub and Foutch's mixed bed ion exchange model.

The resins used in this study are different from those in Harries and Ray's work and the used resins were sampled from PSO (Public Service Oklahoma).

The experimental data are analyzed emphasizing of influent concentration and flow rate, and particle diffusion effects are explained for the used resins.

The mass transfer coefficients estimated in this study will be used in the model to predict column breakthrough curves at industrial operating conditions and be a basis for developing new mass transfer coefficient correlations in the future.

CHAPTER II

LITERATURE REVIEW

There are many useful references that explain the ion exchange process. Kunin (1960), Helfferich (1962, 1966), and Naden and Streat (1984) present the fundamentals, kinetic theories, industrial applications, and the modeling of ion exchange reactors. Haub (1984), Yoon (1990), Zecchini (1990), and Noh (1992) reviewed the ion exchange process in mixed beds of cationic and anionic resins. In addition to the fundamentals and the modeling of ion exchange process, Yoon, Noh, and King (1991) have discussed experimental techniques with mixed beds. This chapter reviews three major fields: ion exchange kinetics, non-ionic and ionic mass transfer coefficients.

Ion Exchange Kinetics

The ion exchange process involves three rate controlling mechanisms: mass transfer through a static liquid film surrounding the resin surface, mass transfer into the resin particle, and the exchange reaction between counterions in the solid and solution phase (Boyd et al., 1947). The slowest mechanism among these determines the ion exchange rate. Boyd et al. were the first to analyze ion exchange kinetics and apply the Nernst concept of a liquid-film diffusion layer. Bieber et al. (1954) found that the exchange reaction rate was fast enough to be

5

ignored. He concluded that mass transfer of counterions was the rate controlling factor for the shallow bed technique. Therefore, the rate of exchange is generally described by the interdiffusion of counterions in the adherent film, the particle diffusion into ion exchange resin, or the combination of both film and particle diffusion. In contrast, Streat (1984) proposed a case which was controlled by the reactions at the exchange site. For most applications, however, ion exchange is purely a diffusion phenomenon (Helfferich and Plesset, 1958).

Particle diffusion control is accounted for phenomenologically when film diffusion is much faster than particle diffusion. Thus, the concentration gradient disappears in the film and exists only in the resin. Petruzzelli et al. (1987b) reviewed various mathematical models for ion exchange kinetics with solid phase rate control. When the particle diffusion rate is much faster than the film diffusion rate, film diffusion controls the exchange rate. This leads to a concentration gradient that exists only in the film. Particle diffusion control is, in general, adequate for concentrated solutions, large resin diameters, high degree crosslinking of resin beads, low concentration of fixed ionic groups and a high degree of agitation. Film diffusion control is the general phenomenon when conditions of a high concentration of fixed ionic groups, low cross linking of the resin phase, dilute solutions, and low agitation exist (Helfferich, 1962; Gopala Rao and Gupta, 1982a).

Helfferich (1962) proposed theoretical criteria for film and particle diffusion rate control using quantitative expressions for the effects of the various factors. Helfferich (1965) also derived similar criteria when ion exchange accompanies reactions such as: neutralization and complex formation. He showed that the derived rate laws with ionic reaction differed from those for ordinary ion exchange in the absence of reactions. Gopala Rao and Gupta (1982b) verified Helfferich's theoretical development experimentally. Kataoka and Yoshida (1988)

analyzed ion exchange accompanied by a neutralization reaction when the bulk solution contained a neutral salt and an acid or a base. They developed a theory to account for the neutralization reaction using the Nernst-Planck equation with combined resistances of both particle and liquid-phase diffusion. Helfferich (1990) compared four different mathematical models of ion exchange kinetics: Nernst-Planck film model, shell-core models with or without reaction and a kinetic model for macro-porous resins. He pointed out their deficiencies from physical reality. Other investigators (Omatete et al., 1980a,b; Kataoka et al., 1987; Zecchini, 1990) extended the theory of ion exchange kinetics to multi-component systems.

The diffusion rate process for ordinary ion exchange is described by the Nernst-Planck equation, while Fick's first law is used for nonelectrolytes or isotopic exchange of counterions with equal mobility (Schlogl and Helfferich, 1957; Helfferich and Plesset, 1958; Turner et al., 1966). The Nernst-Planck equation accounts for electric field effects in addition to ordinary diffusion in fluxes of ions. The ion exchange process must always preserve electroneutrality in the film and inside the resin particle. The difference between mobilities of counterions generates the electric potential. The electric potential influences the diffusion rate of both the slow and fast counterions due to the constraint of electroneutrality. The net fluxes of the counter ions, therefore, are equivalent to one another. The one-dimensional Nernst-Planck equation is expressed by Equation (1), and the second term in the right hand side of the equation accounts for the effect of the electric potential.

$$J_i = -D_i \left(\frac{dC_i}{dy} \right) - D_i z_i C_i \left(\frac{F}{RT} \right) \left(\frac{d\varphi}{dy} \right) \tag{1}$$

Schlogl and Helfferich (1957) and Helfferich and Plesset (1958) first calculated the kinetics of film and particle diffusion controlled ion exchange processes for mutually diffusing ions with dissimilar mobilities using the Nernst-Planck equation. They proposed an explicit empirical formula approximating the numerical results. Hering and Bliss (1963) observed ion exchange rates for six pairs of ions under particle diffusion control and interpreted the results with Fick's law and the Nernst-Planck model. Both models fitted the results well. They recommended that Fick's diffusion model be used for design purposes because of its simplicity, even though the Nernst-Planck model was more theoretical. Smith and Dranoff (1964) carried out binary ion exchange experiments in a batch reactor. Experimental data were used to validate predictions using the Nernst-Planck equation, assuming film diffusion control.

The Nernst-Planck equation for counterions in binary exchange is used to obtain the effective liquid-phase or solid-phase diffusivity. The effective diffusivity is used to calculate ionic mass transfer coefficient in the rate expression (Kataoka et al., 1973; Van Brocklin and David, 1972). The effective diffusivity is generally not constant but changes with the concentrations of both counterions in the solution or particle (Helfferich and Plesset, 1958; Schlogl and Helfferich, 1957; Kataoka et al., 1968). The breakthrough curve for an ion exchange packed bed is obtained by solving simultaneously a column material balance, an equilibrium relationship, and a rate expression with initial and boundary conditions in order to predict the bed outlet concentrations. This procedure is carried out separately for both cation and anion resins in an ion exchange mixed bed. Haub and Foutch (1984, 1986a,b) discussed the derivation and the numerical technique for solving the equations for liquid-film control ion exchange in a mixed bed of cation and anion resins. Divekar et al. (1987) expanded Haub and Foutch's

model to include the effects of temperature on the model parameters and the solution properties.

Boyd et al. (1947) showed that two rate-controlling steps, film and particle diffusion, governed ion exchange rate with experimental data for cation exchange kinetics. The rate controlling mechanism depended on influent concentration. They concluded that the rate was controlled by particle diffusion for solution concentrations of 0.1 M or greater, and film diffusion was controlled when solution concentrations were 0.003 M or less. It was found that the two rate processes acted in series at the intermediate concentration between 0.003 and 0.1 M. Other investigators (Gilliland and Baddour, 1953; Reichenberg, 1953; Moison and O'Hearn, 1969) also claimed that the ion exchange process is controlled by diffusion across a liquid boundary layer at low inlet concentrations. This was validated by experiments (Frisch and Kunin, 1960; Turner and Snowdon, 1968).

Gopala Rao and David (1964) discussed film and particle diffusion in packed beds with the effects of solution concentration and flow rate. Liberti et al. (1987) showed that the ion exchange rate was controlled by particle diffusion at high solution concentrations. Petruzzelli et al. (1988) visually confirmed the particle diffusion mechanism by autoradiography and light microscopic observation inside a resin bead. Bolden et al. (1989) predicted amine concentration in a solution and in a resin as a function of position in the bed and time. The system was a complexation of amine with an immobilized metal ion on a pellet type resin for more than 0.1 M amine feed concentration. The shrinking-core model for particle diffusion was used. Gopala Rao and Gupta (1982a,b) showed an exception that the particle diffusion resistance was dominant even in extremely dilute solutions, when the acid sorption took place between weak-base anionic resins and acidic solutions. Tittle (1981) verified experimentally the poor kinetics on used anion exchange resin. He reported that particle diffusion is the

rate controlling process in anion resins at even very low ionic concentrations. Van Brocklin and David (1972) predicted the effects of ionic migration on cation exchange for the case of liquid-phase controlled mass transfer based upon three different mass transfer models such as film, boundary layer, and penetration theory.

Graham and Dranoff (1972) conducted kinetic experiments of anion exchange accompanied by fast irreversible reaction in a well-stirred batch reactor. Results were analyzed with film diffusion control at low concentration and low stirring rates, and with intraparticle diffusion control at high concentration and high stirring rates. The stirring rates accounted for the hydrodynamic effects on the film thickness. The analyses showed that the film diffusion model was appropriate, but the combined model, which takes into account the effects of both film and particle diffusion, fit the experimental data very well. They explained that the exchange rate must be controlled in the initial stages by film diffusion, since the rate of particle diffusion will approach infinity until the outer layers of the exchanger are exhausted. Other investigators (Helfferich et al., 1985; Petruzzelli et al., 1987a) confirmed that the combined model was appropriate for exchange at low concentration with a high selectivity of the anion exchange resin towards the entering ion. Huang and Li (1973) also claimed that the ion exchange mechanism was dependent on stirring speeds for isotopic exchange reactions in a batch reactor. They obtained the intraparticle diffusivity from isotopic ion exchange data for high stirring speeds and the film mass transfer coefficient for low stirring speeds. Huang and Tsai (1977) and Tsai (1982b) derived the isotopic exchange rate equations for film diffusion controlled kinetics assuming linear and nonlinear concentration profiles in the film, respectively. Goto et al. (1981a,b) proposed a method of simultaneous evaluation of the interphase mass transfer coefficient and intraparticle diffusivity from batchwise stirred tank reactor

experiments using linear and nonlinear isotherms similar to Huang and Li (1973). The film mass transfer coefficient was used to obtain interphase mass transfer coefficients which involved both film and particle resistances. Tsai (1982a) derived a theoretical equation to predict the fractional attainment of equilibrium in a batch reactor for an isotopic ion exchange reaction controlled by combined film and particle diffusion. The criteria depended on the distribution coefficient, the ratio of the film thickness to particle radius, and the ratio of particle to film diffusion mass transfer coefficients.

Non-ionic Mass Transfer Coefficient

The non-ionic mass transfer coefficient is a concept that gives a simpler driving force description of mass transfer phenomenon by concentration difference. In general, it is expressed by a correlation with dimensionless numbers for various systems when complex geometrical flow patterns are involved. Cussler (1984) presented the fundamentals of mass transfer coefficients and their correlations for various systems with solid-liquid interfaces and liquid-liquid interfaces.

The many empirical correlations for mass transfer coefficients in fixed and fluidized beds were initially based on experimental results (Wilke and Hougen, 1945; Maccune and Wilhelm, 1949; Gaffney and Drew, 1950). The general empirical equations for nonelectrolyte packed bed mass transfer had the form (Lightfoot et al., 1966):

$$k_l = A \frac{u_f}{\varepsilon}(Sc)^{-\frac{2}{3}}(Re)^n \tag{2}$$

Carberry (1960) developed a theoretical equation for fluid-particle mass transfer in fixed beds at Reynolds numbers less than 1,000 by applying simplified boundary-layer theory. The transfer process between the fluid and particle occurs across a boundary with a velocity gradient. He assumed that a boundary layer developed and collapsed over a distance approximately equal to one particle diameter. Pfeffer (1964) proposed an equation with the assumption of a free surface model in the same flow region as Carberry's equation. Carberry's equation showed deviation from experimental data in the low Reynold number region (Wilson and Geankoplis, 1966; Kataoka et al., 1972). Kataoka et al. (1972) derived a mass transfer equation applying the hydraulic radius model to laminar flow in a packed bed. He assumed that mass transfer is similar to that between a pipe surface and a stream of liquid with a steady laminar velocity profile. The steady laminar velocity profile within the pipe is instantly formed and collapsed over a distance equivalent to one particle diameter. They insisted that their equation agreed well with data for Reynolds number less than 10 and that Carberry's equation was best for Reynolds numbers greater than 100. Both equations could be applied to the region between 10 and 100. They explained the reason for the deviation of Carberry's equation at low Reynolds numbers as boundary layer effects when flow in void regions collide with each other. At smaller Reynolds number, the larger the boundary layer thickness based on the flat-plate boundary layer theory. Pan and David (1976) applied Carberry's equation to Reynolds numbers greater than 30 and Kataoka's equation for lower flow rates to the mixed bed ion exchange model development. Haub and Foutch (1986a) used Carberry's equation for Reynold numbers greater than 20 and Kataoka's equation for lower than 20. Equations (3) and (4) show Carberry's and Kataoka's equations, respectively. The equations are popular for calculations concerning ion exchange fixed beds.

Carberry's equation

$$k_1 = 1.15 \frac{u_f}{\epsilon} (Re_c)^{-\frac{1}{2}} (Sc)^{-\frac{2}{3}}$$ (3)

Kataoka et al.'s equation

$$k_1 = 1.85 \frac{u_f}{\epsilon} \left(\frac{\epsilon}{1-\epsilon}\right)^{\frac{1}{3}} (Re_k)^{-\frac{2}{3}} (Sc)^{-\frac{2}{3}}$$ (4)

where

Re_c = Reynold number, $(d_p \, u_f \, \rho)/(\epsilon \, \mu)$

Re_k = Reynold number, $(d_p \, u_f \, \rho)/[(1-\epsilon) \, \mu]$

These equations account for the effects of bed geometry and the flow field on the mass transfer rate with dimensionless groups.

For systems with both particle and film diffusion control, the overall mass transfer coefficient can be related to the individual coefficients by the usual sum of resistances (Gilliland and Baddour, 1953; Levenspiel, 1972; Wankat, 1990; Cooney, 1991). It can be expressed by

$$\frac{1}{k} = \frac{1}{k_f} + \frac{1}{k_p}$$ (5)

where

k = the overall mass transfer coefficient

k_f = the film mass transfer coefficient

k_p = the particle mass transfer coefficient.

Rosen (1954) developed a solution for linear sorption systems, assuming negligible dispersion and constant fluid velocity, to sum resistances for systems which showed film and particle mass tra

showed the sum of resistances as in Equation (5), i.e. particle and film mass transfer coefficients,

$$k_m a_p = \left[\frac{1}{k_f a_p} + \frac{d_p^2}{60 D_{mp} A (1 - \varepsilon_e) \rho_p} \right]^{-1} \tag{6}$$

where the second term on the right hand side explains the particle diffusion resistance. The film mass transfer coefficient can be estimated by Equation (3) or (4), and the particle mass transfer coefficient with the physical and design properties, d_p, ε_e, A, ρ_p, and D_{mp}.

Ionic Mass Transfer Coefficient

While the mass transfer coefficient correlations in the previous section worked reasonably well for non-ionic systems, they do not allow for the effects of ionic migration during ion exchange. This is because the mass transfer of counter ions occurs by simultaneous diffusion and ionic migration. It has been expressed mathematically by the Nernst-Planck flux equation. The effects of ionic migration were accounted for by defining a ratio of ionic to non-ionic mass transfer coefficients, R_i (Van Brocklin and David, 1972, 1975), symbolizing the ratio of Fick's law flux to Nernst-Planck flux. Van Brocklin and David (1972) investigated the effects of ionic migration on cation exchange for the case of liquid-phase controlled mass transfer based upon three mass transfer models, film, boundary-layer, and penetration theory. Pan and David (1978) claimed that the two-dimensional boundary-layer model is appropriate in packed bed ion exchange when flow rates are low. In addition, the R_i factor was connected with an

effective ionic liquid phase diffusivity to explain ionic effects (Kataoka, 1973). The ionic mass transfer coefficient was calculated by the following relationship.

$$R_i = \frac{k_l^{'}}{k_l} = \left(\frac{D_e}{D_B}\right)^{\frac{2}{3}}$$ (7)

The rate of exchange accounting for ionic effects in film diffusion controlled systems can be determined by Equation (8).

$$\frac{\partial q_i}{\partial t} = k_l R_i a_p C_t \left(x_i^{\circ} - x_i^{*}\right)$$ (8)

k_l in equation (8) can be calculated by Equation (3) or (4) depending on the flow rates, and R_i can be estimated by Equation (7). The effective diffusivity, D_e in Equation (7) can be expressed as a function of bulk and interface concentrations between the resin surface and film. The effective diffusivities of cation and anion, are derived using the Nernst-Planck flux equations for each species in a film with neutralization reaction and water dissociation (Haub, 1982).

Frisch and Kunin (1960) proposed a mass transfer coefficient correlation based on a film mass transfer mechanism for mixed bed deionization of a salt solution. The correlation was the same type as Wilke and Hougen's (1945) equation, but its coefficient was much greater. They assumed that a mixed bed was a salt-removing bed, with identical exchange rates for cations and anions. In this system the solute, both in the liquid and resin phase, would be a salt rather than individual ions. Therefore, their mass transfer equation did not account for the ratio of cation to anion resins and resin particle size because the equation used the effective diameter of all resins present. In addition, their mass transfer

coefficient equation could not explain ionic migration effects for cations and anions.

Harries and Ray (1984) modified Frisch and Kunin's equation dimensionally, based on resin volume and volumetric flow rate, rather than resin mass and mass flow rate. Their equation introduced the volume fraction of anion or cation exchange resins in the mixed bed in order to evaluate a specific resin. They measured the mass transfer coefficients for chloride and sulphate, with both new and fouled resins in a mixed bed. In addition, they discussed the experimental results qualitatively using the simple relationship:

$$k_f = \frac{D}{\delta} \qquad (9)$$

where δ is the fixed boundary layer thickness (a function of the Reynolds number). The relationship accounts for the hydrodynamic effect in mass transfer. They concluded that the mass transfer coefficients of new resins were independent of polymer/matrix type and influent concentrations and dependent on flow rates. The dependency of the mass transfer coefficient on flow rate resulted from the decrease of δ as the flow rates increase. The experimental results showed that the mass transfer coefficients of new resins were greater than those of organically fouled resins, and those of organically fouled resins were dependent on the influent concentrations. The large organic foulants can not diffuse into resins easily because of their size, and they form a barrier layer on the resin surface. The layer will disturb the diffusion into the resin. This gives the clue that the kinetic mechanism of fouled resins is not explained by only a liquid film diffusion model. The experimental results, in addition, showed the mass transfer coefficients of sulphate were smaller than those of chloride under the same condition. McNulty (1984) also observed the same trend. The diffusion coefficient of sulphate is

greater than that of chloride, but that of sodium sulphate is smaller than that of sodium chloride. Therefore the differences in mass transfer coefficients could be described by the effects of the diffusions of both ion and molecular species across a concentration gradient.

In order to determine the effects of the ratio of cation to anion resins, Harries (1987) carried out measurements of the mass transfer coefficients of anion exchange resins for chloride and sulphate in mixed and single beds. The results showed that the mass transfer coefficients of chloride and sulphate decreased with the increase in the proportion of anion resins in mixed beds. The mass transfer coefficient of sulphate decreased more than that of chloride. He concluded that anion exchange is strongly affected by the pH of the bulk solution within the bed. In a mixed bed of the resin ratio 2:1, cation:anion, the cations in the injected salt ($NaCl$ or Na_2SO_4) are more rapidly exchanged for hydrogen ions than anions are for hydroxyl ions, due to the excess of cation exchanger. The pH of the bulk solution, therefore, becomes acidic during the exchange process. As the proportion of cation exchanger decreases, the pH of the bulk solution will rise. This means that anion in a single bed will be processed in alkaline conditions during the exchange process. Harries et al. concluded that the optimum ratio must be balanced between exchange zone depth (Michaels, 1952) and loss of cation exchange capacity. The increase of the proportion of anion resins results in the decrease of anion exchange zone. From Equation (9), the ratios between the mass transfer coefficients for two anions should be constant under liquid film layer control, and the same as the ratios between diffusion coefficients, because D and δ are constant at specific operating conditions. However, in fact, the ratios had some variation and differed from the ratios of diffusion coefficients. This accounts for the effects of exchange reaction or particle diffusion for processes with film diffusion control. This can explain the phenomenon observed by Harries

et al. (1984), where the mass transfer coefficients of used and organically fouled resins depended on influent concentrations.

Harries and Tittle (1986) proposed that the kinetic deterioration in anion exchangers comes from the chemical degradation of the exchange groups at the bead surface. Both strongly and weakly basic groups are on the surface. The strongly basic groups retain their activity over a wide range of pH, but the weakly basic groups are active only under acidic conditions. This means that more exchange sites can be used in acidic solutions. This trend was more significant for sulphate exchange, because a divalent ion needs two adjacent active exchange sites. McNulty et al. (1986) estimated mass transfer coefficients of sulphate in new and used resins using the same method as Harries and Ray (1984). They also identified the deterioration of anion resin performance. Harries (1988) carried out the X-rays photoelectron spectroscopy analysis with new and used resins to identify the proportion of strongly and weakly basic groups on the resin surface and within the beads. While the bead surface contained a mixture of strongly and weakly basic groups, the bulk resin consisted mostly of strongly basic groups for both new and used resins. The analysis for the used resins confirmed the existence of a sulphur-containing contaminant on the surface. It is believed that the contaminant causes the fouling effect. The experimental results, in addition, showed that the equilibrium uptake of Cl^- or SO_4^{-2} on the surface from alkaline solutions was less than from acidic solutions. He concluded that both exchange group degradation and fouling had a significant effect on anion exchange kinetics. This effect will reduce the concentration gradient across the liquid film, because the exchange reaction on the surface is no longer fast relative to film diffusion.

Experiments on the dependence of anion and cation exchange kinetics on pH in mixed beds was carried out for used and new resins by Harries (1988, 1991). In 2:1, cation:anion volume ratio, the mass transfer coefficients of chloride

and sulphate for both new and used resins decreased as the pH of the aqueous phase varied from acid to alkaline, while for cations, ammonia and sodium, mass transfer coefficients increased. This feature was more sensitive for sulphate and ammonia. The decrease was not monotonic, but there were two separate regions where the mass transfer coefficients were almost constant. There is a sharp drop or rise between these two regions. The drop of mass transfer coefficient for sulphate was sharper than for chloride. Harries (1988) measured the effects of cation resin bead size on the mass transfer coefficients for chloride and sulphate. Increased size caused a reduction of mass transfer coefficients for both ions, and the mass transfer coefficients of sulphate were influenced more strongly. Additionally, the exchange rate of cations associated with sulphate was a little faster than cations associated with chloride. This is not simply interpreted by pH, but by the complicated interactions of anion and cation exchange processes in a mixed bed.

Harries (1991) measured the anion exchange rate for chloride and sulphate as salt, when the corrosion controlling agent, ammonia or morpholine, was dosed into a mixed bed. The rates were slower than without the corrosion controlling agent. This feature was interpreted again by the pH of aqueous phase and showed that the type of cation being exchanged can affect the anion exchange kinetics in a mixed bed. He also ascribed poor cation exchange in a mixed bed to fouling of cation resins by residual polymeric material eluted from regenerated anion resins.

The mass transfer coefficient is lower for lower influent concentration because the film thickness increases as the influent concentration decreases. Yoon (1990), therefore, claimed that Equation (4) is not appropriate for the condition of ultra-low influent concentrations, because the mass transfer coefficients under these conditions needs to be reduced. He proposed a new correlation using his experimental results over a range of cation to anion resin ratios in mixed bed

performance at ultra-low concentrations. The result was of the same type as Equation (2) with -0.5 as the exponent of Reynolds number. The constant, A, is calculated from fitting experimental results to the mixed bed ion exchange model of Haub and Foutch (1986a). Consequently, A was linearly correlated with cation and anion resin ratio. Equation (10) is Yoon's correlation.

$$k_1 = A \frac{u_f}{\epsilon} (Sc)^{-\frac{2}{3}} (Re)^{-\frac{1}{2}} \tag{10}$$

where

$A = 0.454 - 0.168 * log(R_{C/A})$ for cation (sodium)

$A = 0.364 + 0.028 * (R_{C/A})$ for anion (chloride)

$R_{C/A}$ = the ratio of cation to anion resin

CHAPTER III

EVALUATION OF MASS TRANSFER COEFFICIENT
DATA FOR NEW AND USED ION
EXCHANGE RESINS

Introduction

Compared with other separation processes, ion exchange technology has an advantage to treat a large volume of condensate at high flow rate economically. Therefore, most condensate purification plants normally use an ion exchange mixed bed to remove continuously ionic impurities to produce ultra-pure water. Bead and powder type ion exchange resins are utilized popularly. In mixed bed operation, a major problem has been the deterioration of anion exchange resin (Harries and Ray, 1984; Harries, 1986, 1987). The problem is first identified by an increase of anion leakage. This results from fouling of the anion exchange resin by several mechanisms, such as organic molecules that exist in the raw water. McNulty et al. (1986) explained the deterioration of anion resin by thermal degradation of strong base capacity as well as resin fouling. In addition, sulphate leakage was observed from mixed beds due to cross contamination of anion exchange resin by sulfuric acid and insufficient rinse time for cation exchange resins after regeneration. Cross contamination arises from incomplete cation and anion resin separation prior to regeneration (Harries and Ray, 1978; Emmett, 1983).

The kinetics of cation and anion exchange in gelular resins were measured by kinetic leakage experiments and are described in this chapter. The kinetics were estimated by mass transfer coefficients. Used resins from an industrial plant were tested in addition to new resins. The result were compared with data of previous investigators (Harries and Ray, 1984; Harries, 1987).

Mass Transfer Equation

The mass transfer equation for kinetic leakage was first derived by Frisch and Kunin (1960) and modified appropriately to ion exchanger mixed beds by Harries (1984). Kinetic leakage differs from equilibrium leakage, which is based on selectivity coefficients. Kinetic leakage is related to the physical characteristics of the ion exchanger and hydraulics of the system.

Ignoring axial dispersion and diffusion, the material balance of a packed bed is

$$\frac{u}{\varepsilon}\frac{\partial C}{\partial z} + \frac{\partial C}{\partial t} + \frac{1-\varepsilon}{\varepsilon}\frac{\partial q}{\partial t} = 0 \tag{11}$$

The first term of Equation (11) is for the movement of ions axially due to bulk fluid movement, the second term is ion accumulation in the mobile fluid, and the third term is ion adsorption on the resin. Equation (11) is written for a certain ion, i, in a mixed bed by introducing x_i and R_i :

$$\frac{u}{\varepsilon}\frac{\partial x_i}{\partial z} + \frac{\partial x_i}{\partial t} + \frac{R_i(1-\varepsilon)Q_i}{C_i^f(\varepsilon)}\frac{\partial y_i}{\partial t} = 0 \tag{12}$$

where

R_i = volumetric fraction of cation or anion resin in a mixed bed

$$x_i = \frac{C_i}{C_i^f}$$

$$y_i = \frac{q_i}{Q_i}$$

The ion exchange rate based on Nernst film diffusion is expressed by

$$\frac{\partial q_i}{\partial t} = k_1 a_s \left(C_i - C_i^* \right) \tag{13}$$

Equation (13) is expressed with the definition of y_i by Equation (14).

$$\frac{\partial y_i}{\partial t} = \frac{k_1 a_s}{Q_i} \left(C_i - C_i^* \right) \tag{14}$$

Dimensionless distance and time coordinates are used to make Equation (12) an ordinary differential equation (Kataoka, 1976) :

$$\xi = \frac{k_1(1-\varepsilon)}{u} \frac{z}{d_p} \tag{15}$$

$$\tau = \frac{k_1 C_i^f}{d_p Q_i} (t - \frac{Z\varepsilon}{u}) \tag{16}$$

ξ and τ are substituted for z and t in Equation (12) and (14), and simplified to:

$$\frac{\partial x_i}{\partial \xi} + R_i \frac{\partial y_i}{\partial \tau} = 0 \tag{17}$$

$$\frac{\partial y_i}{\partial \tau} = \frac{d_p a_s}{C_i^f} \left(C_i - C_i^* \right) \tag{18}$$

The concentration of a certain ion at the surface of the resin, C_i^*, is assumed zero in all calculations (Frisch and Kunin, 1960; Koloini et al., 1977; Rahman and Streat, 1981). This assumption is appropriate for low levels of resin loading observed in kinetic leakage analysis. Actually, maximum percentage loadings of sodium and chloride in this study were 3.35 and 5.79 %, respectively, where the maximum loading is assumed based on total influent ions without ionic leakage at the highest flow rate (900 ml/min). Thus, Equation (18) is simplified to:

$$\frac{\partial y_i}{\partial \tau} = d_p a_s \frac{C_i}{C_i^f} \tag{19}$$

Equation (19) is substituted into Equation (17) and integrated with the following boundary conditions :

$$C_i = C_i^f \qquad \text{at } z = 0 \ (\xi = 0)$$
$$C_i = C_i^{eff} \qquad \text{at } z = Z \ (\xi = \xi)$$

The final mass transfer equation for a certain ion is:

$$\ln \frac{C_i^{eff}}{C_i^f} = -\frac{k_1 SZAR_i}{V} \tag{20}$$

where $S = a_s(1-\varepsilon)$ and C_i^{eff} is the effluent ionic concentration at the end of bed depth, Z. In this experiment, the exchange zone needed for C_i^f decrease to C_i^{eff} at the outlet is equal to the bed depth, Z. R_i is 1.0 for a single bed. From the outlet concentration, the mass transfer coefficient of a certain ion, k_1, can be calculated using Equation (20) with the arbitrarily determined values of C_i^f, V, Z, A, R_i and a_s, and the effluent concentration, C_i^{eff}, measured from experiment.

The objectives of this study are to determine the mass transfer coefficients for anions (Cl⁻) and cations (Na⁺), to compare the kinetics of new resin with those of used resins, and to evaluate the differences between the kinetics in mono and mixed beds.

Experimental Methods

The experiments were carried out to determine the effects of influent concentration and flow rate. Seven influent concentrations and three flow rates were used. The flow rates were chosen due to similar superficial linear velocities as operating flow rates in industry. Table I shows for anion and cation exchange experiments, respectively. In addition, two types of new and used Dow resins were tested; 650C-H and HGR-W2-H for cation, and 550A-OH and SBR-P-C-OH for anion. The experimental system, procedure and analysis of outlet samples with ion chromatography are described in Appendix A, B and C, respectively.

TABLE I

EXPERIMENTAL INFLUENT CONCENTRATIONS AND FLOW RATES

Influent Concentration (ppb)		Superficial Velocity	
Cation (Na)	Anion (Cl)	volumetric (ml/min)	$linear \times 10^{-2}$ (m/s)
64.9	100	500	1.65
159	245	700	2.30
324	500	900	2.96
486	750		
649	1000		
1590	2450		
3240	5000		

The used resins were obtained from PSO (Public Service of Oklahoma), and sampled from two sites, Riverside and Northeastern station, of PSO. Table II shows sources of used resins and their ages. Tables III and IV show physical properties of the resins. All resins, new and used, were regenerated separately in order to maximize their capacities, before being used. The regeneration procedures for both resins are described in Appendix B. Polyethylene bottles, for sampling effluent from a bed, were filled with deionized water for at least a week in order to soak impurities inside. The effluent samples were analyzed within 3 days by ion chromatography, because the storage of the samples for a long time can cause the penetration of impurities through sample bottles. All experiments were carried out at room temperature, 24±0.5 °C. The inside diameter of the test column was one inch. All experimental data are listed in Tables XVII and XVIII (Appendix E).

The measurements of mass transfer coefficients in a single bed were conducted with new HGR-W2-H and SBR-P-C-OH resins. Bed depth was 7.6 cm (40 ml by volume) for both cation and anion resins, respectively. The experimental conditions for influent concentrations and flow rates were the same as in Table I.

The mass transfer coefficient of ions in a mixed bed were determined using two types of resins, HGR-W2-H and 650C-H cation resins and SBR-P-C-OH and 550A-OH anion resins. Bed depths were 11.5 and 11.6 cm for each, respectively. The ratio of cation to anion resin was 2 (40 ml) to 1 (20 ml) by volume for all experiments. This ratio was determined to coincide with a common value used in industry. The large proportion of cation resin in a mixed bed is generally required because amines are dosed with the feed in order to prevent the corrosion of reactor surfaces.

TABLE II

SOURCE OF USED ION EXCHANGE RESINS USED IN EXPERIMENTS

Name of Resin		Used Resin from Plants		
Cation	Anion	Name of Plant	Installation	Sampling
650C-H	550A-OH	Riverside PSO No.1 C.P.	Oct., 1990	Mar., 1993
		Riverside PSO No.2 C.P.	Mar., 1992	Mar., 1993
		Northeastern Station No.3 C.P.	Dec., 1991	Apr., 1993
		Northeastern Station No.4 C.P.	Feb.,1992	Apr., 1993
HGR-W2-H	SBR-P-C-OH	Northeastern Station No.2 C.P.	May, 1986	Apr., 1993

C.P. : Condensate Polisher.

TABLE III

PHYSICAL PROPERTIES OF DOWEX RESIN* (I)

Parameter	Cation	Anion
Name	HGR-W2-H	SBR-P-C-OH
Capacity (meq/ml)	2.18 (Na^+ form)	1.1 (Cl^- form)
Selectivity	1.13 for Na-H	22.0 for Cl-OH
Void fraction	0.335-0.340	0.335-0.340
Diameter (cm)	0.08	0.06
Density (lb/ft^3)	50.0	41.0
Water retention capacity (%)	48.2	54.3
Appearance	light yellow to amber solid (bead)	white to dark amber solid (bead)

* From the vender

TABLE IV

PHYSICAL PROPERTIES OF DOWEX RESIN* (II)

Parameter	Cation	Anion
Name	Monosphere 650C-H	Monosphere 550A-OH
Capacity (meq/ml)	1.90 (Na^+ form)	1.1 (Cl^- form)
Selectivity	1.13 for Na-H	22.0 for Cl-OH
Void fraction	0.33-0.35	0.33-0.35
Diameter (cm)	0.065	0.059
Density (lb/ft^3)	50.0	40.0
Water retention capacity (%)	46 - 51	44 - 50
Diameter (cm)	0.065	0.059
Cross linkage (%)	8	6
Appearance	hard, black, spherical beads	hard, white, spherical beads
Particle within range of ± 0.01cm from diameter (%)	95 minimum	95 minimum

* From the vender

Accuracy and Reproducibility

Errors always exist in experimental studies. Therefore, the source of errors should be discovered and removed as much as possible. Errors in this study resulted from several sources; the preparation of a certain amount of crystal sodium chloride and resin, the measurement of bed depth, the inaccurate flow rates of feeding and dosing pumps, and the inaccuracy of the analysis of effluent samples by ion chromatography. The errors affected the calculation of mass transfer coefficients.

The reproducibility of experimental data was estimated with the source of errors. It was carried out by repeating an experimental run and comparing the results. The reproducibility of this experiment was relatively good. The error analysis and the reproducibility of experimental data are described in Appendix D.

Results and Discussion

Single Bed Experiments

Figures 1 and 2 show the mass transfer coefficient data of Na^+ and Cl^- for various influent concentrations and flow rates. The mass transfer coefficients were increased for both cation and anion resin as flow rate becomes higher. This verified that ion exchange kinetics are controlled by film diffusion. Namely, the film thickness is decreased as flow rate increases. The resistance of film diffusion, therefore, becomes weak and the mass transfer coefficient increases in Equation (9) assuming constant ionic diffusivity in solution at a certain temperature. The mass transfer coefficients were also affected by influent concentrations, even though Harries and Ray (1984) had indicated experimentally the independence of mass transfer coefficients for new resins on influent concentration. Harries and
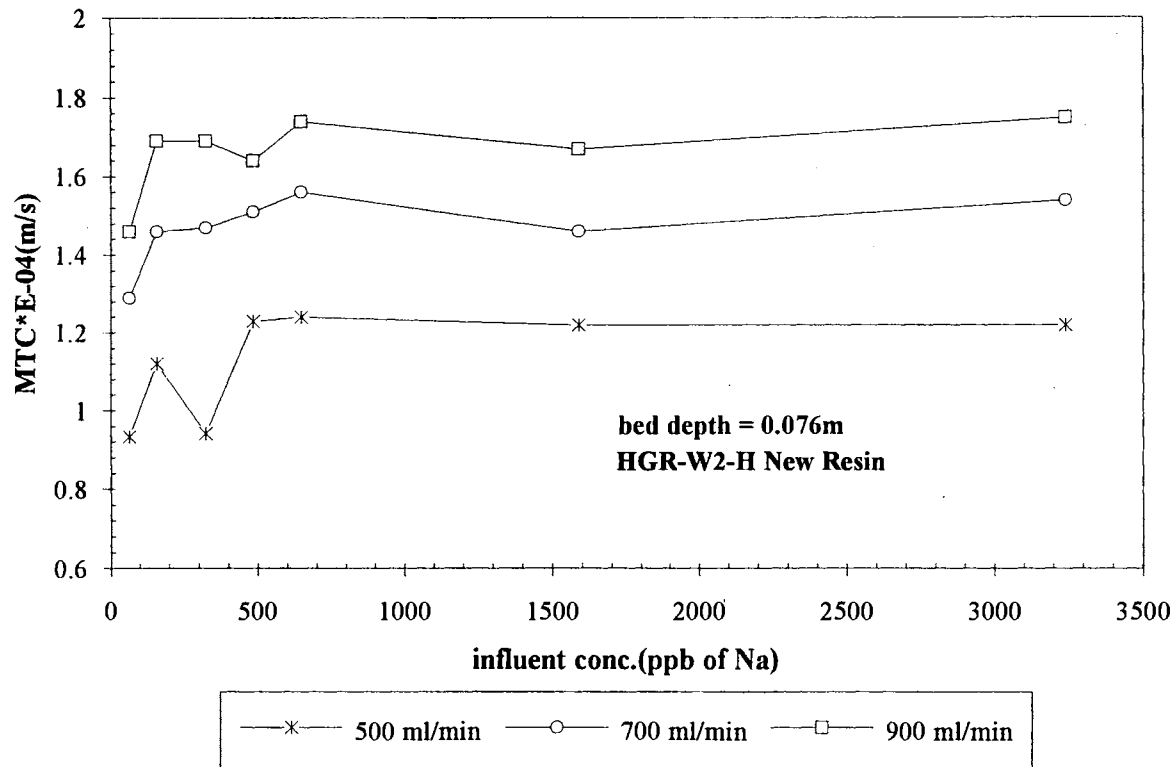
Figure 1. Mass Transfer Coefficients of Sodium in Single Beds
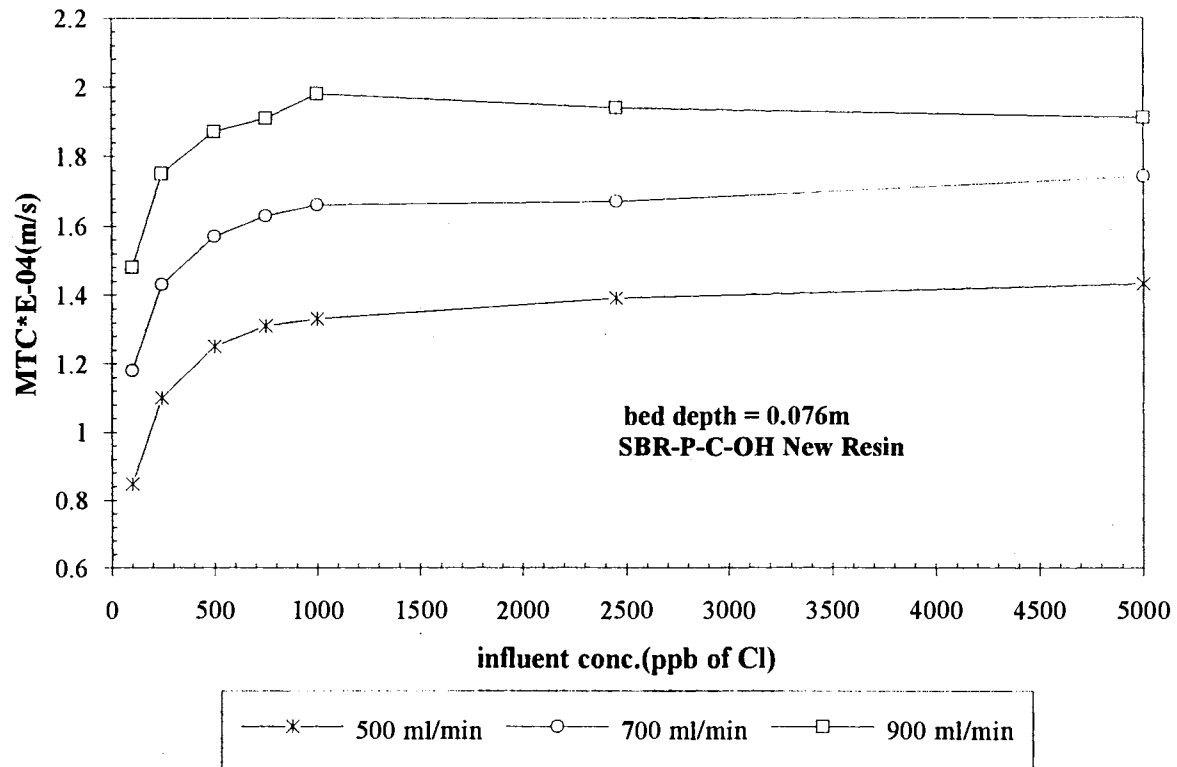
Figure 2. Mass Transfer Coefficients of Chloride in Single Beds

Ray (1984) used three influent concentrations, 1480, 2960 and 5920 ppb of Cl⁻ in mixed bed experiments, and three superficial velocities, 1.53×10^{-2}, 2.5×10^{-2} and 3.33×10^{-2} m/s. In this study, the measurements of mass transfer coefficient were carried out in a broader influent concentration range than Harries and Ray (1984). The mass transfer coefficients at the lower concentrations depend on influent concentration, and becomes lower as influent concentration decreases. This results from the driving force for mass transfer becoming weak as the influent concentration decreases. The phenomenon was generally significant at influent concentrations below 245 ppb chloride and 159 ppb sodium. At higher influent concentration, mass transfer coefficients were almost constant. This phenomenon coincides with Harries and Ray's (1984) results.

TABLE V

EFFLUENT CONCENTRATIONS FOR NEW MONOSPHERE RESIN IN
MIXED BED AT DIFFERENT FLOW RATES

inlet conc. (ppb)		outlet concentration (ppb)					
		500 ml/min		700 ml/min		900 ml/min	
anion	cation	anion	cation	anion	cation	anion	cation
100	64.9	11.7	3.61	11.1	5.54	14.3	4.54
245	159	12.4	5.64	17.9	8.29	22.3	9.49
500	324	20.0	10.4	30.7	13.1	45.4	20.0
750	486	28.2	12.5	43.9	18.4	71.1	30.2
1000	649	36.6	16.0	53.3	22.0	90.8	39.6
2450	1590	108	42.9	148	60.3	250	98.2
5000	3240	206	87.5	302	114	511	230

On the other hand, a higher mass transfer coefficient does not mean smaller ionic leakage, even though the mass transfer coefficient increases as flow rate becomes high. Table V shows the effluent concentrations for new Monosphere resin at three flow rates. At low flow rates, the residence time through the bed is greater than at high flow rate. The increase of the residence time compensates for the decrease of mass transfer coefficient, thus ionic leakage at the bed outlet becomes lower than at high flow rate.

The mass transfer coefficients of both cations and anions in a single bed were lower than those in a mixed bed. This trend was more significant for anions. Table VI shows the percentage difference of the average mass transfer coefficients between a single and mixed bed for influent concentrations over 750 ppb anion and 480 ppb cation. The mass transfer coefficient of anion is high in acidic solution and low in basic solution, and that of cation is high in basic solution and low in acidic solution (Harries, 1991). Following Harries' explanation, the low mass transfer coefficient of single bed compared with mixed bed can be explained by solution pH. In the case of an anion single bed, the OH^- concentration of a solution inside the bed will increase during the exchange reaction, so the exchange reaction takes place in more basic solution than in a mixed bed where the initial state of exchange takes place in acidic solution due to the excess of cation resin. Figure 3 shows the difference of mass transfer coefficients of chloride between single and mixed bed. In contrast with anion exchange, cation exchange in a single bed occurs in more acidic solution than in a mixed bed. Figure 4 indicates the difference of mass transfer coefficients of sodium between a single and mixed bed. Both figures show that mass transfer coefficients of chloride are higher than those of sodium in both single and mixed beds.
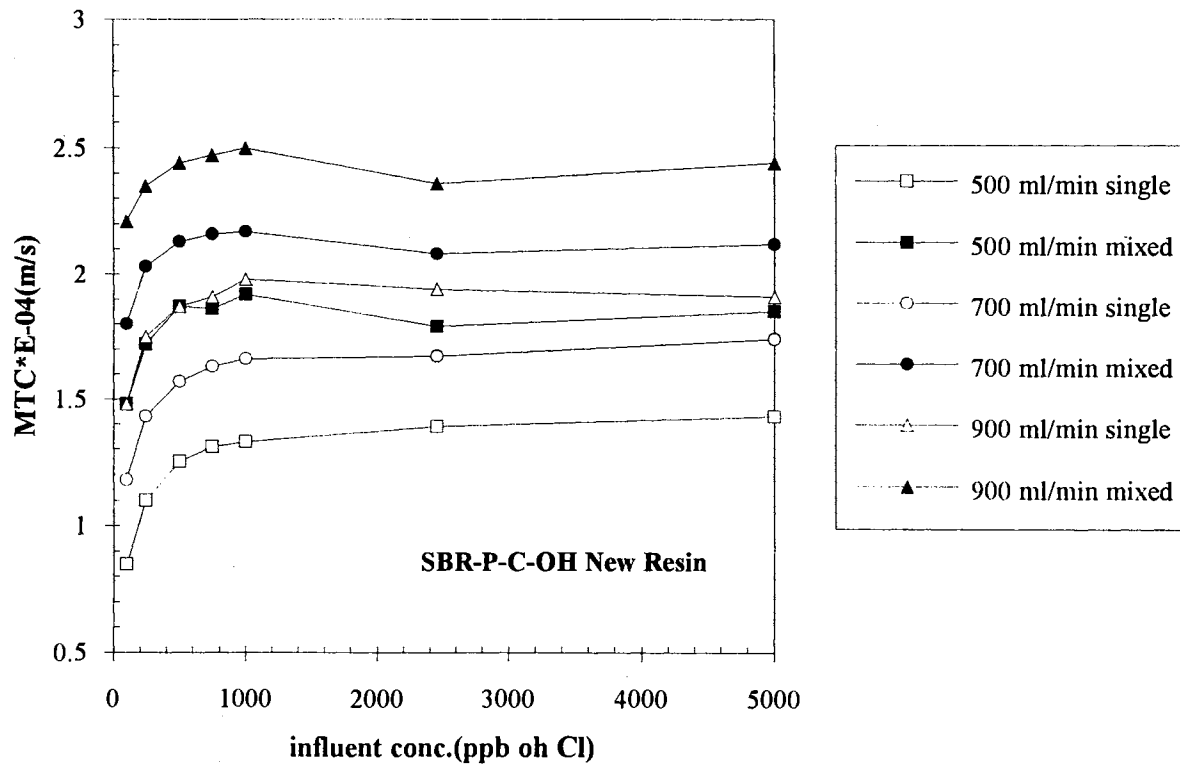
Figure 3. Comparison of Mass Transfer Coefficients of Chloride in Single and Mixed Beds
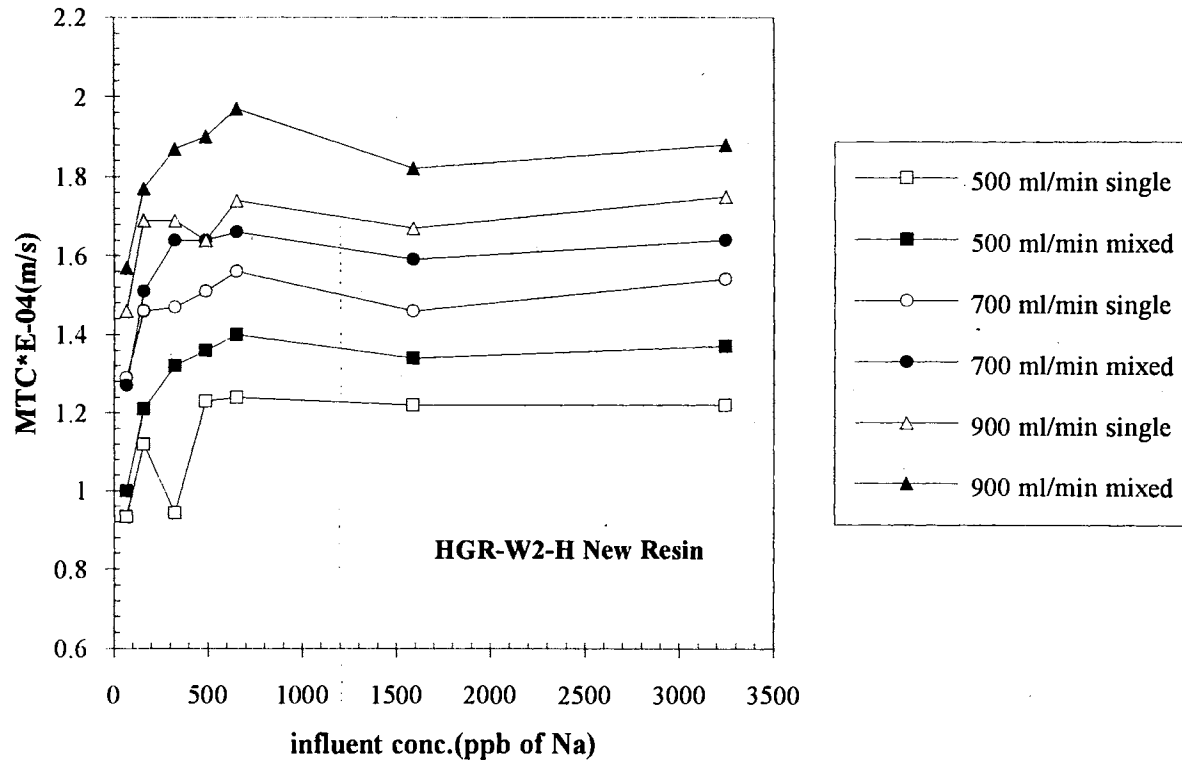
Figure 4. Comparison of Mass Transfer Coefficients of Sodium in Single
and Mixed Beds

TABLE VI

THE DIFFERENCES OF AVERAGE MASS TRANSFER COEFFICIENTS
BETWEEN SINGLE AND MIXED BEDS

flow rate (ml/min)	single bed ($\times 10^{-4}$ m/s)		mixed bed ($\times 10^{-4}$ m/s)		% increase of MTC in mixed bed	
	cation	anion	cation	anion	cation	anion
500	1.228	1.365	1.368	1.855	11.4	35.9
700	1.518	1.675	1.633	2.133	7.6	27.3
900	1.700	1.935	1.893	2.443	11.4	26.3

MTC : mass transfer coefficient
HGR-W2-H & SBR-P-C-OH resin

The higher mass transfer coefficient of anion in mixed bed can be explained by neutralization in bulk and liquid film (Haub and Foutch, 1986b). The neutralization reaction is described by the following stoichiometric equations.

$$R\text{-}OH^- + Cl^- \Leftrightarrow R\text{-}Cl^- + OH^- \text{ (anion exchange)}$$

$$R\text{-}H^+ + Na^+ \Leftrightarrow R\text{-}Na^+ + H^+ \text{ (cation exchange)}$$

$$OH^- + H^+ \Leftrightarrow H_2O \text{ (neutralization)}$$
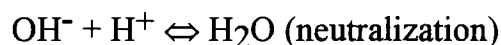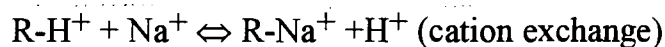
The neutralization in mixed beds initially occurs at the interface between bulk solution and film layer. During the exchange reactions of cation and anion, the inside solution becomes acidic solution due to the excess of cation resin. The increased hydrogen ions starts diffusing into the liquid film on anion resin. Therefore, the neutralization reaction plane is shifted from the bulk phase into the liquid film. The shift of reaction front decreases the effective film thickness and increases the concentration gradient of hydroxide ion in the film.

For ultra-low feed concentration, neutralization reaction occurs in the bulk phase. Equation (21) shows the effective diffusivity for cation exchange between sodium and hydrogen, when neutralization reaction occurs in the bulk phase. The derivations of effective diffusivities for cations and anions were explained by Haub (1984).

$$D_e = \frac{2\alpha D_{Na}}{(1-\alpha)(1-X)}(SX + X - Y - 1) \tag{21}$$

where

$$\alpha = \frac{D_H}{D_{Na}}$$

$$S = K_H^{Na} \frac{1 - y_{Na}}{y_{Na}}$$

$$X = \frac{C_{Na}^*}{C_{Na}^o} = \left[\frac{(\alpha Y + 1)(Y + 1)}{(\alpha S + 1)(S + 1)} \right]$$

$$Y = \frac{C_H^o}{C_{Na}^o}$$

In bulk neutralization, as hydrogen concentration increases due to cation resin excess, effective diffusivity of cation decreases. At the same time, effective diffusivity of anion increases, because the increase of hydrogen concentration in the bulk solution makes hydroxide concentration decrease by the water dissociation constant. Therefore, the anion exchange rate becomes faster than the cation exchange rate, and this explains higher mass transfer coefficients of chloride compared with those of sodium.

In the case of a single bed, there is no neutralization. Therefore, concentration gradients of hydrogen and hydroxide are smaller than in a mixed

bed. This affects diffusion of sodium and chloride across the liquid film in cation and anion beds, respectively, because of the restraint of electroneutrality in the film. Therefore, mass transfer rates of both ions become slow.

This phenomenon accounts for the higher mass transfer coefficients of both cation and anion in mixed bed compared with a single bed. In Table VI, the increase of mass transfer coefficient in a mixed bed is larger for anion than cation. The excess of cation resin in a mixed bed increases hydrogen concentration in bulk solution. In addition, diffusion coefficients of hydrogen and hydroxide are 9.31 and 5.28 $\times 10^{-9}$ m^{2}s^{-1}, respectively (Robinson and Stokes, 1968). Therefore, this fast mobility of hydrogen in solution makes neutralization in a film on anion resin fast. This explains the larger increase of mass transfer coefficients of chloride in the mixed bed compared with sodium.

The mass transfer coefficients of anions were always higher than those of cations in the specific operating conditions. In addition to the effect of the shift of the neutralization reaction plane and effective diffusivities of sodium and chloride explained previously, this trend can be explained by ionic diffusion coefficients and selectivities which show the relative affinity of a certain resin between counter ions in solution and the resin phase. The diffusivities of chloride and sodium at 25 °C are 2.03 and 1.33$\times 10^{-9}$ m^{2}s^{-1} (Robinson and Stokes, 1968), and the selectivity of anion resin for chloride with respect to hydroxide is much higher than that of cation resin for sodium with respect to hydrogen (Table III). Therefore, chloride is consumed fast on resin surface compared with sodium. It affects anion exchange rate, so chloride mass transfer coefficients are generally higher than sodium.

Mixed Bed Experiments

Figures 5 and 6 show mass transfer coefficient data for new Monosphere resins, and Figures 7 and 8 present data for new HGR-W2-H and SBR-P-C-OH resins. The effects of influent concentration and flow rate on mass transfer coefficient were similar to those in a single bed. The mass transfer coefficients of anion resin were higher than those of cation resin. This phenomenon is accounted for with pH in the bed, in addition to the effects of the difference of ionic diffusivities, the position of the neutralization reaction plane and the effective diffusivities as in the previous section.

Mass Transfer Coefficients of Used Resins

The mass transfer coefficients of used resins were calculated from data obtained by experiments using the same operating conditions as those in new mixed bed experiments. Table VII shows the actual operating conditions in the plant where used resins were sampled.

Figures 9 through 11 show the mass transfer coefficients for sodium and Figures 12 through 14 for chloride in the new and used Monosphere resins at different flow rates. Figures 15 through 18 and 19 through 22 show the mass transfer coefficients for sodium and chloride at different flow rates for used resin. Figures 23 and 24 show the mass transfer coefficients for new and used HGR-W2-H and SBR-P-C-OH resins, respectively. The mass transfer coefficients in the used resin were smaller than those in the new resin at every flow rate. In the case of anion exchange, the mass transfer coefficients of the anion resins sampled from Riverside PSO Number 1 and 2 condensate polishers (C.P.) were smaller than those from Northeastern Stations Number 3 and 4 C.P. in Figures 12 through 14. This means that the anion resins from the Riverside plant are deteriorated more

TABLE VII

OPERATING CONDITIONS OF A CONDENSATE POLISHER AT TULSA
RIVERSIDE AND NORTHEASTERN PLANTS

Number of Unit	2
Number of Bed per Unit	4
Bed Depth	
Actual, ft	8.24
Resin Packed, ft	4.12
Bed Diameter, ft	6.0
Working Pressure, psig	500
Flow Rate per Bed, GPM	500 - 1300
pH of Feed Solution	9.1 - 9.3
Resin	
Cation	Dowex Monosphere 650C-H
Anion	Dowex Monosphere 550A-OH
Fraction of Cation Resin	0.667
Maximum Design Temperature, °F	140
Regeneration Period, day	21
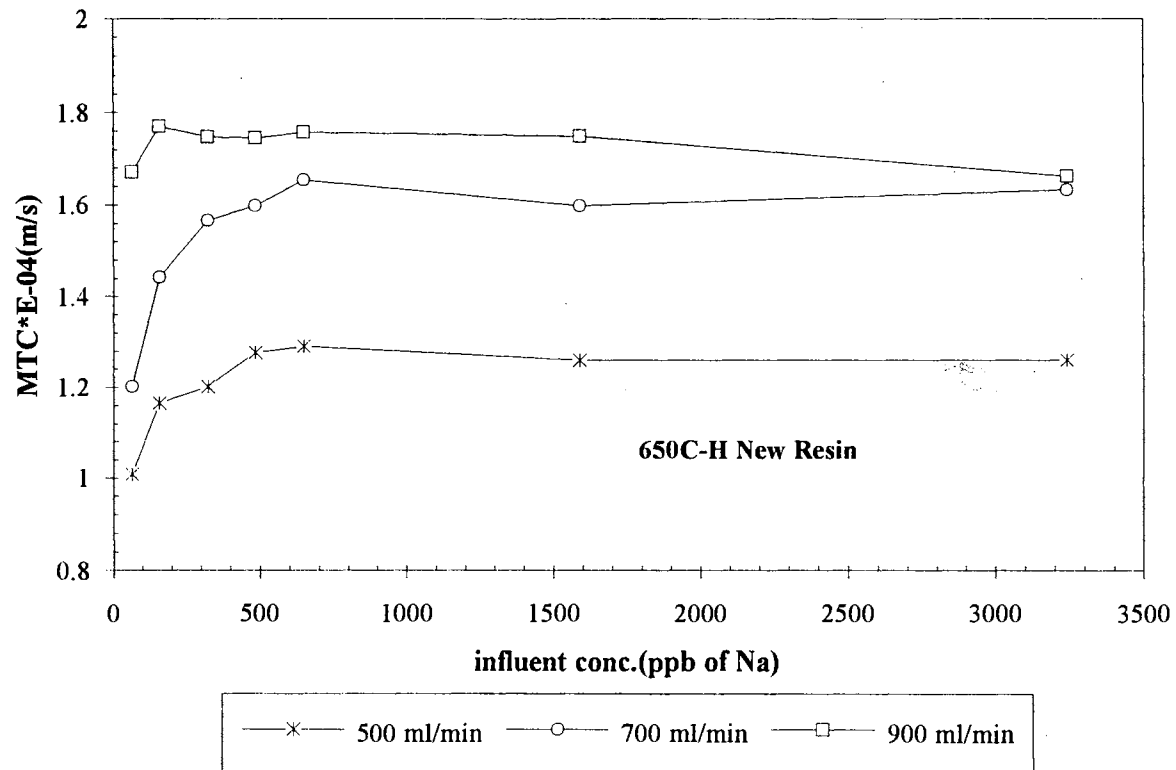
Figure 5. Mass Transfer Coefficients of Sodium in Mixed Beds of New
Monosphere Resin
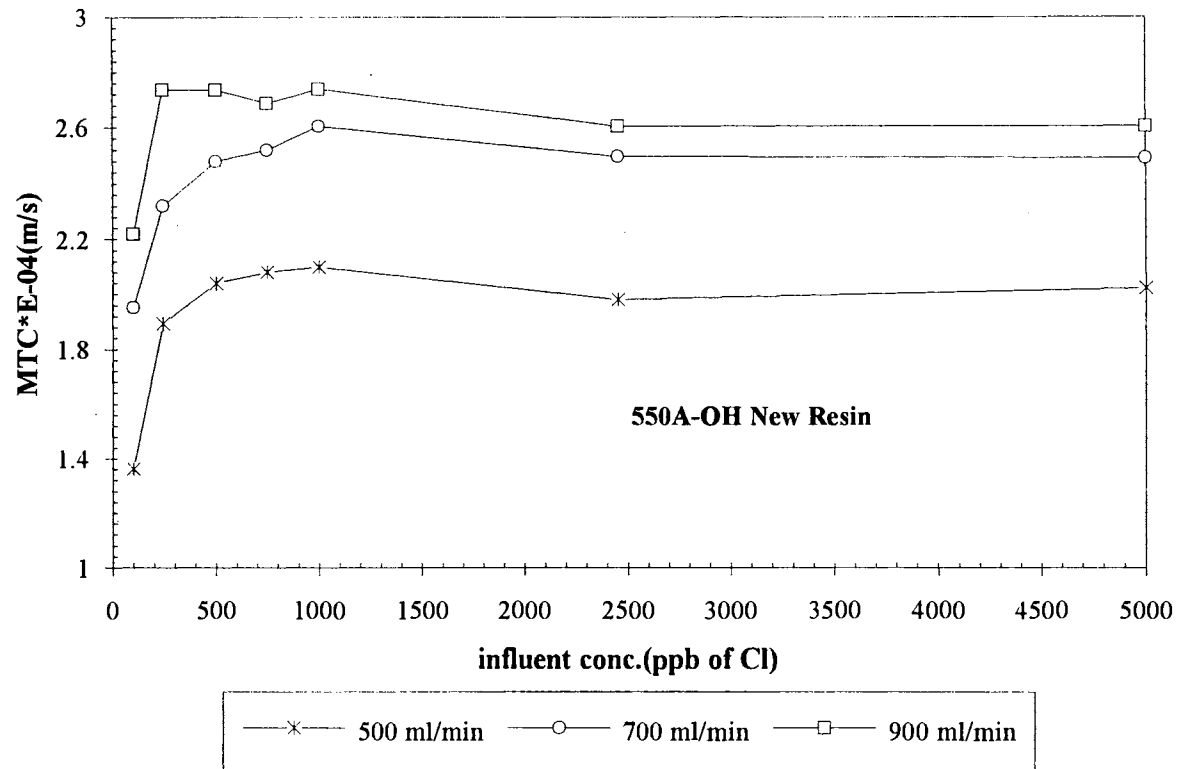
Figure 6. Mass Transfer Coefficients of Chloride in Mixed Beds of New
Monosphere Resin
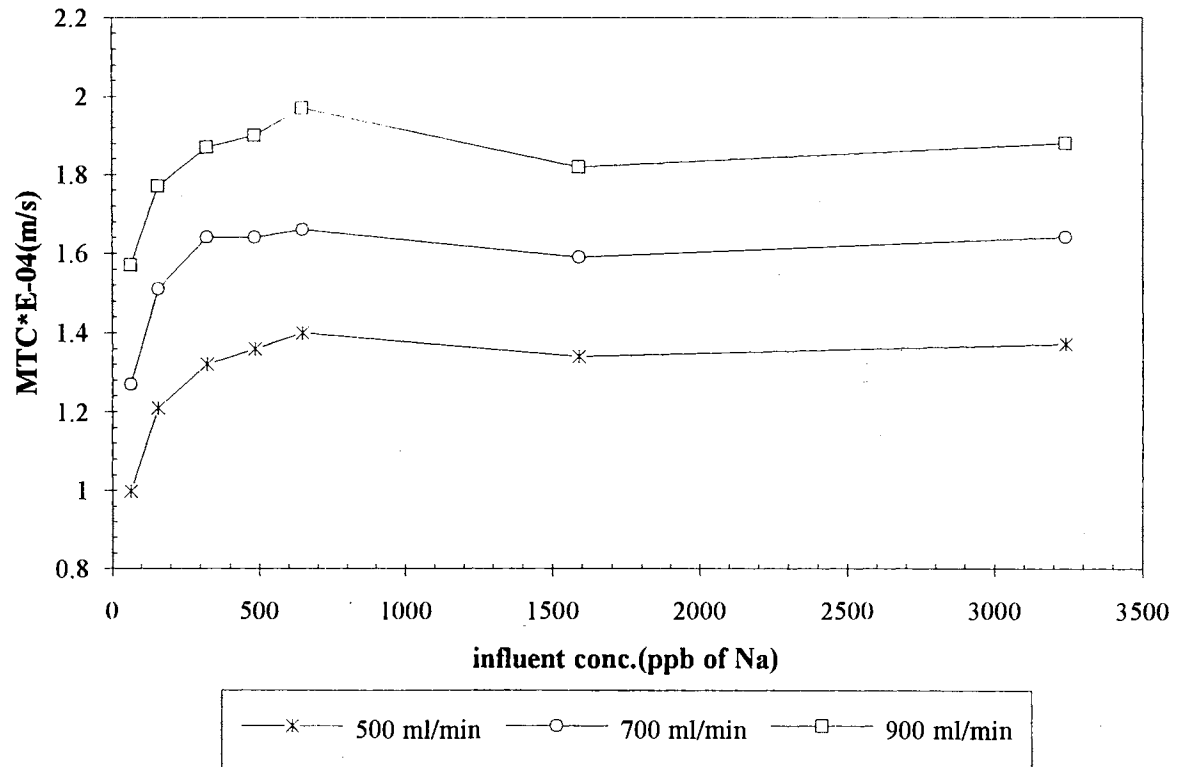
Figure 7. Mass Transfer Coefficients of Sodium in Mixed Beds of New
HGR-W2-H and SBR-P-C-OH Resin
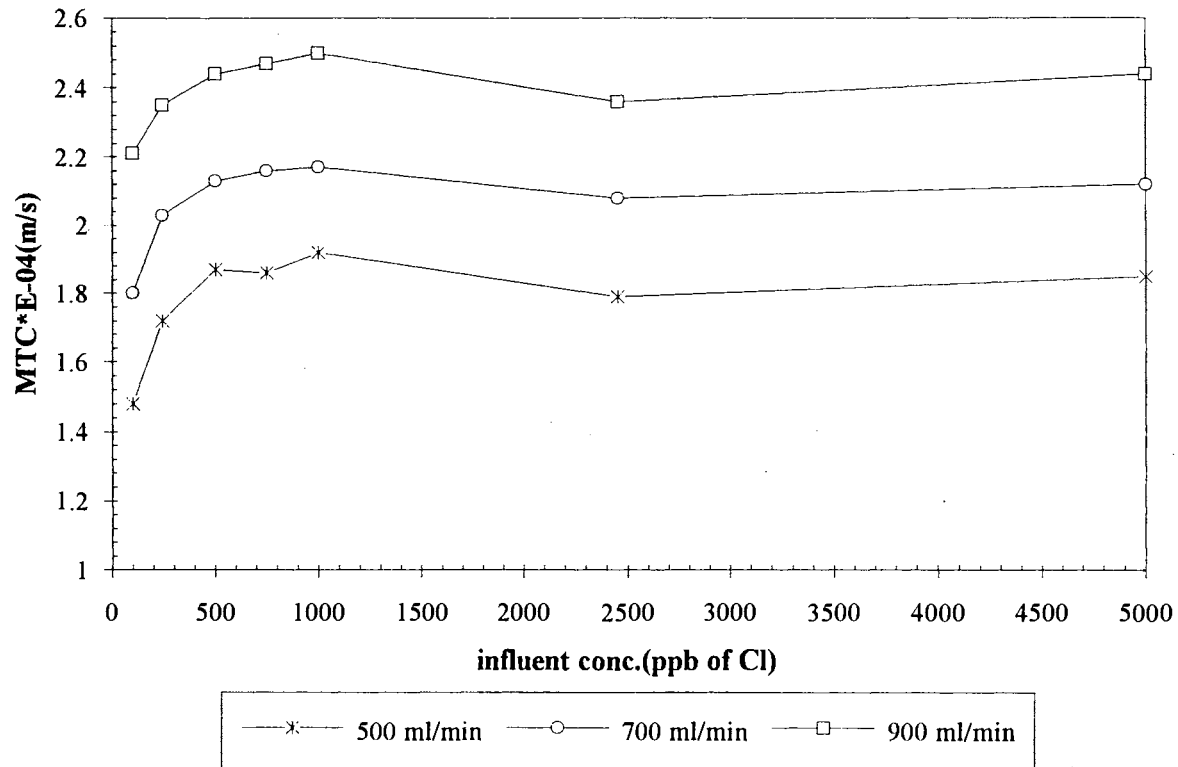
Figure 8. Mass Transfer Coefficients of Chloride in Mixed Beds of New
HGR-W2-H and SBR-P-C-OH Resin
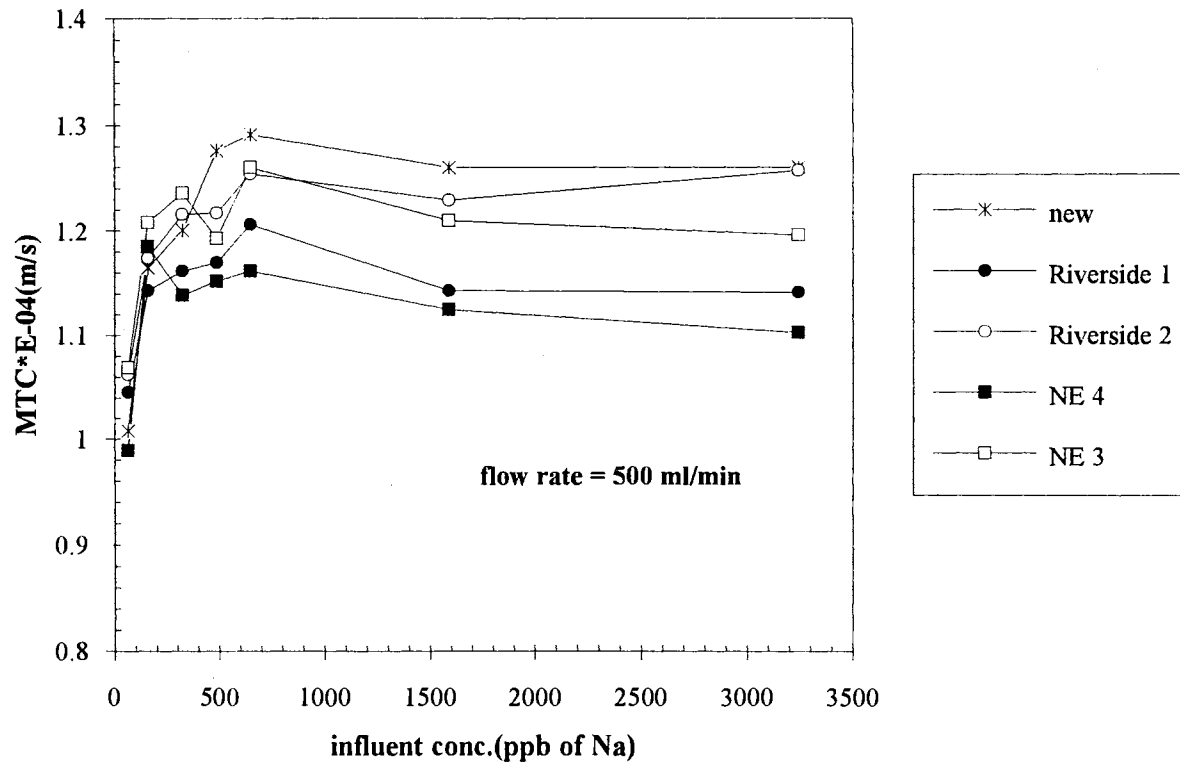
Figure 9. Mass Transfer Coefficients of Sodium in Mixed Beds of New and
Used Monosphere Resins at 500 ml/min
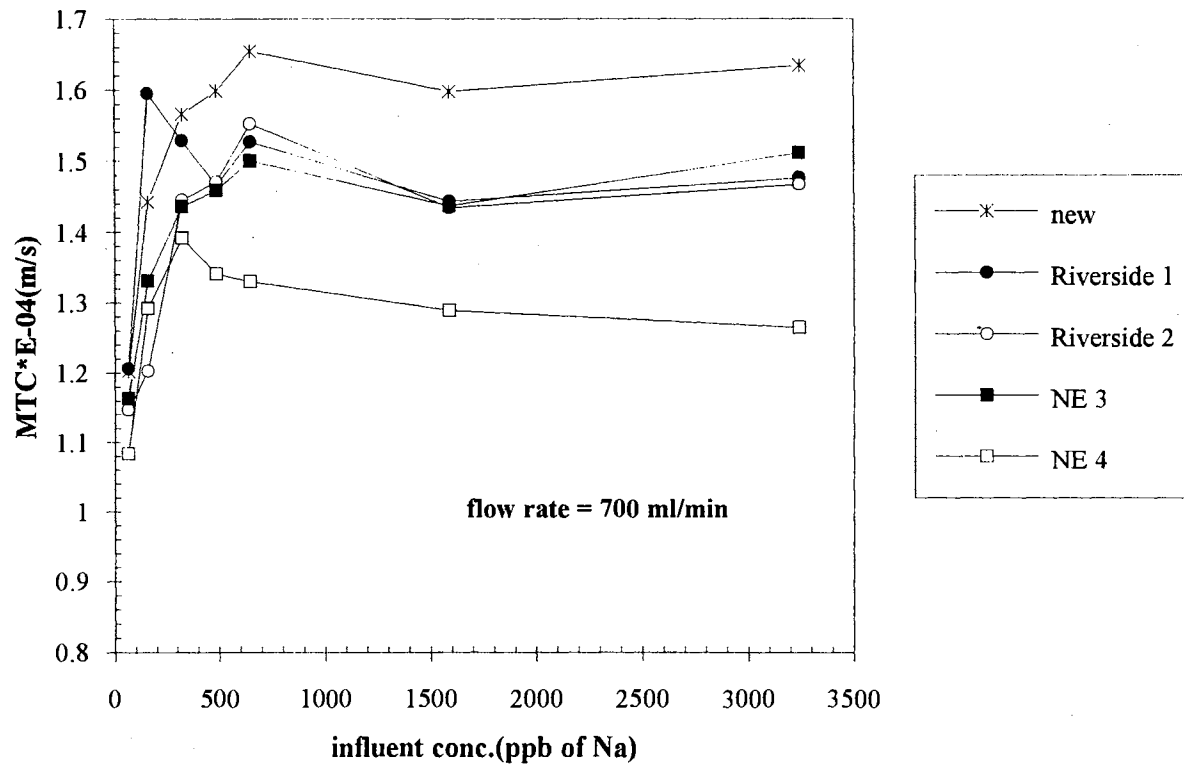
Figure 10. Mass Transfer Coefficients of Sodium in Mixed Beds of New
and Used Monosphere Resins at 700 ml/min
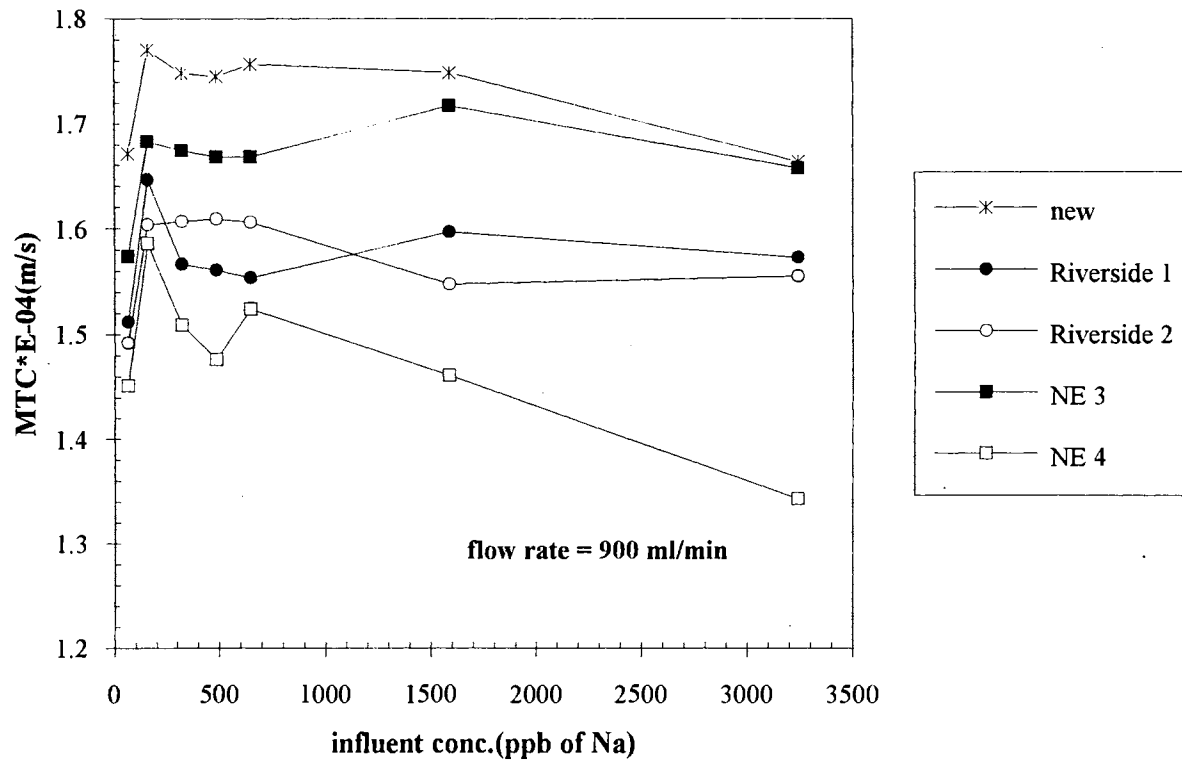
Figure 11. Mass Transfer Coefficients of Sodium in Mixed Beds of New
and Used Monosphere Resins at 900 ml/min
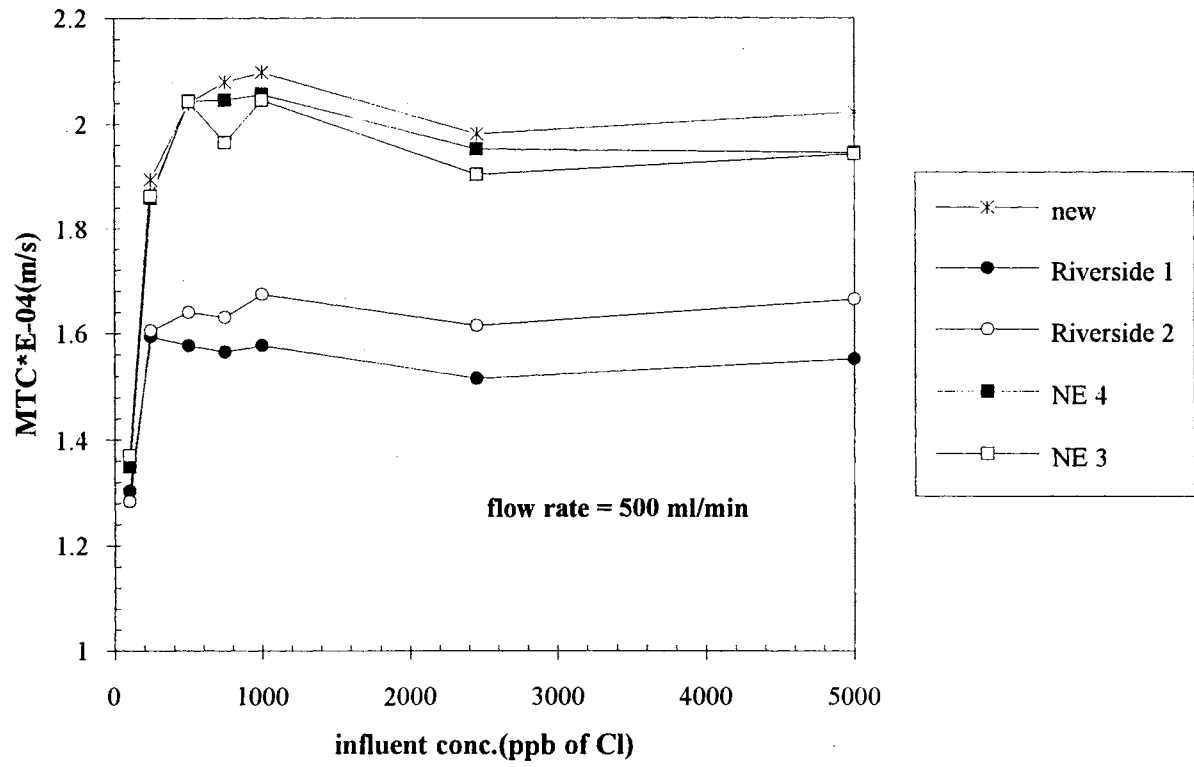
Figure 12. Mass Transfer Coefficients of Chloride in Mixed Beds of New
and Used Monosphere Resins at 500 ml/min
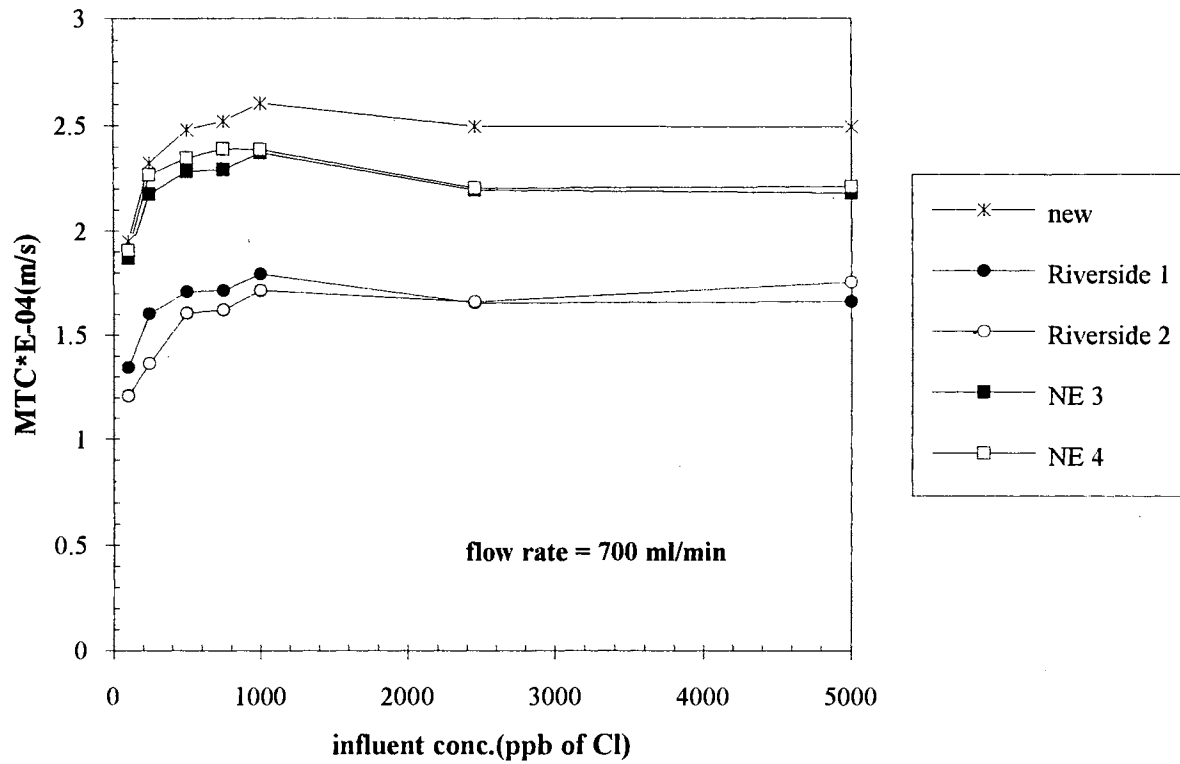
Figure 13. Mass Transfer Coefficients of Chloride in Mixed Beds of New
and Used Monosphere Resins at 700 ml/min
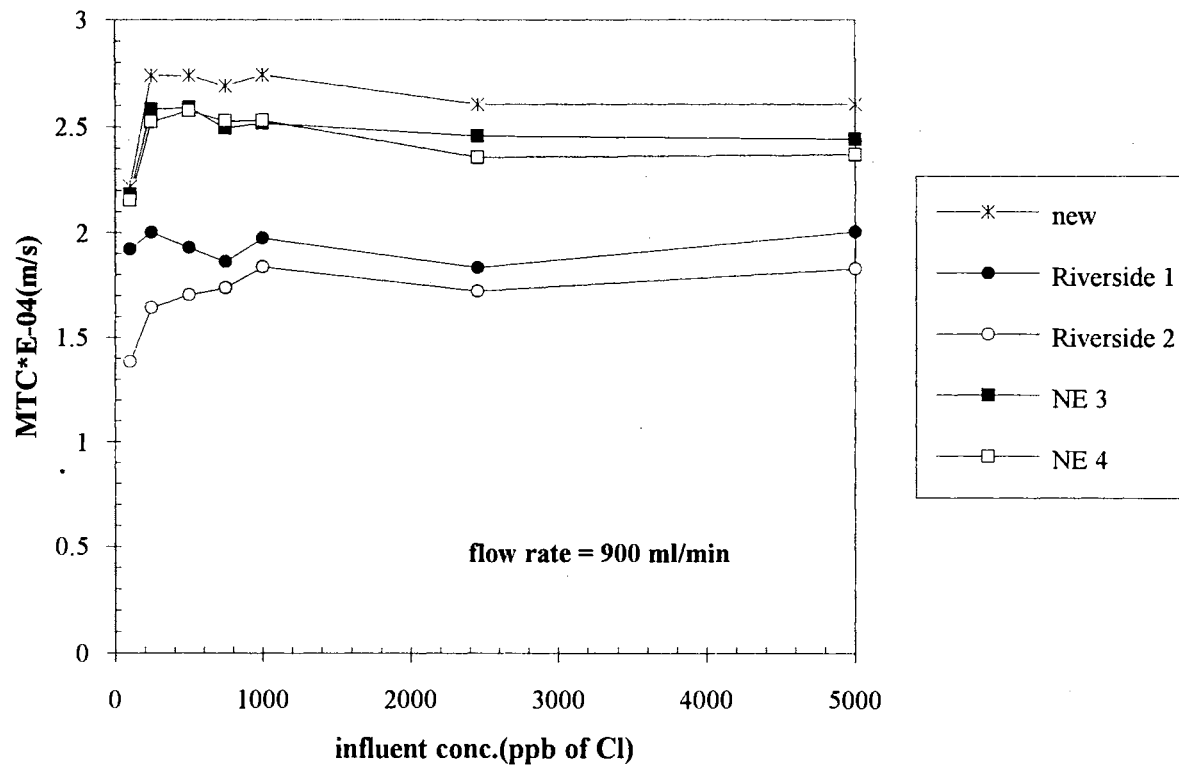
Figure 14. Mass Transfer Coefficients of Chloride in Mixed Beds of New
and Used Monosphere Resins at 900 ml/min
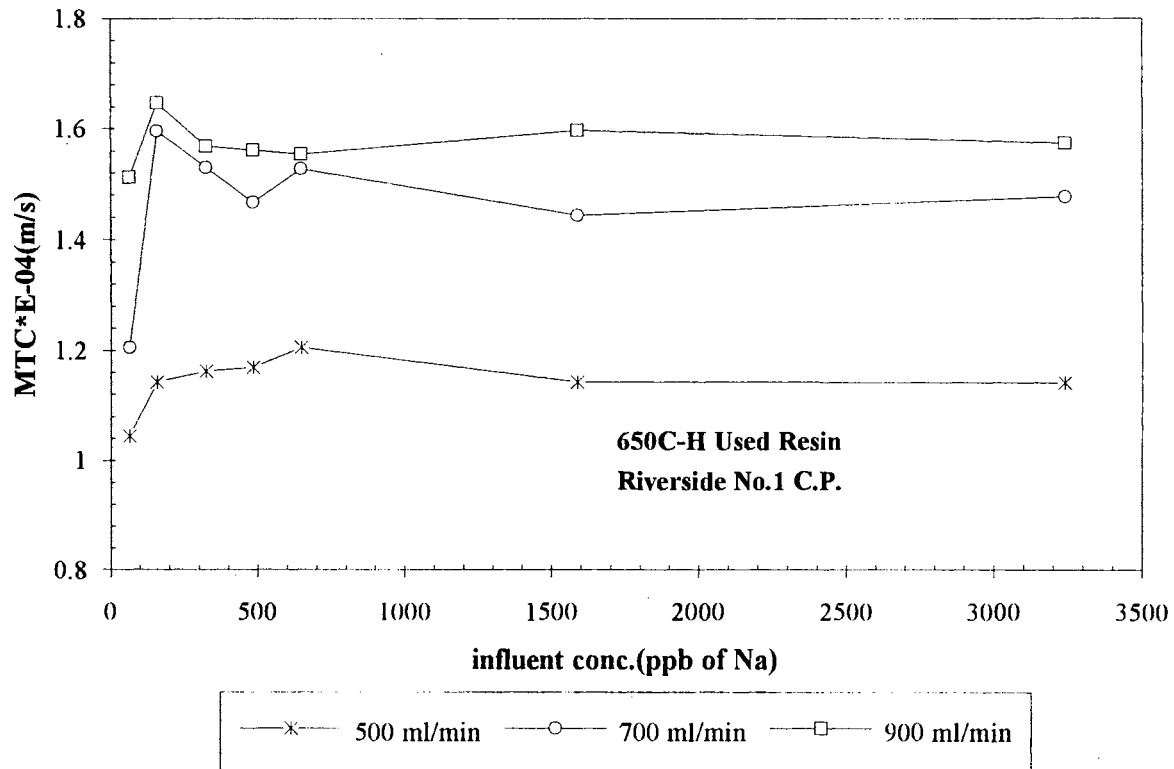
Figure 15. Mass Transfer Coefficients of Sodium in Mixed Bed of Used
Monosphere Resins from Riverside Number 1 Condensate
Polisher
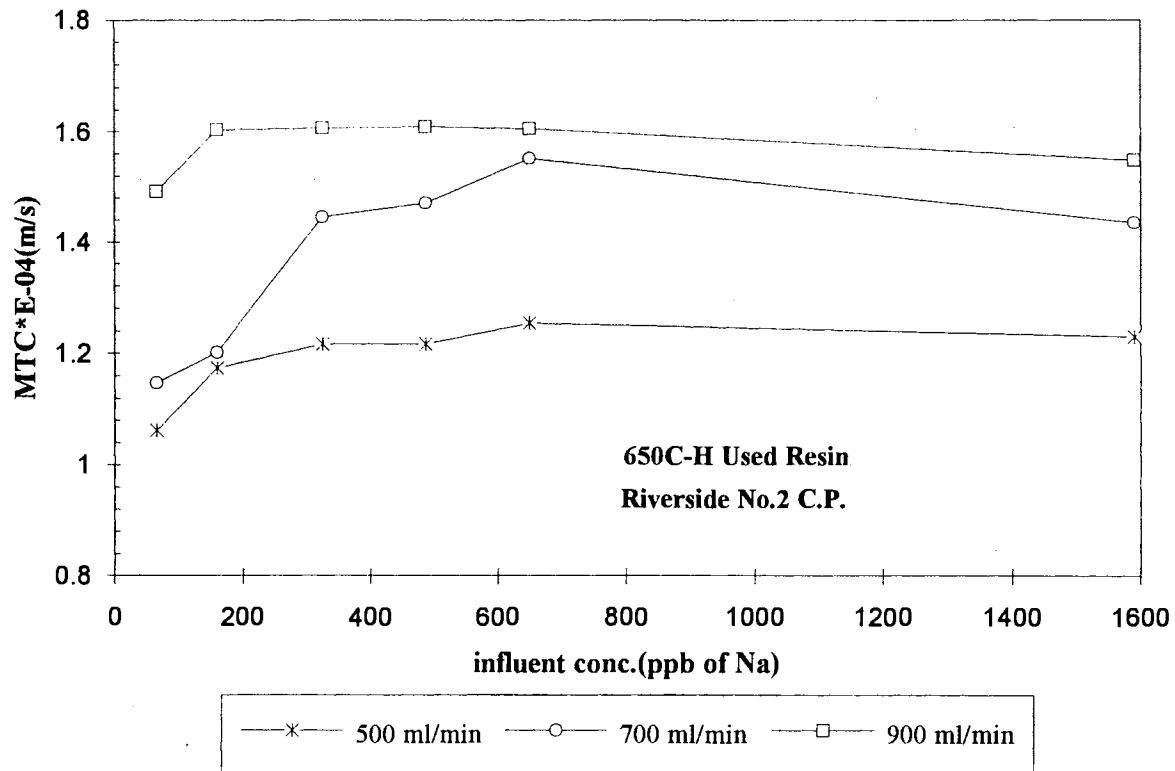
Figure 16. Mass Transfer Coefficients of Sodium in Mixed Bed of Used Monosphere Resins from Riverside Number 2 Condensate Polisher

MTC*E-04(m/s)

1.8

1.6

1.4

1.2

. 1

0.8

0   500   1000   1500   2000   2500   3000   3500

650C-H Used Resin

Northeastern Station No.3 C.P.

influent conc.(ppb of Na)

—✻— 500 ml/min   —○— 700 ml/min   —□— 900 ml/min
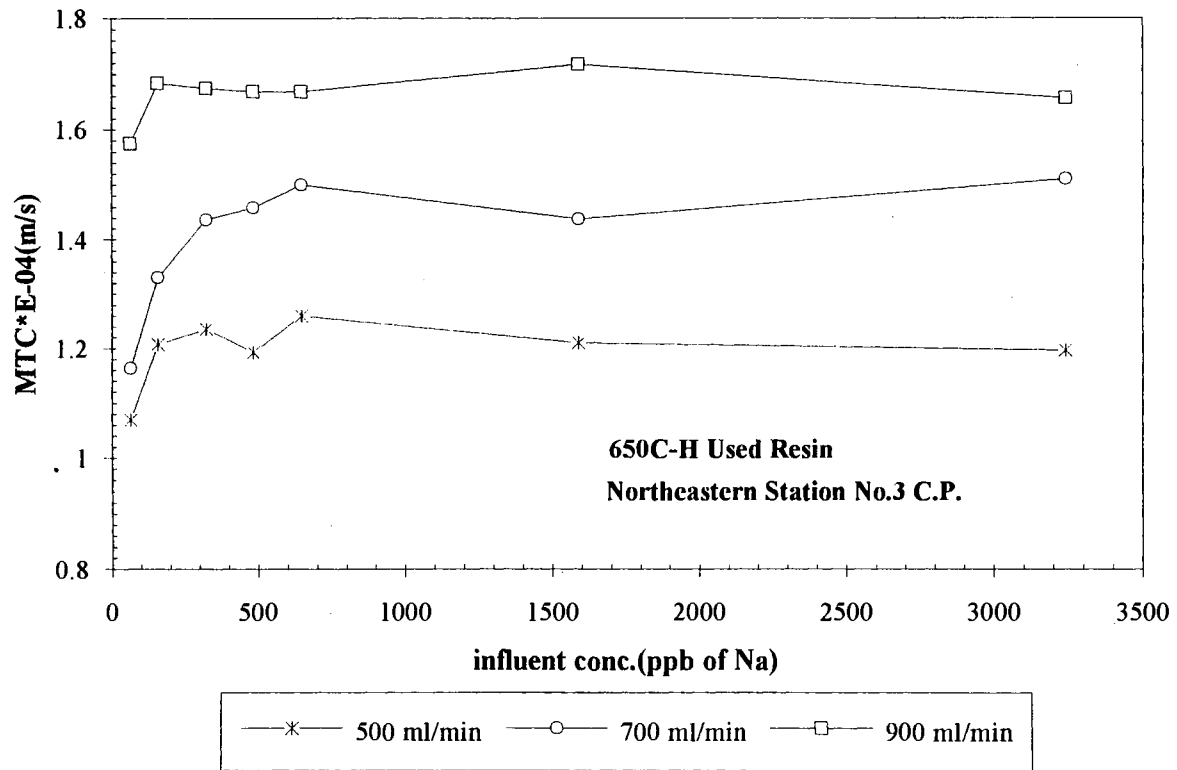
Figure 17. Mass Transfer Coefficients of Sodium in Mixed Bed of Used
Monosphere Resins from Northeastern Station Number 3
Condensate Polisher
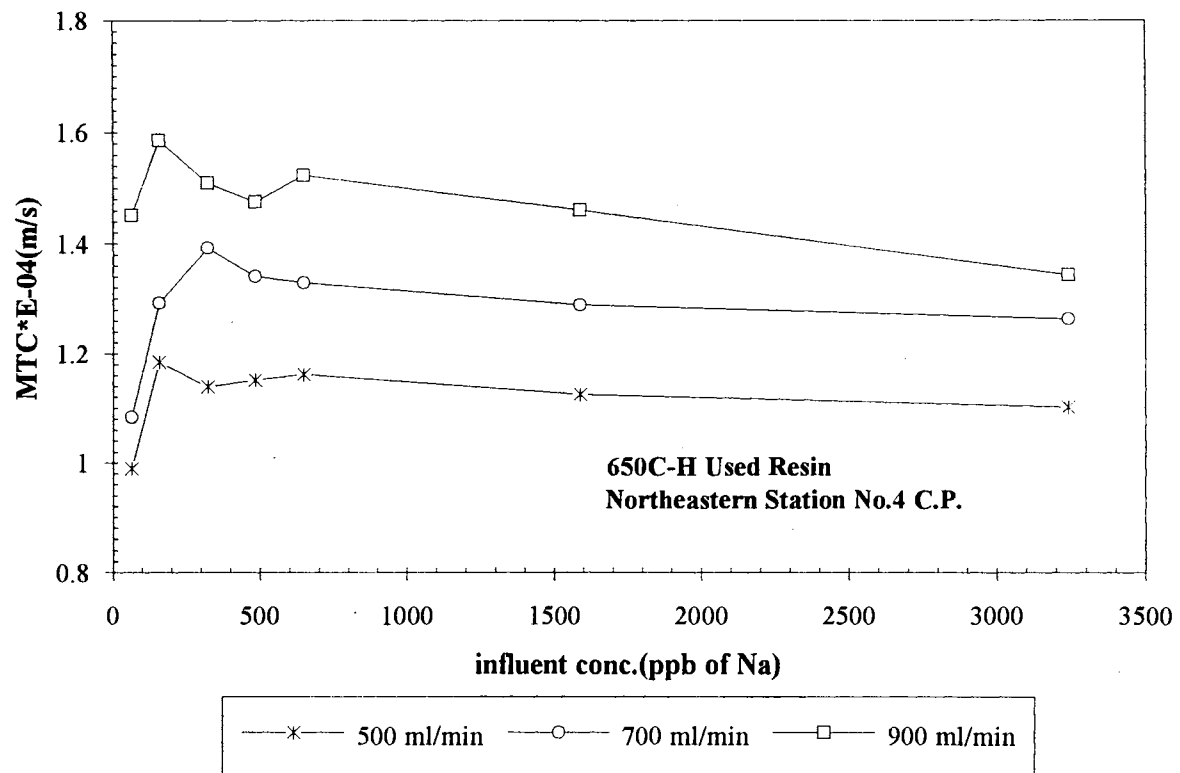
Figure 18. Mass Transfer Coefficients of Sodium in Mixed Bed of Used Monosphere Resins from Northeastern Station Number 4 Condensate Polisher
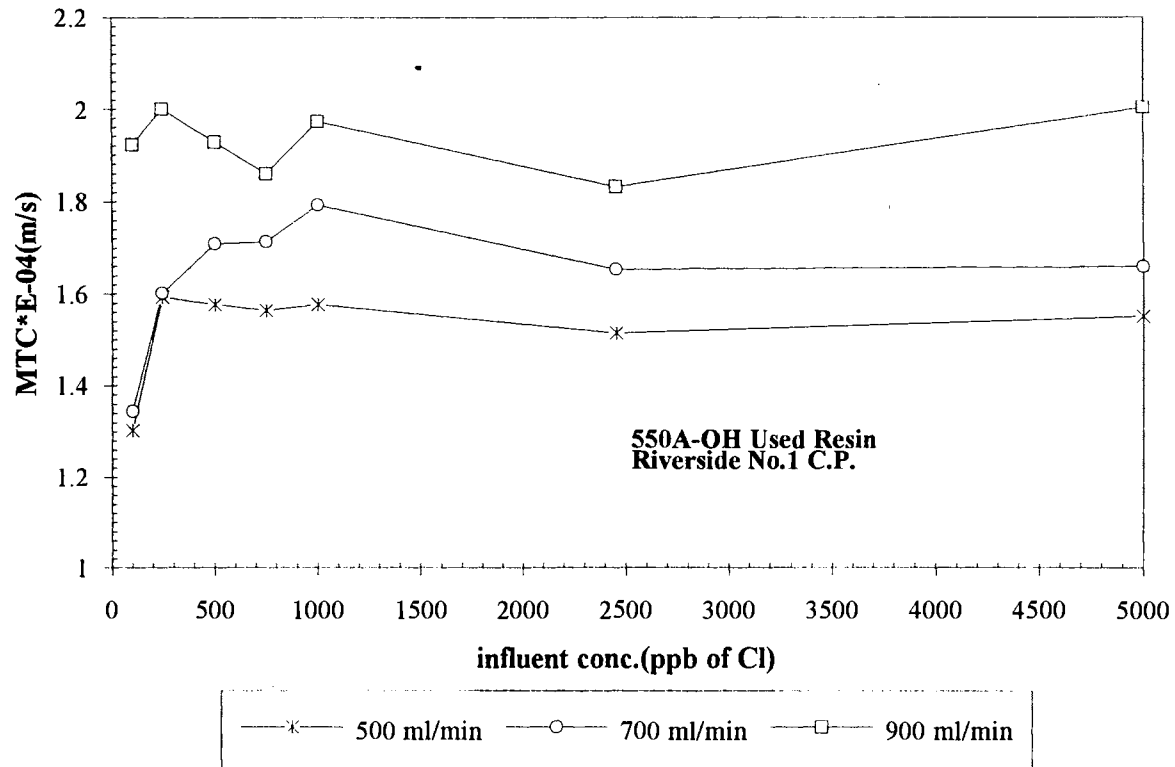
Figure 19. Mass Transfer Coefficients of Chloride in Mixed Bed of Used
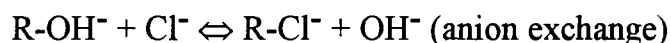Monosphere Resins from Riverside Number 1 Condensate
Polisher
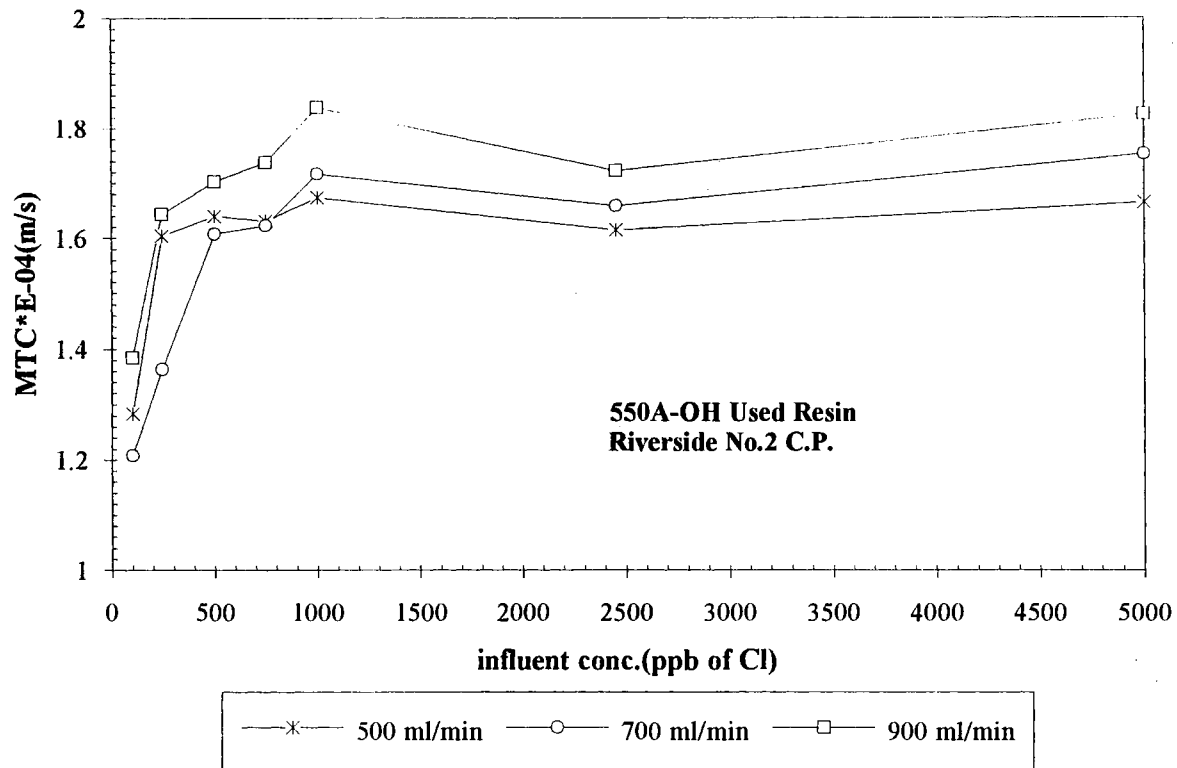
Figure 20. Mass Transfer Coefficients of Chloride in Mixed Bed of Used
Monosphere Resins from Riverside Number 2 Condensate
Polisher
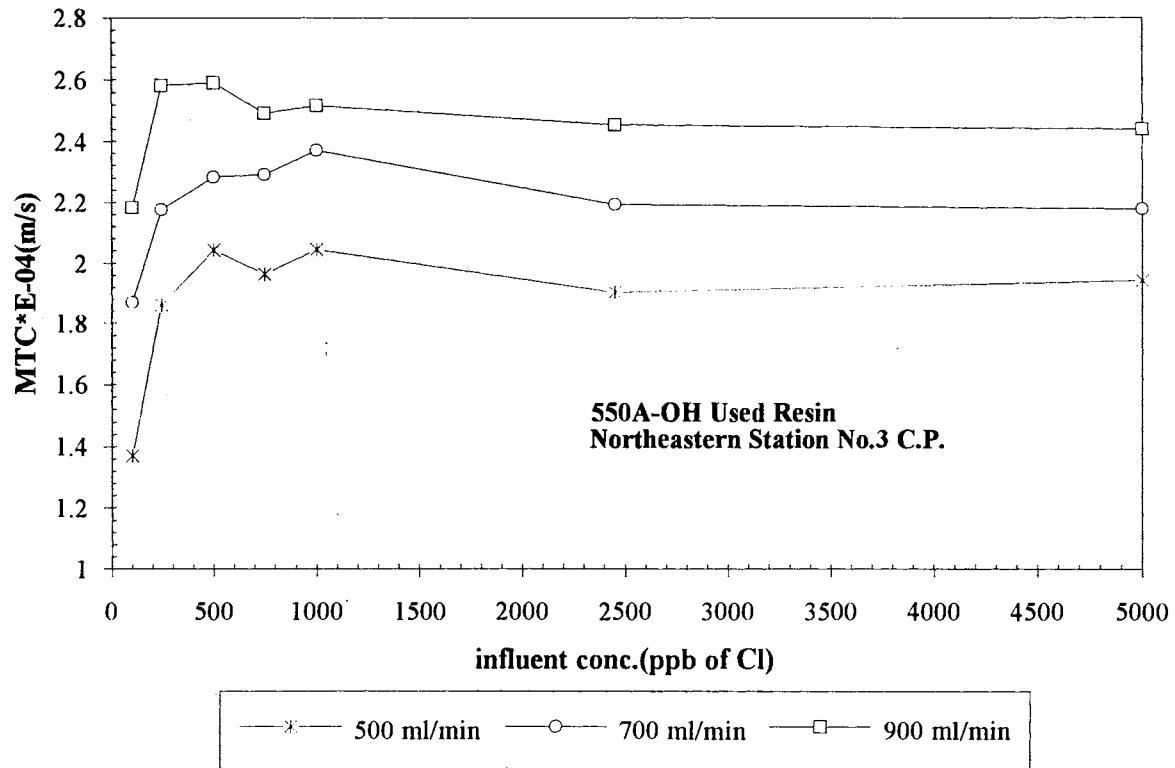
Figure 21. Mass Transfer Coefficients of Chloride in Mixed Bed of Used
Monosphere Resins from Northeastern Station Number 3
Condensate Polisher
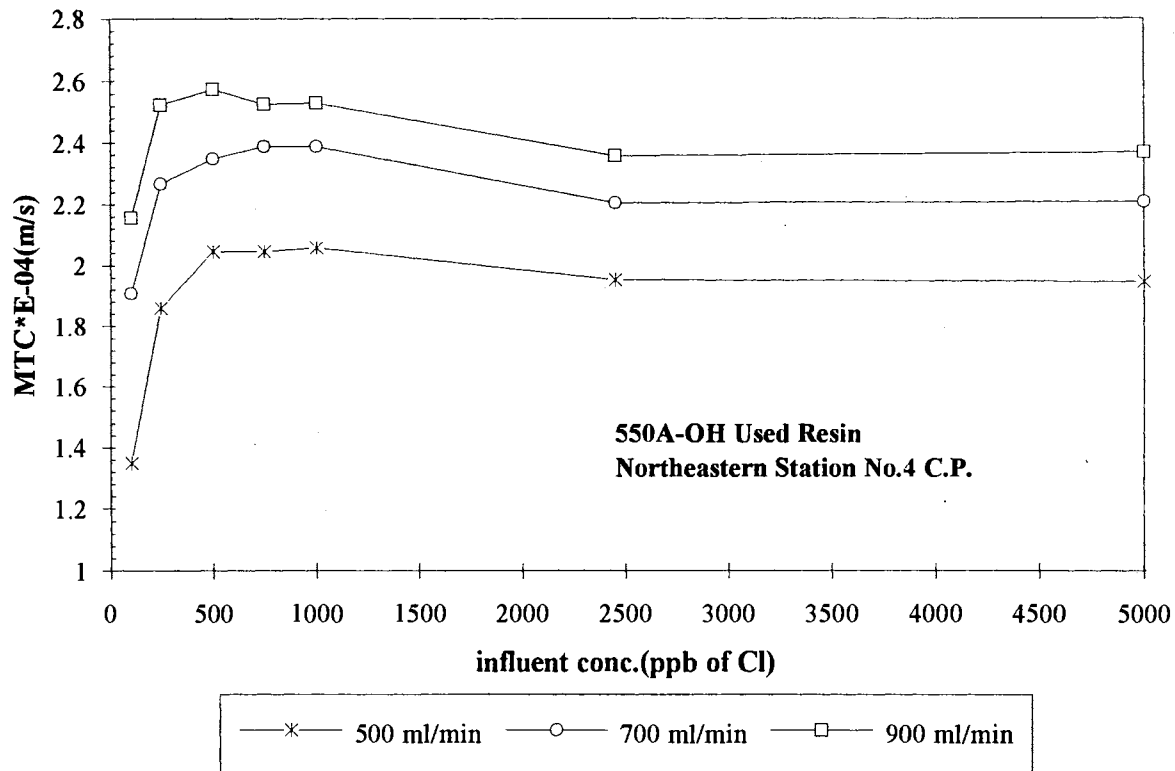
Figure 22. Mass Transfer Coefficients of Chloride in Mixed Bed of Used
Monosphere Resins from Northeastern Station Number 4
Condensate Polisher
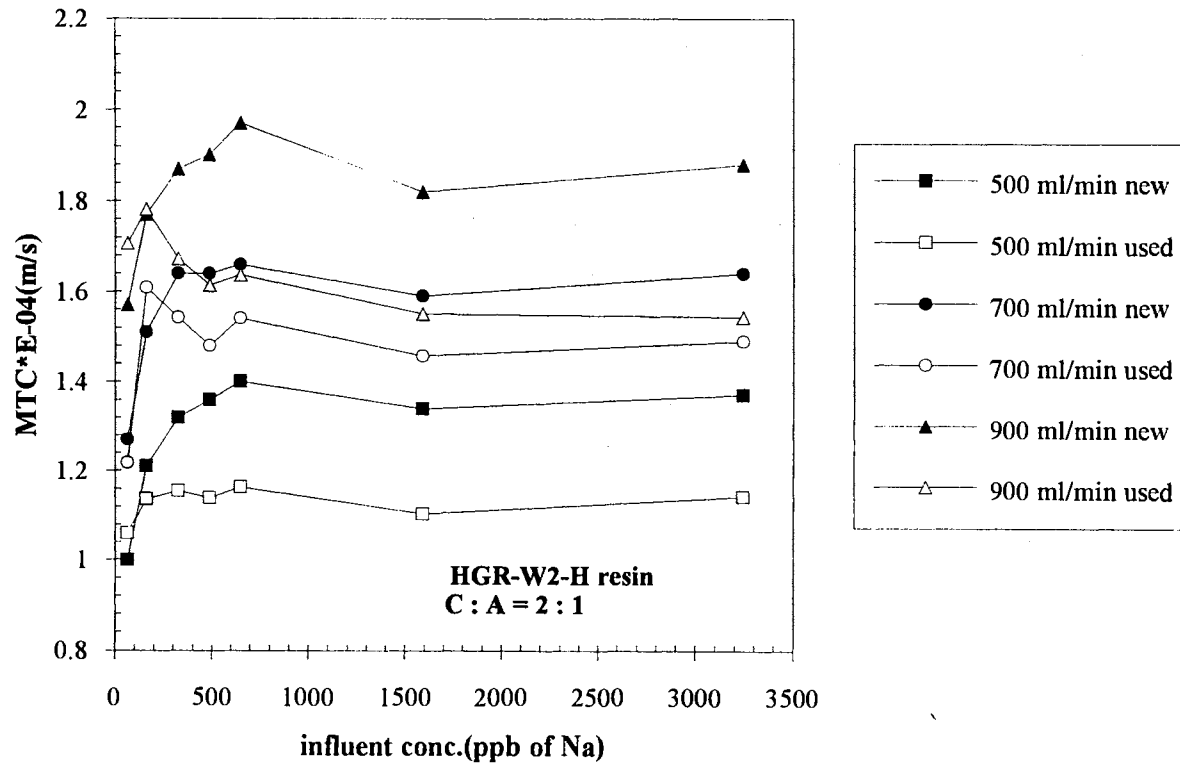
Figure 23. Mass Transfer Coefficients of Sodium in Mixed Beds of New
and Used Resins (HGR-W2-H and SBR-P-C-OH)
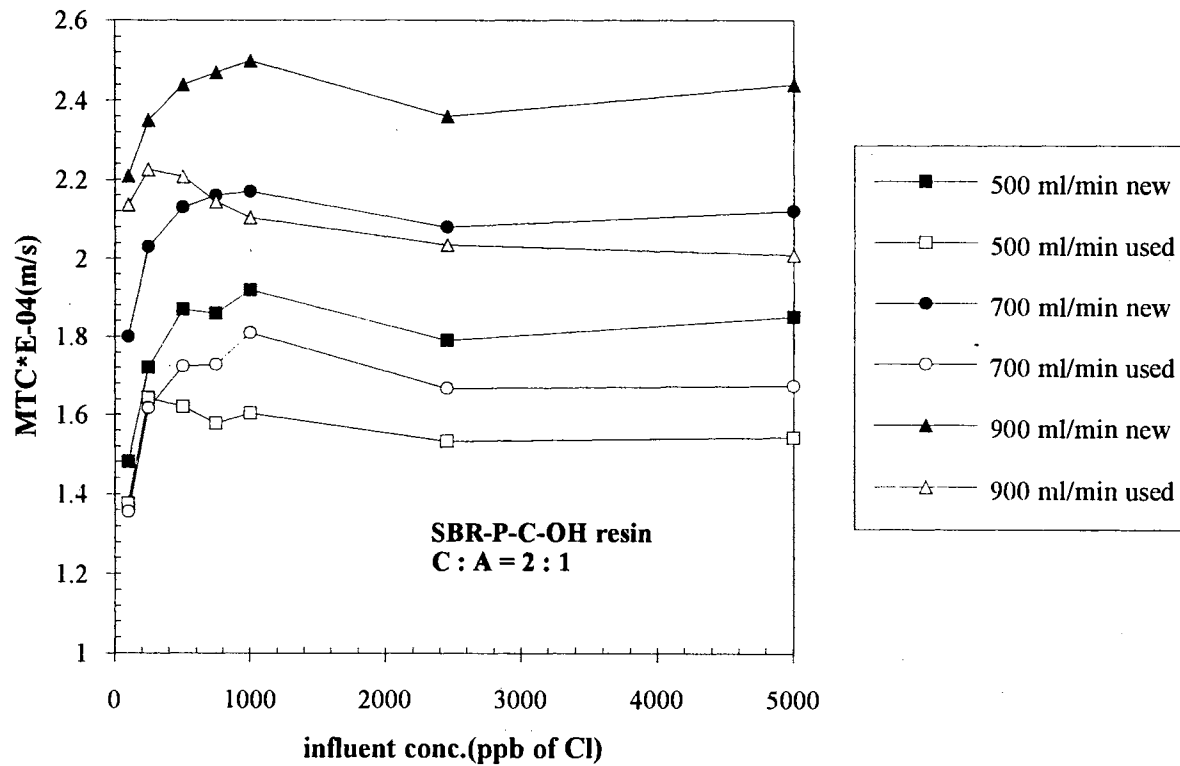
Figure 24. Mass Transfer Coefficients of Chloride in Mixed Beds of New
and Used Resins (HGR-W2-H and SBR-P-C-OH)

significantly than other used resins. In Table II, the used resin from Riverside No. 1 C.P. is actually the oldest, and the ages of others are not much different. Therefore, the mass transfer coefficient of the resin from Riverside Number 1 C.P. should be lowest theoretically for both anion and cation at the same operating conditions, based on the resin age. There, however, is not much difference between the mass transfer coefficients of the anion resins from Riverside Number 1 and 2. For cation resin, the used resin from Northeastern Station Number 4 C.P. showed smaller mass transfer coefficients than from Riverside Number 1 C.P. From this result, the cation resin from Northeastern Number 4 C.P. is deteriorated more than other used resins. Therefore, this phenomenon could not be simply explained by the resin age without the information of the fouling and the characteristics of feed solution, and it is also considered that there are other effects on resin kinetics like resin breakage during the resin separation of mixed bed for regeneration and deactivation of active sites in resins.

As in new resins, mass transfer coefficients of the used resins depended on influent concentration below 245 ppb for chloride and 159 ppb for sodium. This trend coincided with Harries and Ray's results (1984) for fouled resins. They showed that mass transfer coefficients of chloride decreased as the influent concentration is decreased for the range from 500 to 100 ppb chloride. However, the mass transfer coefficients did not depend on influent concentration above this range.

The differences of mass transfer coefficients among the used resins indicates the degree of deterioration from new resin. The kinetic deterioration of anion resin is the general phenomenon for an aged resin in a mixed bed, but that of cation resin is not common compared with anion resin. The deterioration of anion resins, which is observed by chloride or sulphate leakage, has been known due to the existence of organic foulants in feed solution and other reasons like the

deactivation of exchange sites on resin. Some foulants in anion resin are humic and fulvic acids, the degradation products of cation resins like short chain aromatic sulphonates and the manufacturing residues from cation resins like sulphonated polystyrene (Harries, 1986). McNulty et al. (1986) pointed out thermal degradation of strong base capacity and coating of the resin surface by dense iron oxide films as the reasons of the normal deterioration of anion resin. The poor kinetics of cation exchange is observed by sodium or ammonium leakage and caused by residual polymeric material like oligomeric species eluted from the anion resin (Harries, 1991). The foulants form a physical barrier on the resin surface because they cannot diffuse into the resin due to their large molecular size, inhibit the penetration of counter ions into the resin, and interrupt the exchange sites (Tittle, 1981; Harries, 1984). The effect of interruption of the sites to the exchange kinetics is more severe for multivalent ions than monovalent, because multivalent ions need at least two neighboring exchange sites at the same time. Harries (1987) verified this effect for sulphate exchange kinetics experimentally. This phenomenon cannot be accounted for by film diffusion mechanism that the reaction rate and the particle diffusion rate are very fast in comparison with the film diffusion rate. Therefore, the exchange kinetics in the used resins is no longer controlled by film diffusion only, but by the combination of film and particle diffusion or only by particle diffusion because the chemical reaction offers negligible resistance to exchange.

Resin type

Harries (1984, 1987) observed that the mass transfer coefficient of the new resin does not depend on polymer/matrix type at a particular flow rate. The mass transfer coefficients of the new resins used in this study, Monosphere and HGR-

W2-H and SBR-P-C-OH resins, indicated the different phenomenon from Harries' (1987) results. Figures 25 and 26 show the difference of mass transfer coefficients of two types of new resins for cation and anion exchange, respectively.

The mass transfer coefficients of new anionic Monosphere resins were generally greater than those of SBR-P-C-OH, and those of new cationic Monosphere resins were smaller than those of HGR-W2-H. Table VIII shows the average values of mass transfer coefficients for both resins at different flow rates and influent concentrations greater than 1000 ppb of anion and 600 ppb of cation and the percentage differences between two resin types. The differences of mass transfer coefficients between two types of resins were more serious in anion exchange at the flow rate of 700 ml/min.

The mass transfer coefficient in Equation (20) is a function of specific surface area of resin, and the specific surface area depends on diameter of a resin. The diameter of Monosphere cation resin is smaller than that of HGR-W2-H, and the diameters of anion resins of both types are almost the same. The specific surface areas of 650C-H and HGR-W2-H resins, which is S in Equation (20), are 6090 and 4950 m^2/m^3. The difference between the specific surface areas of both cation resins leads to the difference in exchange rates. Therefore, the exchange rate of cation in Monosphere resin is a little faster than that in HGR-W2-H. Faster cation exchange rate increases hydrogen concentration in bulk solution, and the anion exchange rate in a Monosphere type mixed bed becomes fast due to film neutralization as discussed previously. It gives the reason why the mass transfer coefficient of anion in a Monosphere type mixed bed is higher than that in another mixed bed.

In the mixed bed of Monosphere resins, the faster increase of hydrogen concentration in bulk solution makes the effective diffusivity of cation to decrease.
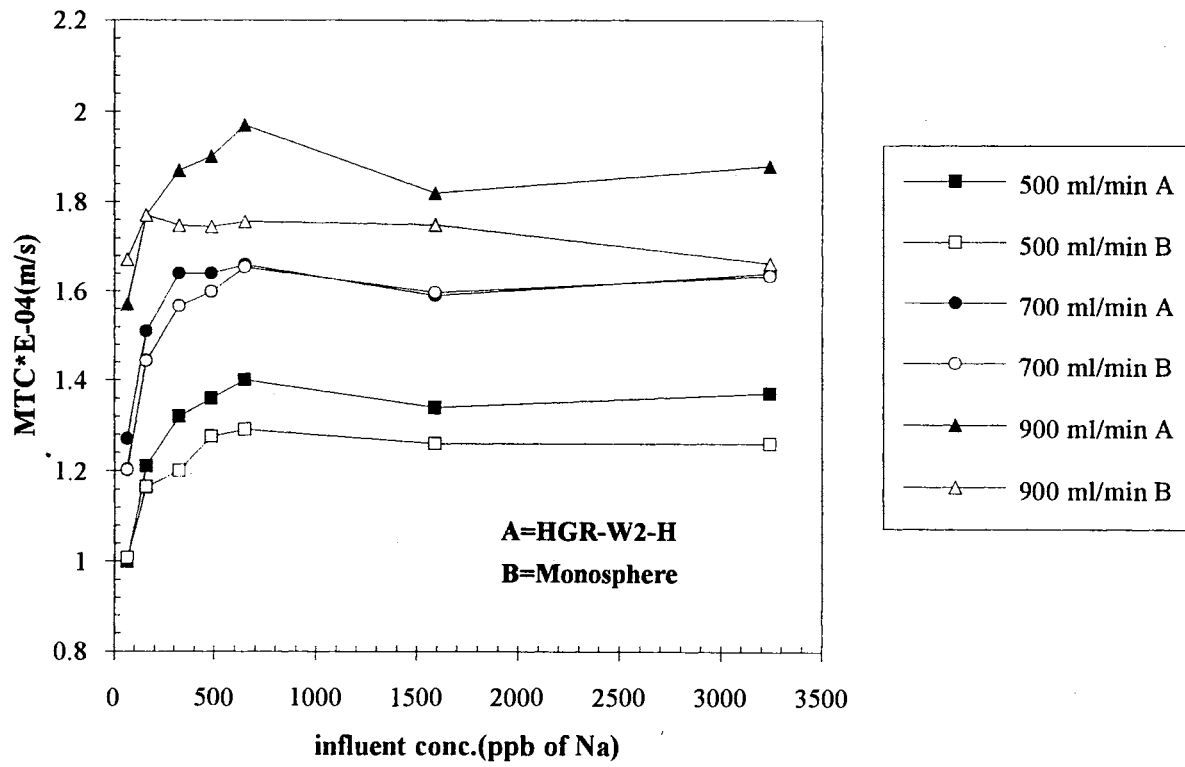
Figure 25. Difference of Mass Transfer Coefficients of HGR-W2-H and
650C-H resin for Sodium in Mixed Bed
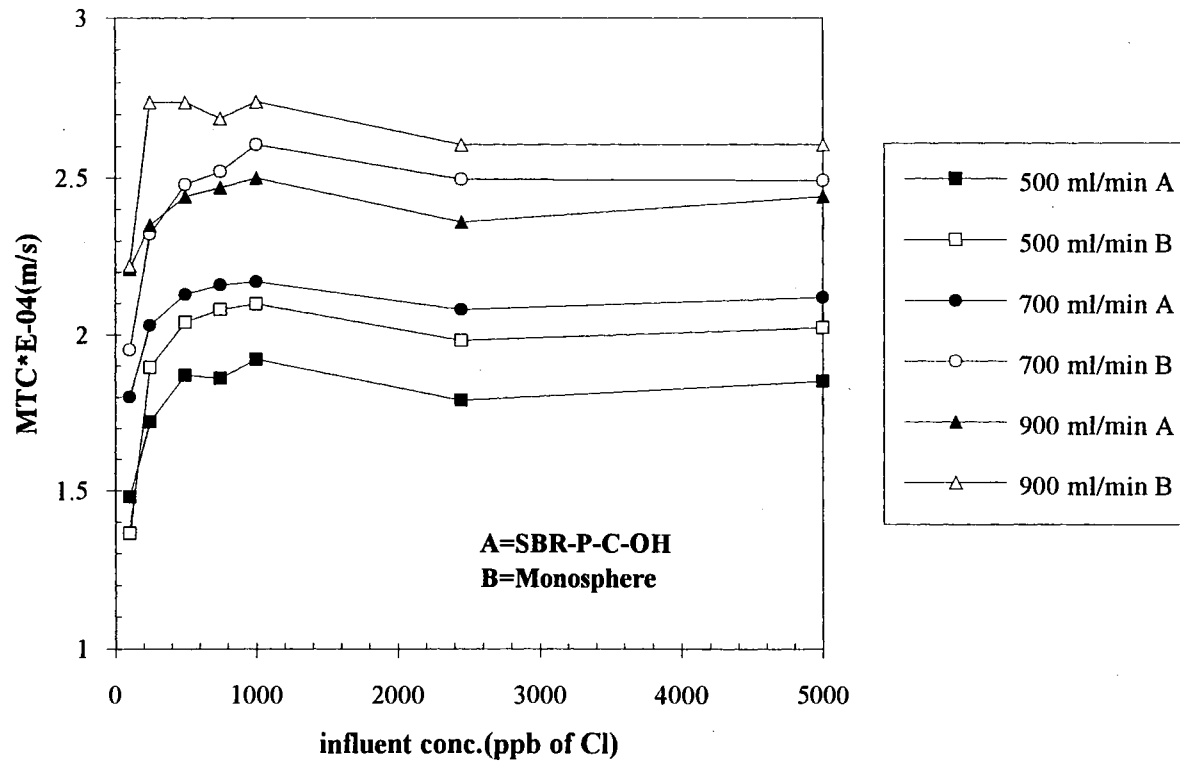
Figure 26. Difference of Mass Transfer Coefficients of SBR-P-C-OH and
550A-OH resin for Chloride in Mixed Bed

Mass transfer coefficients of Monosphere cation resin, therefore, are lower than those of HGR-W2-H resin.

TABLE VIII

THE DIFFERENCES OF AVERAGE MASS TRANSFER COEFFICIENTS BETWEEN TWO TYPES OF NEW RESINS IN MIXED BEDS

flow rate (ml/min)	average MTC of Monosphere resins $(\times 10^{-4}$ m/s)		average MTC of HGR-W2-H and SBR-P-C-OH resins $(\times 10^{-4}$ m/s)		% differences (of MTC of Monosphere resins from MTC HGR-W2-H and SBR-P-C-OH resins)	
	cation	anion	cation	anion	cation	anion
500	1.270	2.034	1.370	1.853	-7.3	9.8
700	1.629	2.531	1.630	2.123	-0.1	19.2
900	1.723	2.650	1.890	2.433	-8.8	8.9

The ratio of cation and anion

The ratio of cation and anion resins, R_i in Equation (20), affects the mass transfer coefficient. This results from the fact that the mass transfer coefficient depends on pH of the solution inside a bed and the pH of solution is affected by the resin ratio. If the fraction of anion resin in a mixed bed increases, pH of solution inside the bed will approach neutrality. If the fraction is over 0.5, the exchange will occur in basic solution because of faster anion exchange rate resulted from the excess of anion resin. The mass transfer coefficient of anion will decrease and that of cation will increase, as the fraction of anion resin increases. In addition, the increase of anion resin fraction arises from the reduction of the total capacity of cation resin. The reduction makes the regeneration period short.

Harries (1987) verified this phenomenon for anion exchange kinetics experimentally.

Yoon (1990) carried out the experiment for the effect of various ratios of cation to anion resin to breakthrough curves. He indicated that the breakthrough curve is affected by selectivity, bed depth and the ratio of both resins. His experimental breakthrough curves showed that the increase of the fraction of anion resin reduces the exchange zone of sodium and increase that of chloride. The reduction of sodium exchange zone accounts for the increase of sodium mass transfer coefficient. However, breakthrough time for chloride was increased and decreased for sodium. For design purpose, the benefit from the reduction of the sodium exchange zone must be balanced with the decrease of sodium breakthrough time.

Conclusions

The experimental results of mass transfer coefficient elucidated the following conclusions in this study:

1. The errors in mass transfer coefficients result from the uncertainties of experimental measurements. The maximum and minimum relative errors in mass transfer coefficient measurements were obtained by combining maximum and minimum uncertainties in experimental measurements of parameters in Harries and Ray's equation, and they were 12.6 and -12.6 %, respectively. However, most errors were between 7 and 9 % (Appendixes D and E).

2. The mass transfer coefficients of both cation and anion for new and used resin were affected by influent concentration and flow rate. As flow rate increased, the mass transfer coefficients increased. For low influent concentration, under 245 ppb of chloride and 159 ppb of sodium, the mass transfer coefficients

increased according to the increase of influent concentration. This trend indicates that the exchange kinetics is controlled by a film diffusion mechanism. For high influent concentration the mass transfer coefficients were near constant.

3. The mass transfer coefficients in single beds were lower than those in mixed beds. It was more significant for anion exchange than for cation exchange. There is no neutralization in a single bed. Therefore, concentration gradients for both hydrogen and hydroxide are lower than in mixed bed. Because of the restraint of electroneutrality in liquid film, this affects diffusion of sodium and chloride across the film in cation and anion beds, respectively. Therefore, mass transfer rates of both ions become slow, and the mass transfer coefficients in single beds are lower than in mixed beds.

4. The mass transfer coefficient of chloride was always higher than that of sodium in a mixed bed. This was explained by effective diffusivities of sodium and chloride for bulk phase neutralization. The excess of cation resin made effective diffusivity of sodium to decrease and that of chloride to increase. The effective diffusivities accounted for exchange rates for both ions and higher mass transfer coefficients of anion than cation.

5. The mass transfer coefficients of both cation and anion in the used resin were lower than those in the new resin. The difference between mass transfer coefficients in used and new resin was accounted for by the effect of foulants on the surface of used resin. Therefore, the diffusion mechanism is explained no longer by film diffusion only, but by the combination of particle and film diffusion or by particle diffusion only.

6. The degree of degradation of used resins was not exactly proportion to resin age. It is considered that the resin degradation results from the combination of various source: resin age, an efficiency of regeneration, a breakage of resin beads during resin separation and mixing, and characteristics of feed water, etc.

7. Two types of resin, Monosphere and another (HGR-W2-H and SBR-P-C-OH) had different mass transfer coefficients of both cation and anion. The diameters of two types of resin used in this study were different. The different specific surface area gives different mass transfer coefficient because the specific surface area affects the mass transfer coefficient in Equation (20).

CHAPTER IV

APPROXIMATION OF PARTICLE MASS TRANSFER COEFFICIENT
AND ESTIMATION OF FILM MASS TRANSFER
COEFFICIENT FROM A MIXED BED ION
EXCHANGE MODEL

Introduction

The mass transfer coefficient model is used to estimate mass transfer kinetics for process design rather than the diffusion model because of its simplicity. While the mass transfer coefficient has been used for film mass transfer kinetics, the diffusion model has been generally utilized for particle mass transfer kinetics (Gopala Rao and Gupta, 1982b). Even if the diffusion model gives an accurate estimate of particle diffusion rate, it can be complex mathematically. A particle diffusion coefficient for gel type exchange resin cannot be calculated theoretically except by curve fitting with experimental data (Bolden et al., 1989). Therefore, the estimation of a particle mass transfer coefficient can be helpful for design purposes and the explanation of mass transfer rates in ion exchange.

In this chapter, the particle mass transfer coefficients for used resin are estimated using a simple series resistance model. The mass transfer coefficients for used resins were lower than those of new resins as in Figures 9 through 14. The exchange kinetics of used resins could not be explained only by a film

diffusion mechanism because the organic foulants or the deterioration of active sites on resin surface can affect the particle diffusion rate. Therefore, the kinetics of used resins must consider both film and particle diffusion mechanisms.

The mass transfer coefficient equation (Equation 20) shows that the coefficient is constant through a bed at a specific operating condition, with the interfacial concentration assumed zero initially. These assumptions are an oversimplification of the exchange phenomena. The concentration of the bulk solution changes continuously through the bed and the interfacial concentration is not zero as the resin is exhausted. Therefore, the mass transfer coefficient is not constant but dependent on the solution concentrations in the bulk and at the interface throughout the bed. Because Equation (20) cannot explain these effects, the mass transfer coefficient is estimated by the mixed bed ion exchange model (Haub and Foutch, 1986a,b) with the experimental data in Chapter III.

Theory

Particle Mass Transfer Coefficient

The kinetics of used resins are explained by both film and particle diffusion mechanisms. The mass transfer coefficients for used resins calculated in Chapter III, therefore, are actually not film mass transfer coefficients but overall mass transfer coefficients which account for both film and particle mass transfer. If Equation (13) is rewritten, appropriately for the overall exchange rate, it expresses the overall rate, assuming that the solute concentration inside the resin is extremely small compared with that in the bulk solution.

$$\frac{\partial q_i}{\partial t} = k_o a_p C_i \tag{22}$$

Equation (22) has the same form as Equation (19) except that k_1 is changed to k_o. Therefore, Equation (20) can be simply rewritten with the overall mass transfer coefficient.

$$\ln \frac{C_i^{eff}}{C_i^{inf}} = -\frac{k_o a_p ZAR_i}{V} \tag{23}$$

Particle mass transfer coefficients can be calculated with k_o and k_1 using the series resistance model. In this case, k_1 is assumed as the same film mass transfer coefficient for the new resin. The assumption seems like an oversimplification, because the driving force of film mass transfer is actually not C_i but $(C_i - C_i^*)$ for the used resin. However, the interfacial fluid-phase solute concentration, C_i^*, is very small compared with the bulk concentration, C_i, so the assumption is appropriate for the approximation of film mass transfer coefficient for the used resin. The particle mass transfer coefficient, k_p, for the used resin is finally calculated from Equation (24).

$$k_p = \frac{k_o k_1}{k_1 - k_o} \tag{24}$$

Equation (24) was obtained by arranging Equation (5) for k_p. The particle mass transfer coefficient accounts for the degradation of both cation and anion resins due to fouling or the deactivation of active sites.

Mixed Bed Ion Exchange Model

The mixed bed ion exchange model for binary exchange was developed by Haub and Foutch (1986a,b). The model was developed with the following

assumptions; static film diffusion control, uniform bulk liquid and surface compositions, equilibrium at the particle-film interface and instantaneous neutralization reaction compared with the exchange rate, activity coefficients are assumed one for ultra-low concentration, pseudo steady state mass transfer across the film, isothermal system and negligible dispersion effect.

The model predicts a bed effluent concentration by solving a column material balance for time and position. Nernst-Planck equation, Equation (1), was used as the ionic flux equation, and the flux equations for each ion were used to obtain the effective liquid-phase diffusivity using the constraints of electroneutrality and no net flux of coions across the film. Selectivity coefficient was introduced to express the interfacial concentrations into the effective diffusivity. In Equation (21), the effective diffusivity depends on diffusivity ratio of counterions, α, selectivity coefficient, K_H^{Na}, and equivalent fraction of sodium in resin phase, y_{Na}. Therefore, the mass transfer coefficient is not constant inside the bed, but a function of the effective diffusivity. The exchange rate is determined by Equation (25)

.

$$\frac{\partial q_i}{\partial t} = k_1 R_i a_s \left(C_i - C_i^* \right) \tag{25}$$

where R_i is expressed by Equation (7). R_i accounts for the effect of effective diffusivity on exchange rate. The mass transfer coefficient, k_1 was determined by Equation (3) or (4) depending on the flow rate. The effluent concentration is predicted by integrating the column material balance, Equation (17), with initial and boundary conditions.

The first step of the calculation procedure is to check whether the model estimates the same effluent concentrations as the experimental data. The mass

transfer coefficients determined in Chapter III are used in Haub and Foutch's (1986a,b) model instead of Carberry's and Kataoka's equations. If there are deviations between effluent concentrations predicted by the model and the experimental data, then new mass transfer coefficients are calculated by trial and error in the model to match the data.

Results and Discussion

Mass Transfer Coefficients from the Model

The Fortran program of Haub and Foutch's model used in this study is the modified version of Haub and Foutch's original code by Yoon (1990). All calculations with the model were carried out for the experimental data of new and used Monosphere resins from Riverside Number 1 condensate polisher (C.P.) and Northeastern Station Number 3 C.P. The mass transfer coefficients from the model are assumed correct, when the effluent concentrations of both cation and anion estimated by the model show less than 5 percent difference from experimental data.

Figures 27 through 29 show the mass transfer coefficients for sodium calculated from Harries and Ray's equation (Equation 20) and Haub and Foutch's model. Figures 30 through 32 are those for chloride. For both cation and anion resins, the model always estimated lower mass transfer coefficients than those determined by Equation (20). In addition, the differences between the mass transfer coefficients determined by the model and Equation (20) were uniform especially for influent concentrations greater than 1000 ppb chloride and 650 ppb sodium. For lesser influent concentrations, the difference, however, was not uniform for some cases. The differences are presented in Appendix E. The
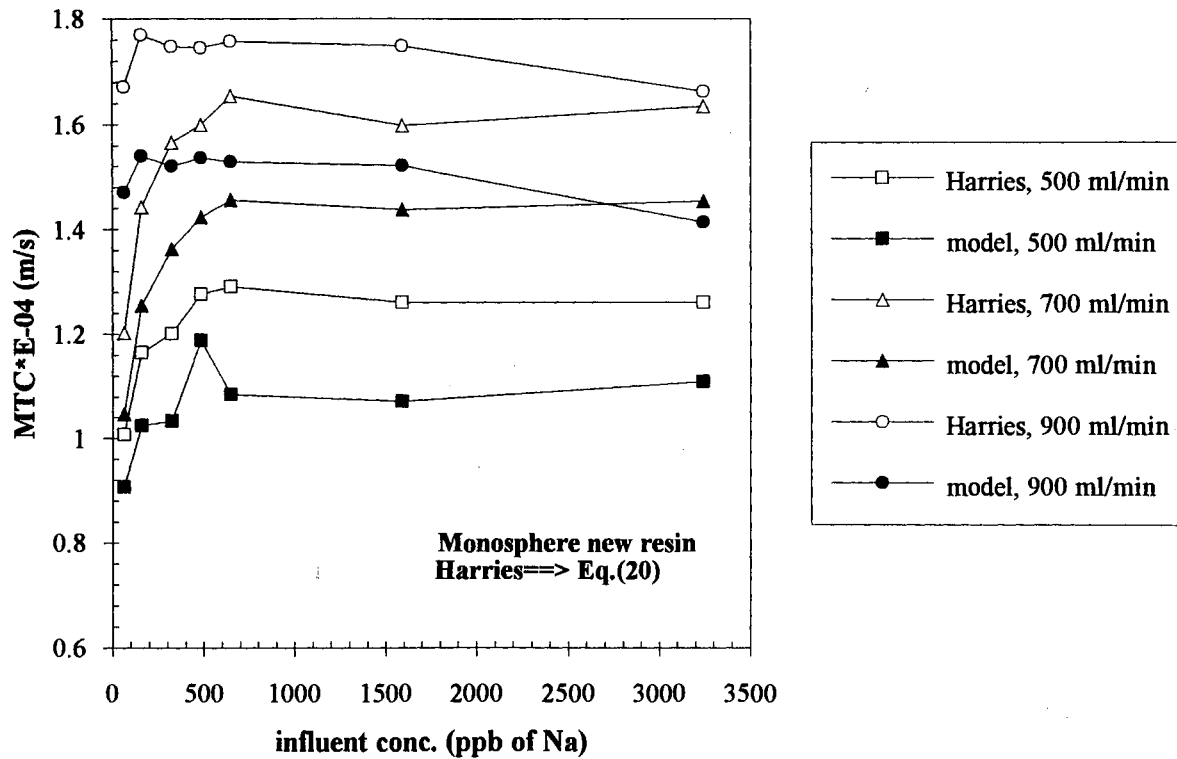
Figure 27. Mass Transfer Coefficients of New Monosphere Resin for Sodium Estimated by Harries and Ray's Equation and Haub and Foutch's Mixed Bed Ion Exchange Model
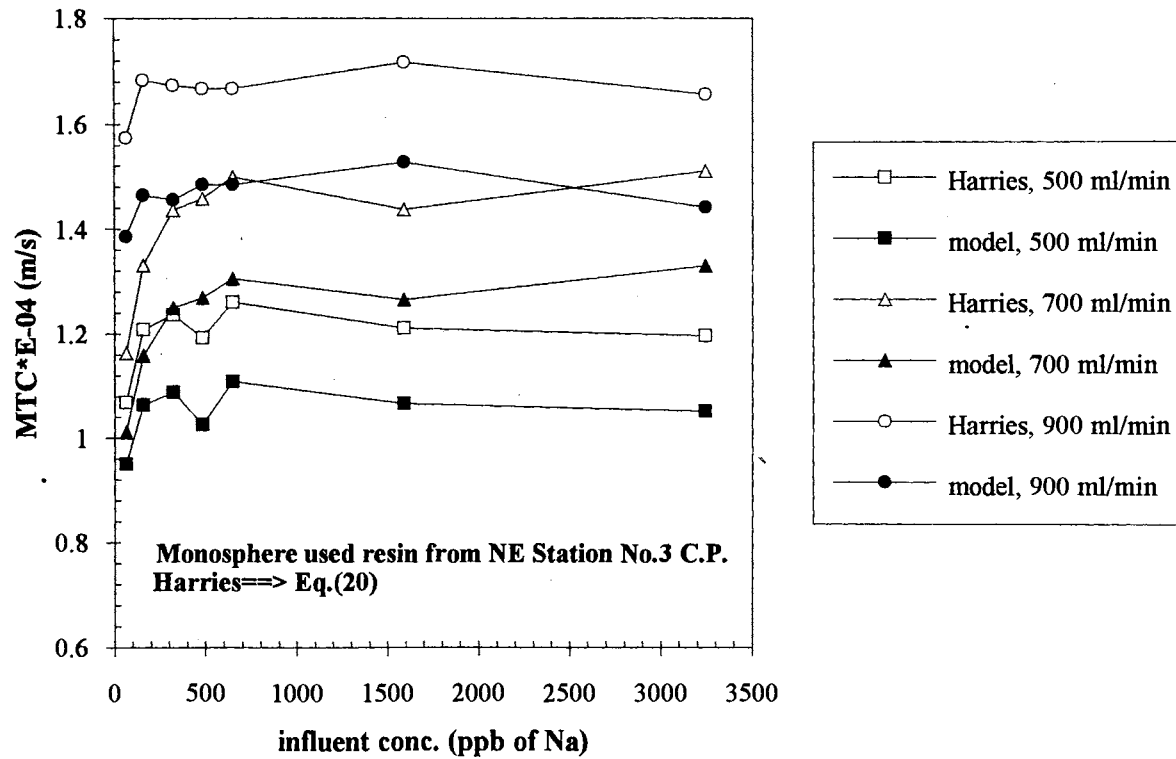
Figure 28. Mass Transfer Coefficients of Used Monosphere Resin (from
Northeastern Station Number 3 Condensate Polisher) for
Sodium Estimated by Harries and Ray's Equation and Haub
and Foutch's Mixed Bed Ion Exchange Model
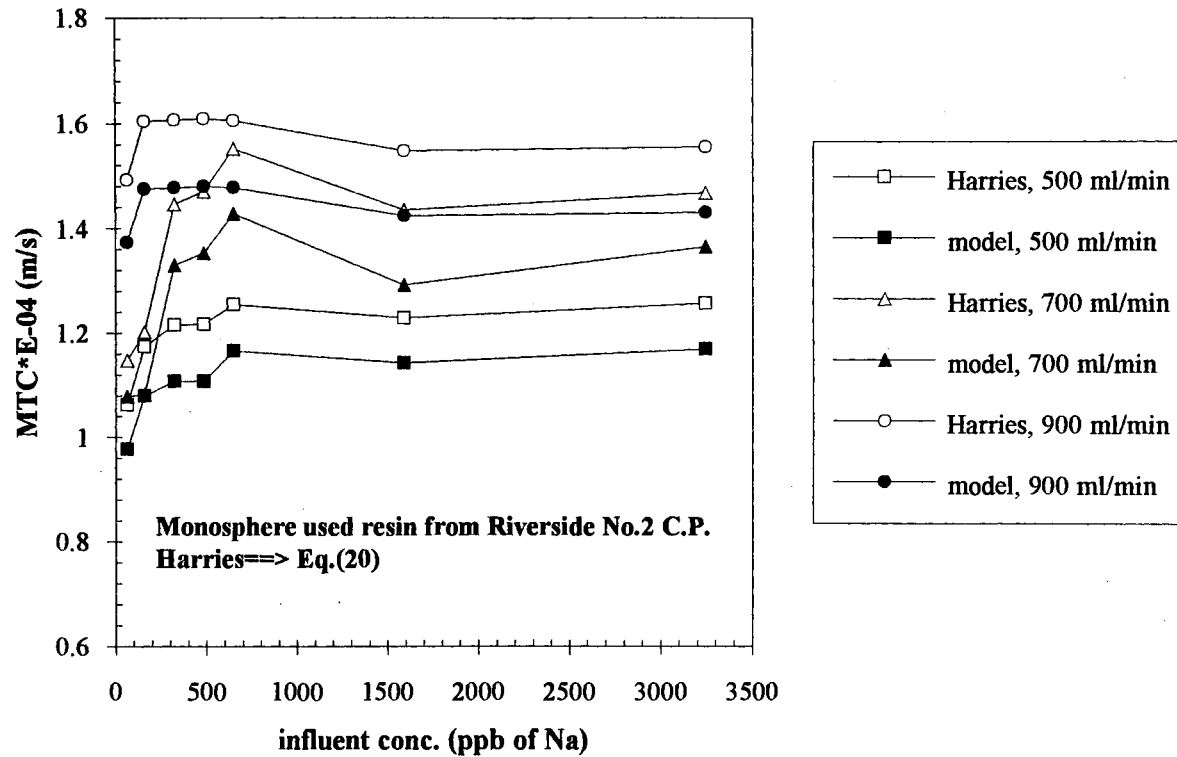
Figure 29. Mass Transfer Coefficients of Used Monosphere Resin (from
Riverside Number 2 Condensate Polisher) for Sodium
Estimated by Harries and Ray's Equation and Haub
and Foutch's Mixed Bed Ion Exchange Model
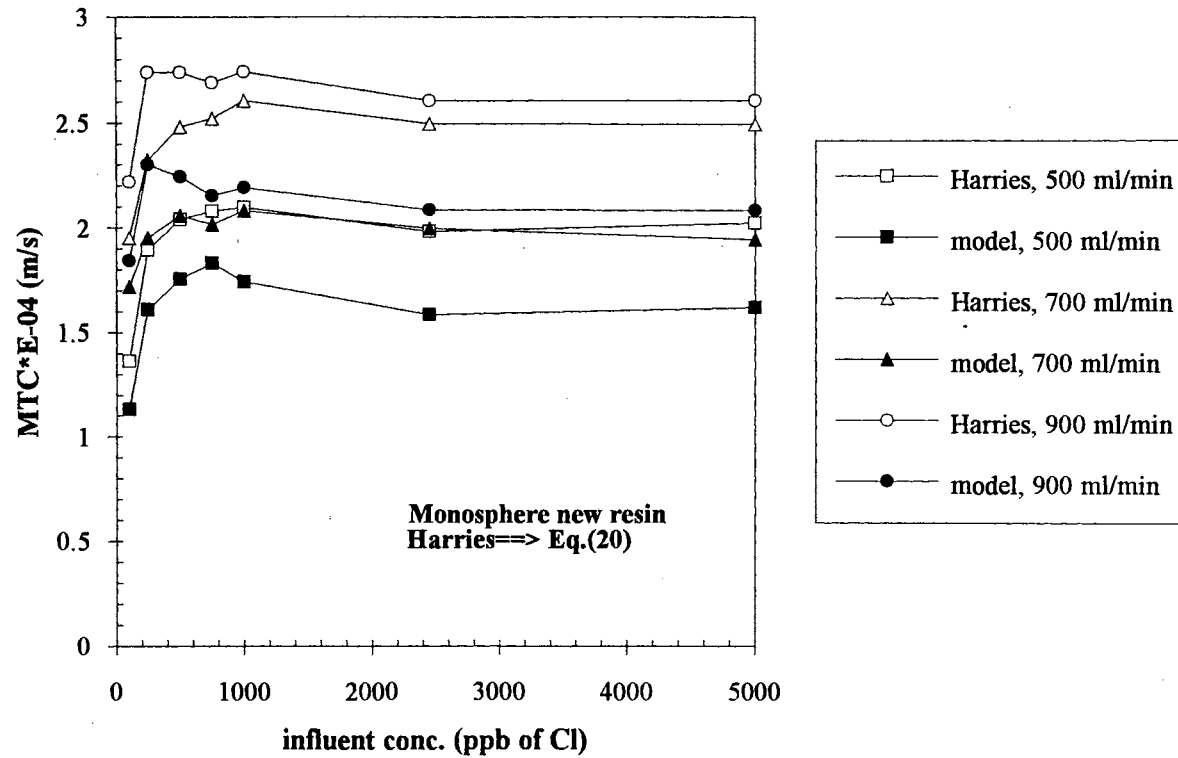
Figure 30. Mass Transfer Coefficients of New Monosphere Resin for
Chloride Estimated by Harries and Ray's Equation and Haub
and Foutch's Mixed Bed Ion Exchange Model
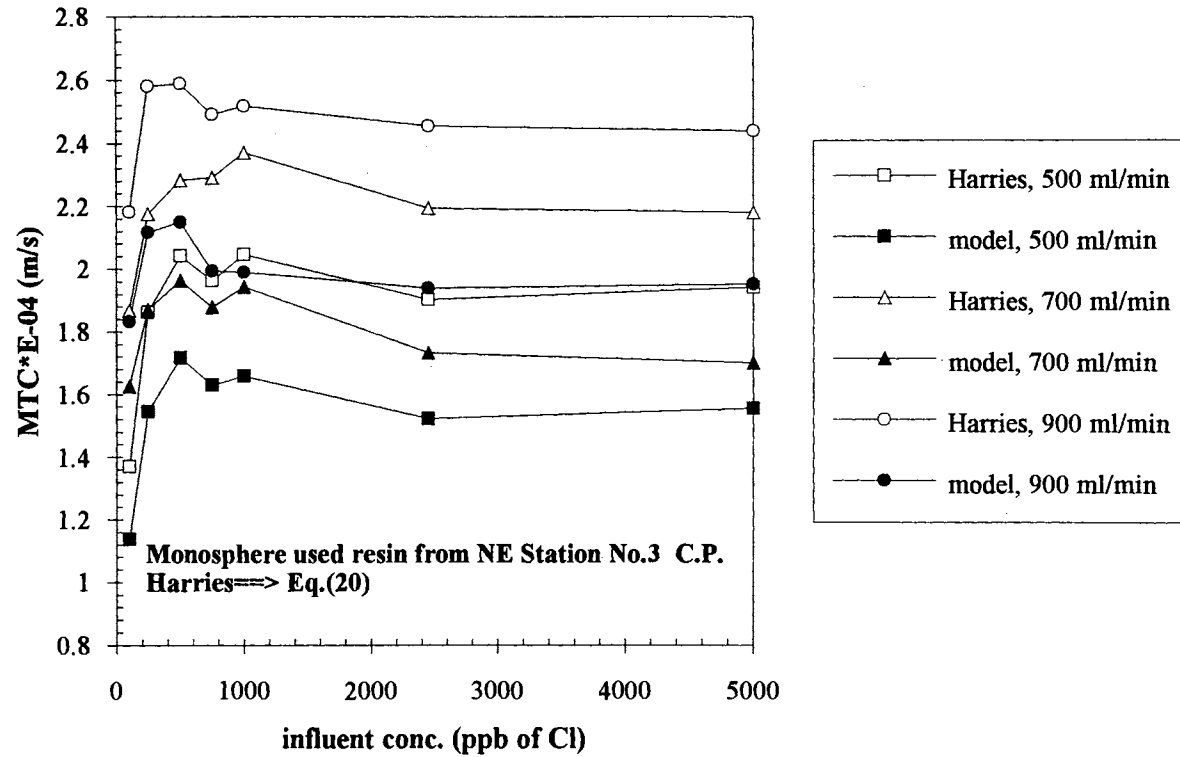
Figure 31. Mass Transfer Coefficients of Used Monosphere Resin (from
Northeastern Station Number 3 Condensate Polisher) for
Chloride Estimated by Harries and Ray's Equation and Haub
and Foutch's Mixed Bed Ion Exchange Model
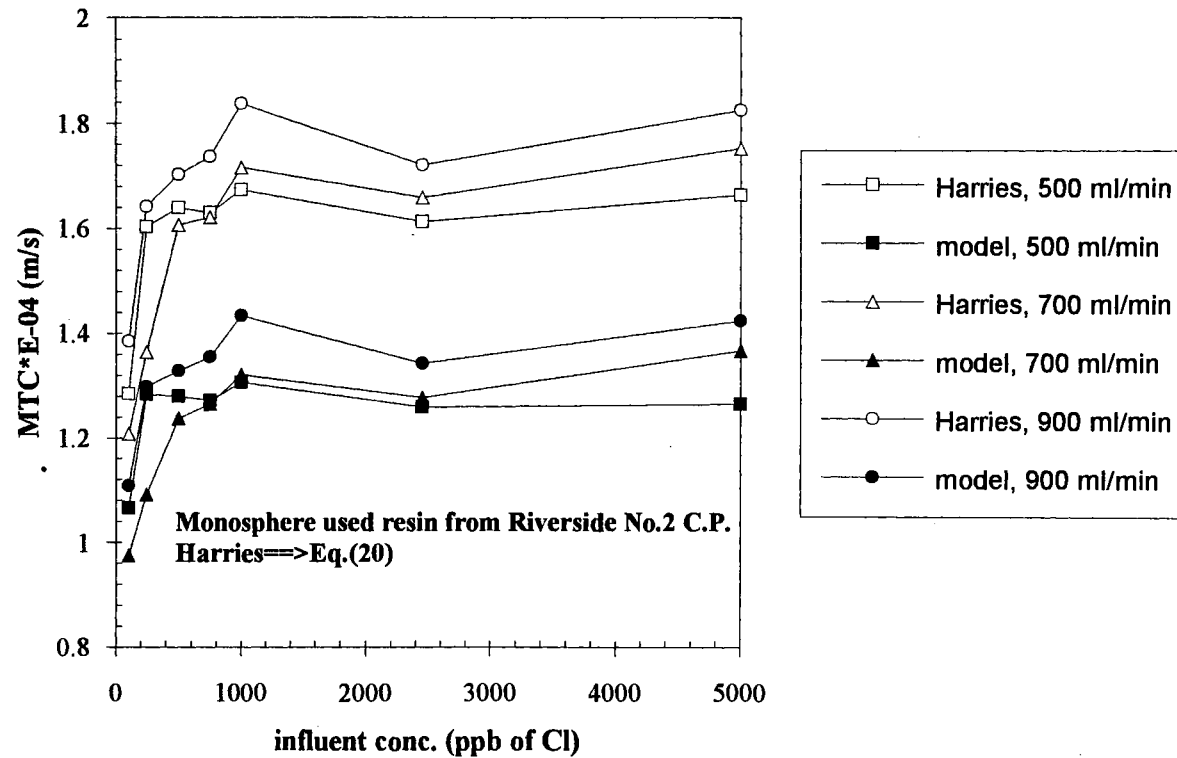
Figure 32. Mass Transfer Coefficients of Used Monosphere Resin (from
Riverside Number 2 Condensate Polisher) for Chloride
Estimated by Harries and Ray's Equation and Haub and
Foutch's Mixed Bed Ion Exchange Model

difference was defined by

$$\text{difference} = \frac{k_H - k_{model}}{k_H} \tag{26}$$

where k_H and k_{model} are the mass transfer coefficients determined by Equation (20) and the model, respectively. This trend was also seen for both the new and used resins. The differences for the used anion resins were almost the same as those of new resin and did not depend on flow rate. In the case of cation resins, the differences were smaller than for anion resins. Table IX shows the average differences for cation and anion resins in the influent concentrations greater than 1000 ppb chloride and 650 ppb sodium. Therefore, the mass transfer coefficients from the model could be estimated by multiplying the mass transfer coefficient from Equation (20) by (1.0 - difference). Table IX shows that the differences for cation at 700 ml/min flow rate are smaller than others.

In the case of anion resins, the average differences for each resin are quite uniform and the arithmetic mean of the average differences for three resins is 0.209. Therefore, the mass transfer coefficients of anion resins from the model and Equation (20) can be related by the following equation.

$$k_{model} = 0.791 k_H \tag{27}$$

However, a particular relationship for cation resins like Equation (27) is impossible because percentage differences at 700 ml/min are quite different from those at other flow rates.

Equation (20) assumes a constant mass transfer coefficient and simply accounts for the effects of operating condition on mass transfer coefficient. The mass transfer coefficient calculated by Equation (20), therefore, does not account

for the effects of the existence of coions, the diffusivities of single ions, and the concentration changes in bulk and interface between resin and liquid-phase. However, Haub and Foutch's model explains those effects with effective diffusivity on the exchange rate, even though Carberry's (Equation 3) and Kataoka's (Equation 4) mass transfer correlations simply account for the effects of column geometry and flow condition. The effect of the position of the reaction plane in the film can be also explained by effective diffusivities based on liquid-film and bulk neutralization (Haub and Foutch, 1986a, b). Therefore, the mass transfer coefficients determined by Equation (20) cannot be used for actual ion exchange process design.

TABLE IX

DIFFERENCE BETWEEN MASS TRANSFER COEFFICIENTS IN MIXED BEDS ESTIMATED BY HARRIES AND RAY'S EQUATION AND HAUB AND FOUTCH'S MIXED BED ION EXCHANGE MODEL

	Percentage Difference (Equation (27) × 100)					
	Cation			Anion		
Fl (ml/min)=>	500	700	900	500	700	900
New	14.4	7.0	12.0	19.0	20.7	20.0
Riverside 2	11.0	8.3	12.3	22.7	22.7	22.0
NE 3	13.6	8.0	11.7	19.7	20.4	20.7
average	13.0	7.8	12.0	20.5	21.3	20.9

average : arithmetic mean at each flow rate
Fl : flow rate

Carberry's correlations estimated much lower effluent concentrations than experimental data and higher mass transfer coefficients for both cation and anion than those by Equation (20). Table X shows the mass transfer coefficients for new resin based on Carberry's correlation and Equation (20) and those estimated in this study.

TABLE X

COMPARISON OF MASS TRANSFER COEFFICIENTS FROM DIFFERENT CALCULATION METHODS

Mass transfer coefficient $\times$ 10^{-2} (cm/sec)								
Fl	Carberry		Equation (20)		this study		Rec	Rea
ml/min	cation	anion	cation	anion	cation	anion	cation	anion
500	1.36	1.92	1.27	2.03	1.09	1.65	18.0	16.3
700	2.01	2.80	1.63	2.53	1.45	2.01	25.2	22.9
900	2.28	3.18	1.72	2.65	1.49	2.12	32.4	29.4

Fl : Volumetric flow rate
Rec & Rea : Reynold numbers of cation and anion at Carberry's equation

The mass transfer coefficients estimated in this study show relatively low values compared with others. Yoon (1990) found new coefficients for Carberry's equation for sodium and chloride, and matched the model prediction with his experimental data (Equation 10). The new coefficients of Yoon's equation are 0.484 and 0.359 for sodium and chloride, respectively, in the case of $R_{C/A}$ = 0.667. These values are smaller than 1.15 in Carberry's equation, so Yoon's correlation estimated lower mass transfer coefficients than Carberry's. Noh (1992) compared various mass transfer correlations and discussed that Yoon's correlation

gave smaller mass transfer coefficient than others except Rowe's correlation (1975) that showed the smallest values. Therefore, it is reasonable that the mass transfer coefficients from this study give lower values than those by Carberry's equation.

Haub and Foutch's model (1986a,b) cannot account for the particle diffusion effect for used resin, because the model is based on film diffusion control. The mass transfer coefficients from the model are estimated by matching effluent concentrations from the experimental data and the model for less than 5 minutes after feed inlet. Therefore, without experimental data, it is impossible to prove whether the mass transfer coefficients from the model can estimate accurate breakthrough curves. In addition, Yoon's correlation was made in his experimental condition which is different from the condition in this study. For example, the superficial linear velocity ranged from 98.7 to 118 cm/min in this study and from 1.34 to 1.48 cm/min in Yoon's experiment.

Particle Mass Transfer Coefficient

Particle mass transfer coefficients were estimated with the mass transfer coefficients of used resins from Equation (20) and Haub and Foutch's model. The mass transfer coefficients are considered overall coefficients, and account for particle and film diffusion effects on the exchange rate, as in Equations (5) and (22). The average overall mass transfer coefficients were actually used for calculation. The average coefficients were taken as arithmetic means of the mass transfer coefficients for the influent concentration range greater than 500 ppb for chloride and 324 ppb for sodium. The concentration range was chosen because the mass transfer coefficients were near uniform in that range. Table XI shows the particle mass transfer coefficients calculated by Equation (24) with the overall

mass transfer coefficients by Equation (23).

Particle mass transfer coefficients were always much higher than film mass transfer coefficients. This means that particle diffusion effect in exchange rate is relatively small compared with film diffusion effect. Especially, the particle mass transfer coefficients for anion resins from Northeastern Station No.3 and 4 C.P. were very high. Figures 12 through 14 shows that the mass transfer coefficients for the resins calculated by Equation (20) were almost equal to those of new resin. That means that the exchange kinetics for the resins are dominantly controlled by the film diffusion mechanism. For anion resins from Riverside No. 1 and 2 C.P., the particle mass transfer coefficients were lower than others. This means that the anion resins were degraded significantly compared to the others. Table XI also shows that the cation resins from Northeastern Station No.4 C.P. were relatively degraded rather than other cation resins, and this coincides with the result in Figures 9 through 11.

TABLE XI

PARTICLE MASS TRANSFER COEFFICIENTS BASED ON OVERALL MASS TRANSFER COEFFICIENTS ESTIMATED BY EQUATION (23)

FR	Particle mass transfer coefficient $\times 10^{-4}$ (m/s)							
	Riverside No.1		Riverside No.2		NE No.3		NE No.4	
ml/min	cation	anion	cation	anion	cation	anion	cation	anion
500	15.7	6.53	67.5	8.41	39.7	62.6	11.8	117
700	19.8	5.29	17.5	4.97	16.8	22.4	7.42	27.5
900	16.8	6.79	18.6	5.19	52.3	37.9	9.39	32.3

NE : Northeastern Station
FR : volumetric flow rate

Table XII shows the particle mass transfer coefficients calculated with the overall mass transfer coefficients estimated by Haub and Foutch's model. The particle mass transfer coefficients for anion resin from Riverside No.2 C.P. were lower than others. A negative value in Table XII occurred when the film mass transfer coefficient for new resin was a little smaller than the overall mass transfer coefficient, but the actual difference was very small. Therefore, it is concluded that the resin is not degraded.

Equation (20) and Haub and Foutch's model are both based on film diffusion control. Therefore, it is only an approximation that the mass transfer coefficients for used resins can be regarded as overall mass transfer coefficients. Thus, particle mass transfer coefficients determined in this chapter permits only the qualitative analysis of mass transfer mechanisms for used resins.

TABLE XII

PARTICLE MASS TRANSFER COEFFICIENTS BASED ON OVERALL MASS TRANSFER COEFFICIENTS ESTIMATED BY HAUB AND FOUTCH'S MIXED BED ION EXCHANGE MODEL

	Particle mass transfer coefficient $\times\ 10^{-4}$ (m/s)			
flow rate	Riverside No.2		Northeastern No.3	
ml/min	cation	anion	cation	anion
500	-30.0	5.07	41.0	30.7
700	26.5	3.60	12.8	21.2
900	47.5	3.83	88.3	29.5

Conclusions and Recommendations

The following conclusions were attained by the estimation of particle mass transfer coefficients and the comparison of mass transfer coefficients determined by Harries equation and a mixed bed ion exchange model.

1. Haub and Foutch's (1986a,b) model estimates lower mass transfer coefficients of both cation and anion than those measured by Harries and Ray's (1984) equation and Carberry's correlation. This trend was the same for new and used resins and coincided with Yoon's (1990) analysis.

2. The percentage differences between the mass transfer coefficients of chloride estimated by Harries and Ray's equation and Haub and Foutch's model were uniform. Thus, the mass transfer coefficients by the model are decreased 21 percent from those by Harries and Ray's equation. For sodium, a small decrease was seen, and the percentage difference was lower at 700 ml/min than at other flow rates.

3. Particle mass transfer coefficients for used resins were estimated based on the overall mass transfer coefficients estimated by Equation (23) and Haub and Foutch's model. The particle mass transfer coefficients calculated by both methods showed similar trends. Smaller particle mass transfer coefficient means stronger effects of particle diffusion resistance on mass transfer rates. Anion resins from Riverside Number 2 condensate polisher had lower particle mass transfer coefficients. This agrees with higher the degradation for this resin than other used resins.

4. From particle mass transfer coefficients based on overall coefficients estimated by Equation (23), anion resins from Riverside Number 1 and 2 condensate polishers and cation resins from Northeastern Station Number 4 condensate polisher were more degraded than others.

From these conclusions, the following recommendations are made:

1. The mass transfer coefficients estimated by Haub and Foutch's model were taken by matching experimental effluent concentrations with those in the model based on initial five minutes feed input. It cannot be proved without experimental breakthrough data whether the mass transfer coefficients will estimate an accurate breakthrough curve. Therefore, column breakthrough experiments at high flow rates used in this work are strongly recommended.

2. In order to explain particle diffusion effect for used resin, Haub and Foutch's model should be modified appropriate for the combined model, where film and particle mass transfer are considered simultaneously. In addition, it should be validated whether some model parameters, like single ionic diffusivity and selectivity coefficient, are appropriate in the experimental condition used in this study.

3. A series resistance model is too simple to estimate particle mass transfer coefficients accurately, and the use of an overall mass transfer coefficient is just an approximation. Therefore, development of a strict model for particle mass transfer coefficient is recommended.

BIBLIOGRAPHY

Bieber, H., Steidler, F. E., and Selke, W. A., "Ion Exchange Rate Mechanism, "Chemical Engineering Progress Symposium Series, No.14, Vol.50, pp.17-21 (1954).

Bolden, W. B., White, T., and Groves, F. R. Jr., "Continuous Fixed Bed Ligand Exchange : The Shrinking-Core Model," AIChE Journal, Vol.35, No.5, pp.849-852 (1989).

Boyd, G. E., Adamson, A. W., and Myers, L. S. Jr., "The Exchange Adsortion of Ions from Aquous Solutions by Organic Zeolites. II. Kinetics," Journal of the American Chemical Society, Vol.69, No.11, pp.2836-2848 (1947).

Carberry, J. J., "A Boundary-Layer Model of Fluid-Particle Mass Transfer in Fixed Beds," AIChE Journal, Vol.6, No.3, pp.460-463 (1960)

Cooney, D. O., "Determining External Film Mass Transfer Coefficients for Adsorption Column," AIChE Journal, Vol.37, No.8, pp.1270-1274 (1991).

Cussler, E. L., "Diffusion, Mass Transfer in Fluid Systems," Cambridge University Press, Cambridge, England, 1984.

Divekar, S. V., Foutch, G. L., and Haub, C. E., "Mixed-Bed Ion Exchange at Concentrations Approaching the Dissociation of Water. Temperature Effects," Industrial and Engineering Chemistry Research, Vol.26, No.2, pp.1906-1909 (1987).

Dowex, "Dowex: Ion Exchange," The Dow Chemical Company, Midland, Michigan, 1958.

Emmett, J. R., "Condensate Polishing: Ammonia Cycle Operation," Effluent and Water Treatment Journal, Vol.23, pp.507-510 (1983).

Foutch, G. L., "Ion Exchange: Predictive Modeling of Mixed-Bed Performance," ULTRAPURE WATER, Vol.8, No.2, pp.47-50 (1991).

Frisch, N. W. and Kunin, R., "Kinetics of Mixed-Bed Deionization: I," AIChE Journal, Vol.6, No.4, pp.640-647 (1960).

Gaffney, B. J. and Drew, T. B., "Mass Transfer from Packing to Organic Solvents in Single Phase Flow through a Column," Industrial and Engineering Chemistry, Vol.42, No.6, pp.1120-1127 (1950).

Gilliland, E. R. and Baddour, R. F., "The Rate of Ion Exchange," Industrial and Engineering Chemistry, Vol.45, No.2, pp.330-337 (1953).

Gopala Rao, M. and David, M. M., "Single-Particle Studies of Ion Exchange in Packed Beds: Cupric Ion-Sodium Ion System," AIChE Journal, Vol.10, No.2, pp.213-219 (1964).

Gopala Rao, M. and Gupta, A. K., "Kinetics of Ion-Exchange in Weak-Base Anion Exchange Resins," AIChE Symposium Series, No.219, Vol.78, pp.96-102 (1982a).

Gopala Rao, M. and Gupta, A. K., "Ion Exchange Processes Accompanied by Ionic Reactions," The Chemical Engineering Journal, Vol.24, pp.181-190 (1982b).

Goto, S., Goto, M., and Teshima, H., "Simplified Evaluations of Mass Transfer Resistances from Batch-Wise Adsorption and Ion-Exchange Data. 1. Linear Isotherms," Industrial and Engineering Chemistry Fundamentals, Vol.20, No.4, pp.368-371 (1981a).

Goto, M., Goto, S., and Teshima, H., "Simplified Evaluations of Mass Transfer Resistances from Batch-Wise Adsorption and Ion-Exchange Data. 1. Linear Isotherms," Industrial and Engineering Chemistry Fundamentals, Vol.20, No.4, pp.371-375 (1981b).

Graham, E. E. and Dranoff, J. S., "Kinetics of Anion Exchange Accompanied by Fast Irrevisible Reaction," AIChE Journal, Vol.18, No.3, pp.608-613 (1972).

Harries, R. R. and Ray, N. J., "Acid Sulphate Leakage from Mixed Beds," Effluent and Water Treatment Journal, Vol.18, pp.487-495 (1978).

Harries, R. R. and Ray, N. J., "Anion Exchange in High Flow Rate Mixed Beds," Effluent and Water Treatment Journal, Vol.24, No.4, pp.131-139 (1984).

Harries, R. R., "Water Purification by Ion Exchange Mixed Bed," Ph.D. Dissertation, Loughborough University of Technology, 1986.

Harries, R. R. and Tittle, K., "Deterioration of Exchange Kinetics in Condensate Purification Plant," in "4th International Conference on Water Chemistry for Nuclear Reactor Systems," London, England, 1986.

Harries, R. R., "Ion Exchange Kinetics in Condensate Purification," Chemistry and Industry, No.4, pp.104-109 (1987).

Harries, R. R., "The Role of pH in Ion Exchange Kinetics," in "Ion Exchange for Industry," Edited by Streat, M., Ellis Horwood Limited, Chichester, England, 1988.

Harries, R. R., "Ion Exchange Kinetics in Ultra Pure Water Systems," Journal of Chemical Technology and Biotechnology, Vol.51, pp.437-447 (1991).

Haub, C. E., "Model Development for Liquid Resistance-Controlled Reactive Ion Exchange at Low Solution Concentrations with Application to Mixed Bed Ion Exchange, M.S. Thesis, Oklahoma State University, Stillwater, Oklahoma, 1984.

Haub, C. E. and Foutch, G. L., "Mixed-Bed Ion Exchange at Concentrations Approaching the Dissociation of Water. 1. Model Development," Industrial and Engineering Chemistry Fundamentals, Vol.25, No.3, pp.373-381 (1986a).

Haub, C. E. and Foutch, G. L., "Mixed-Bed Ion Exchange at Concentrations Approaching the Dissociation of Water. 2. Column Model Application," Industrial and Engineering Chemistry Fundamentals, Vol.25, No.3, pp.381-385 (1986b).

Helfferich, F. and Plesset, M. S., "Ion Exchange Kinetics. A Nonlinear Diffusion Problem," The Journal of Chemical Physics, Vol.28, No.3, pp.418-424 (1958).

Helfferich, F., "Ion Exchange," McGraw-Hill Book Company, New York, 1962.

Helfferich, F., "Ion-Exchange Kinetics. V. Ion Exchange Accompanied by Reactions," The Journal of Physical Chemistry, Vol.69, No.4, pp.1178-1187 (1965).

Helfferich, F., "Chapter 2. Ion Exchange Kinetics," in "Ion Exchange," Vol.1, Edited by J. A. Marinsky, Marcel Dekker, Inc., New York, 1966.

Helfferich, F. G., Liberti, L., Petruzzelli, D, and Passino, R., "Anion Exchange Kinetics in Resins of High Selectivity," Israel Journal of Chemistry, Vol.26, pp.3-8 (1985).

Helfferich, F. G., "Models and Physical Reality in Ion-Exchange Kinetics," Reactive Polymers, Vol.13, pp.191-194 (1990).

Hering, B. and Bliss, H., "Diffusion in Ion Exchange Resins," AIChE Journal, Vol.9, No.4, pp.495-503 (1963).

Huang, T. C. and Li, K. Y., "Ion-Exchange Kinetics for Calcium Radiotracer in a Batch System," Industrial and Engineering Chemistry Fundamentals, Vol.12, No.1, pp.50-55 (1973).

Huang, T. C. and Tsai, F. N., "Kinetic Parameters of Isotopic Exchange Reaction in Finite Bath," Canadian Journal of Chemical Engineering, Vol.55, pp.301-306 (1977).

Kataoka, T., Sato, N., and Ueyama, K., "Effective Liquid Phase Diffusivity in Ion Exchange," Journal of Chemical Engineering of Japan, Vol.1, No.1, pp.38-42 (1968).

Kataoka, T., Yoshida, H., and Ueyama, K., "Mass Transfer in Laminar Region Liquid and Packing Material Surface in The Packed Bed," Journal of Chemical Engineering of Japan, Vol.5, No.2, pp.132-136 (1972).

Kataoka, T., Yoshida, H., and Yamada, T., "Liquid Phase Mass Transfer in Ion Exchange Based on The Hydraulic Radius Model," Journal of Chemical Engineering of Japan, Vol.6, No.2, pp.132-136 (1973).

Kataoka, T., Yoshida, H., and Uemura, T., "Liquid-Side Ion Exchange Mass Transfer in a Ternary System," AIChE Journal, Vol.33, No.2, pp.202-210 (1987).

Kataoka, T. and Yoshida, H., "Breakthrough Curve in Equal Valence Ion Exchange: Liquid Phase Diffusion Control," Journal of Chemical Engineering of Japan, Vol.9, No.5, pp.383-387 (1976).

Kataoka, T. and Yoshida, H., "Kinetics of Ion Exchange Accompanied by Neutralization Reaction," AIChE Journal, Vol.34, No.6, pp.1020-1026 (1988).

King, D.W., "The Influence of Temperature and Amines on Mixed-Bed Ion Exchange Column Performance for Ultra-Low Concentration of Sodium and Chloride," Ph.D. Dissertation, Oklahoma State University, Stillwater, Oklahoma, 1991.

Koloini, T., Sopcic, M., and Zumer, M., "Mass Transfer in Liquid-Fluidized Beds at Low Reynolds Numbers," Chemical Engineering Science, Vol.32, pp637-641 (1977).

Kunin, R., "Elements of Ion Exchange," Reinhold, New York, 1960.

Levenspiel, O., "Chemical Reaction Engineering," John Wiley & Sons, Inc., New York, 1972.

Liberti, L., Petruzzelli, D., Helfferich, F. G., and Passino, R., "Chloride/Sulphate Ion Exchange Kinetics at High Solution Concentration," Reactive Polymers, Vol.5, pp.37-47 (1987).

Lightfoot, E., Massot, C., and Ivani, F., "Approximate Estimation of Heat and Mass Transfer Coefficients," Chemical Engineering Progress Symposium Series, Vol.61, No.58, pp.28-60 (1966).

McCune, L. K. and Wilhelm, R. H., "Mass and Momentum Transfer in Solid-Liquid System: Fixed and Fluidized Beds," Industrial and Engineering Chemistry, vol.41, No.6, pp.1124-1134 (1949).

McNulty, J. T., "Anion Exchange Resin Kinetics in Mixed Bed Condensate Polishing," in "Ion Exchange Technology," Edited by Naden, D. and Streat, M., Ellis Horwood Limited, Chichester, England, 1984.

McNulty, J. T., Eumann, M., Bevan, C. A., and Tan, V. C. T., "Anion Exchange Resin Kinetic Testing an Indispensable Diagnostic Tool for Condensate Polisher Troubleshooting," in "47th Annual Meeting International Water Conference," Pittsburgh, Pennsylvania (1986).

Michaels, A. S., "Symplified Method of Interpreting Kinetic Data in Fixed-Bed Ion Exchange," Industrial and Engineering Chemistry, Vol.44, No.8, pp.1922-1930 (1952).

Moison, R. L. and O'Hern, Jr., H. A., "Ion Exchange Kinetics," Chemical Engineering Progress Symposium Series, No.24, Vol.55, pp.71-85 (1959).

Naden, D. and Streat, M., "Ion Exchange Technology," Ellis Horwood Limited, Chichester, England, 1984.

Noh, B. I., "Effect of Step Changes in Feed Concentration and Incomplete Mixing of Anion and Cation Resin on The Performance of Mixed-Bed Ion Exchange," Ph.D. Dissertation, Oklahoma State University, Stillwater, Oklahoma, 1992.

Omatete, O. O., Clazie, R. N., and Vermeulen, T., "Column Dynamics of Ternary Ion Exchange, Part I: Diffusional and Mass Transfer Relations," The Chemical Engineering Journal, Vol.19, pp.229-240 (1980a).

Omatete, O. O., Clazie, R. N., and Vermeulen, T., "Column Dynamics of Ternary Ion Exchange, Part II: Solution Mass Transfer Controlling," The Chemical Engineering Journal, Vol.19, pp.241-250 (1980b).

Pan, S. H. and David, M. M., "Design Effect of Liquid Phase Ionic Migration on A Moving Packed-Bed Ion Exchange Process," AIChE Symposium Series, No.179, Vol.74, pp.74-82 (1978).

Petruzzelli, D, Liberti, L., Passino, R., Helfferich, F. G., and Hwang, Y. L., "Chloride/Sulphate Exchange Kinetics: Solution for Combined Film and Particle Diffusion Control," Reactive Polymers, Vol.5, pp.219-226 (1987a).

Petruzzelli, D, Helfferich, Liberti, L., Millar, J. R., and Passino, R., "Kinetics of Ion Exchange with Intraparticle Rate Control: Models Accounting for Interactions in the Solid Phase," Reactive Polymers, Vol.7, pp.1-13 (1987b).

Petruzzelli, D., Liberti, L., Boghetich, G., Helfferich, F. G., and Passino, R., "Ion Exchange Kinetics on Anion Resins. Concentration Profiles and Transient Phenomena in the Solid Phase," Reactive Polymers, Vol.7, pp.151-157 (1988).

Pfeffer, R., "Heat and Mass Transport in Multiparticle Systems," Industrial and Engineering Chemistry Fundamentals, Vol.3, No.4, pp.380-383 (1964).

Rahman, K. and Streat, M., "Mass Transfer in Liquid Fluidized Beds of Ion Exchange Particles," Chemical Engineering Science, Vol.36, No.2, pp.293-300 (1981).

Reichenberg, D., "Properties of Ion-Exchange Resin in Relation to Their Structure. III. Kinetics of Exchange," Journal of American Chemical Society, Vol.75, pp.589-597 (1953).

Robinson, R. A. and Stokes, R. H., "Electrolyte Solutions," Butterworths Scientific Publications, London, 1968.

Rosen, J. B., "General Numerical Solution for Solid Diffusion in Fixed Beds," Industrial and Engineering Chemistry, Vol.46, No.8, pp.1590-1594 (1954).

Rowe, P. N., "Particle-To-Liquid Mass Transfer in Fluidized Beds," Chemical Engineering Science, Vol.30, No.1, pp.7-9 (1975)

Schogl, R. and Helfferich, F., "Comment on the Significance of Diffusion Potentials in Ion Exchange Kinetics," The Journal of Chemical Physics, Vol.26, No.1, pp.5-7 (1957).

Smith, T. G. and Dranoff, J. S., "Film Diffusion-Controlled Kinetics in Binary Ion Exchange," Industrial and Engineering Chemistry Fundamentals, Vol.3, No.3, pp.195-200 (1964).

Streat, M., "Kinetics of Slow Diffusing Species in Ion Exchangers," Reactive Polymer, Vol.2, pp.79-91 (1984).

Tittle, K., "Mixed-Bed Performance in a Condensate Polishing Plant," Proceedings of the American Power Conference, Vol.43, pp.1126-1130 (1981).

Tsai, F. N., "Kinetics of Ion Exchange with Combined Film and Particle Diffusion in a Finite Bath," The Journal of Physical Chemistry, Vol.86, No.13, pp.2339-2344 (1982a).

Tsai, F. N., "Film Diffusion-Controlled Kinetics of Isotopic Exchange in a Finite Bath," AIChE Journal, Vol.28, No.4, pp.698-700 (1982b).

Turner, J. C. R., Church, M. R., Johnson, A. S. W., and Snowdon, C. B., "An Experimental Verification of the Nernst-Planck Model for Diffusion in an Ion-Exchange Resin," Chemical Engineering Science, Vol.21, pp.317-325 (1966).

Turner, J. C. R. and Snowdon, C. B., "Liquid-Side Mass Transfer Coefficients in Ion Exchange: An Examination of the Nernst-Planck Model," Chemical Engineering Science, Vol.23, pp.221 (1968).

Van Brocklin, L. P. and David, M. M., "Coupled Ionic Migration and Diffusion During Liquid-Phase Controlled Ion Exchange," Industrial and Engineering Chemistry Fundamentals, Vol.11, No.1, pp.91-99 (1972).

Van Brocklin, L. P. and David, M. M., "Ionic Migration Effects During Liquid Phase Controlled Ion Exchange," AIChE Symposium Series, No.152, Vol.71, pp.191-201 (1975).

Wankat, P. C., "Rate-Controlled Separations," Elsevier Science Publishers Ltd., Essex, England, 1990.

Wilke, C. R. and Hougen, O. A., "Mass Transfer in The Flow of Gases Through Granular Solids Extended to Low Modified Reynolds Numbers," Transactions of American Institute of Chemical Engineers, Vol.41, pp.445-451 (1945).

Wilson, E. J. and Geankoplis, C. J., "Liquid Mass Transfer at Very Low Reynolds Numbers in Packed Beds," Industrial and Engineering Chemistry Fundamentals, Vol.5, No.1, pp.9-14 (1966).

Yoon, T. K., "The Effect of The Cation to Anion Resin Ratio on Mixed-Bed Ion Exchange Performance at Ultra-Low Concentrations," Ph.D. Dissertation, Oklahoma State University, Stillwater, Oklahoma, 1990.

Zecchini, E. J., "Solutions to Selected Problems in Multi-Component Mixed-Bed Ion Exchange Modeling," Ph.D. Dissertation, Oklahoma State University, Stillwater, Oklahoma, 1990.

APPENDIXES

APPENDIX A

EXPERIMENTAL SYSTEM

The experimental system was designed in order to reduce pressure drop due
to high flow rates and reduce contaminants from materials of construction. For
this system polyethylene pipe was used instead of tubing, as was used previously
(Yoon, 1990; King, 1991; Noh, 1992). The previous system of 1/4 in. inside
diameter Tygon tubing was not appropriate for high flow rate experiments, and
produced leakage problems around line connectors and high back pressure to a
feed pump. The pipe used in this system has larger diameter, so the effects of the
pressure drop were reduced. The deionized water, stored in a carboy, can be
contaminated by materials and air. Therefore, pure water to make feed solutions
of a particular ionic concentration was supplied directly into the system on-line
through a big mixed bed.

The system used in this study is composed of an experimental column,
resistivity meters, feeding and dosing pumps, and an ion chromatography to
measure effluent concentrations from the test column. Figure 33 shows the flow
diagram of the main system, and Figure 34 shows the flow diagram for the water
purification process. Distilled water was used to prepare deionized make-up
water. The water purification process satisfied this need. Actually, the water,
which is first deionized from city water, is deionized again in the main system to
make sure the water is clean. Thus, water from the water purification process is
circulated continuously as in Figure 33 without dosing concentrated solution until

IC: Ion Chromatography
RS: Resistivity Meter
PC: Personal Computer

circulation routine

mixed bed purification column

test column

RS2

RS1

RS3

PC

IC

sampling

feed carboy (pure water)

feed pump

dosing pump

waste water carboy
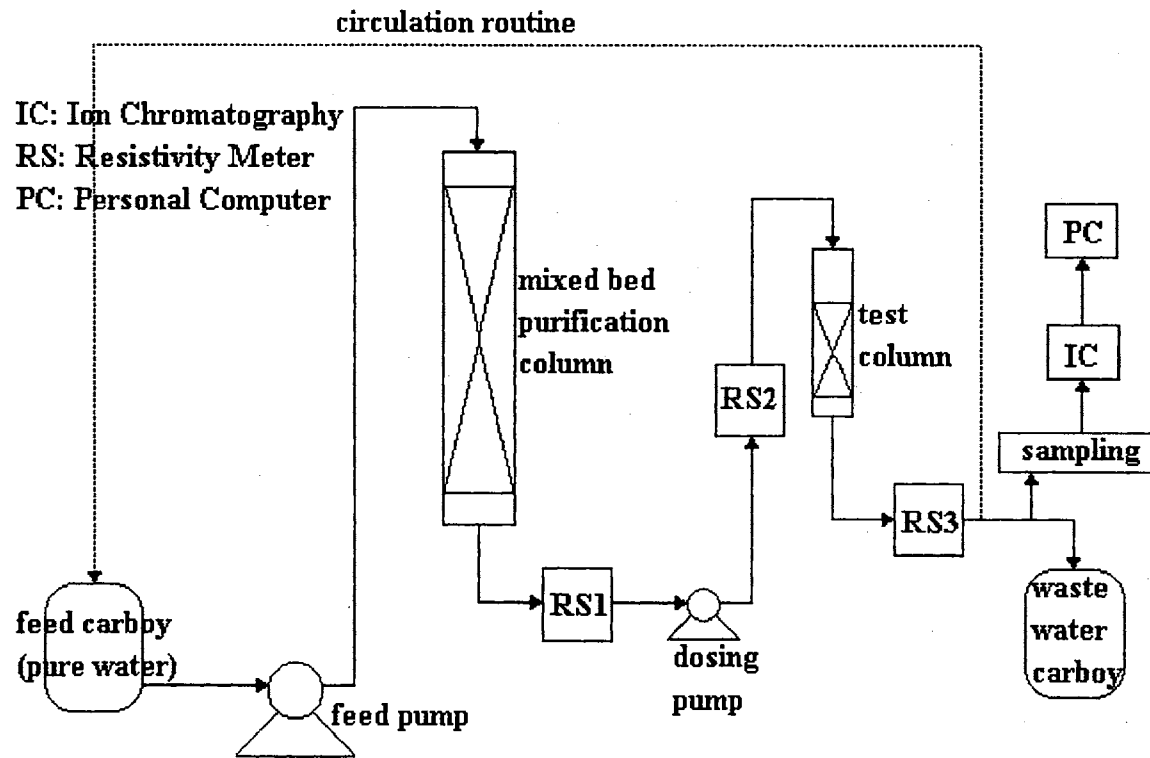
Figure 33. Flow Diagram for Mass Transfer Coefficient Experiment
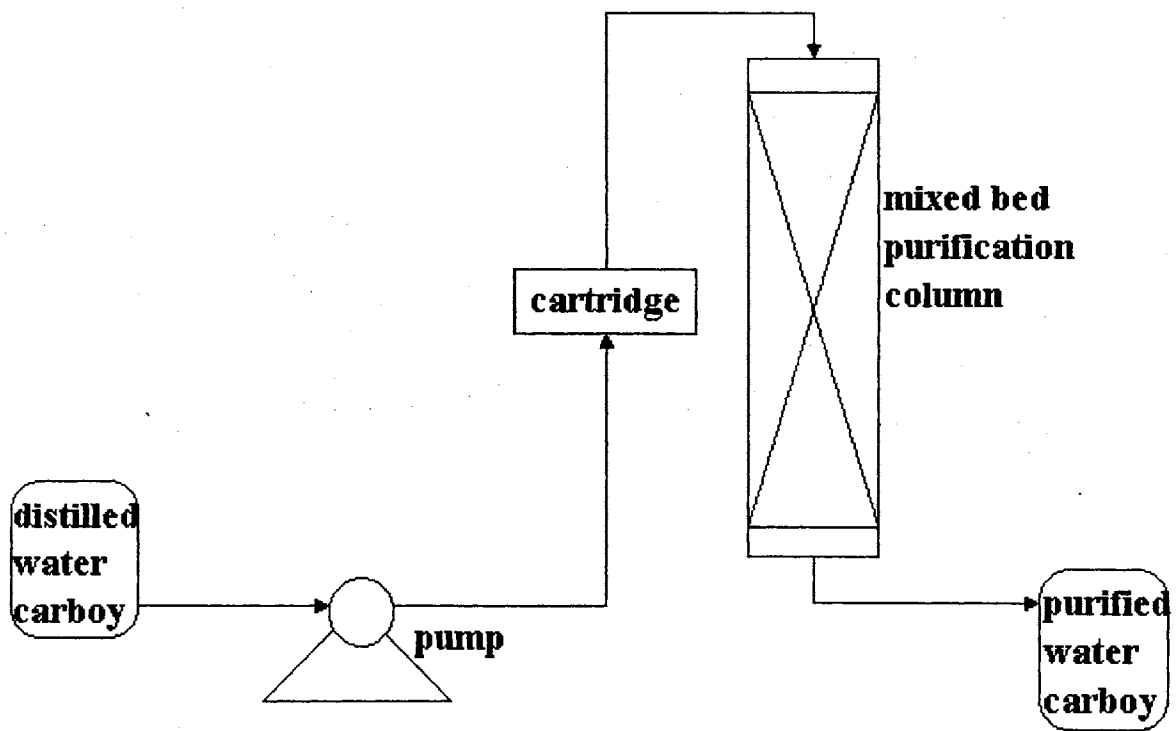
Figure 34. Flow Diagram for Water Purification Process

the resistivity (RS3 in Figure 33) of the water became 16.8 megaΩ-cm. Theoretically, resistivity of deionized water is 18.3 megaΩ-cm. However, the observed resistivity was 18.3 megaΩ-cm in RS1 and 2, after deionization through the circulation routine in Figure 33. Therefore, it was concluded that the lower resistivity in RS3 comes from air bubbles or eddies inside the Pyrex resistivity censor holder. In order to make sure of water purity, 16.8 megaΩ-cm water in RS3 and 18.3 megaΩ-cm in RS1 were analyzed by ion chromatography before every experiment. There were no ions detected in that water.

The ion chromatograph was controlled by a personal computer connected with an interface using Dionex software already installed. The ion chromatograph and the analysis of effluent samples are described in Appendix C.

Test Column

The test column used in this study was Pyrex glass made by the Materials Laboratory at Oklahoma State University. Because Pyrex is transparent, the flow distribution and the resin bed condition inside the column could be checked. The resin supporter was a sponge. The size of the column was one inch inside diameter $\times$ 18 inch length $\times$ 0.13 inch wall thickness (2.54 cm $\times$ 46 cm $\times$ 0.32 cm). The inlet and outlet diameter of the test column was 0.5 inch.

Before the experimental run was started, the deionized water was filled to at least 20 cm above the top level of resin in the test column. This was to give uniform distribution of feed solution through the resin bed and prevent floating the resins in the top portion of the column. Floating separates the mixed resins. The air inside the resin bed was removed by tapping the outside column wall.

Ion Exchange Resin

Two types of Dowex resins were used in this study, Monosphere 650C-H and HGR-W2-H for cation resin, and Monosphere 550A-OH and SBR-P-C-OH for anion resin. Both resins are made by copolymerization with polystyrene and divinylbenzene. The new resins were provided by the Dow Chemical Company, and the used resins were sampled from two different PSO's plants. Table II shows the plant location sampled and dates of the used resins. Tables III and IV show the physical properties of both types resins.

Before the new and used resins were used, the resins were regenerated by the concentrated regenerants for cation and anion resins separately. The regeneration step was needed to ensure the H^+ form on cation resins and the OH^- form on anion resins. However, the foulants on the used resin were not removed. The regeneration process is described in detail in Appendix B.

Accessories

The auxiliary equipment for this experimental study included resistivity meters, pumps, cartridge, carboys and a personal computer. The ion chromatograph is explained in detail in Appendix C. Table XIII shows the list of equipment. The syringe pump, which was used as a dosing pump, made it possible to feed the solution of very low influent concentration. The calibration curves for chloride and sodium were prepared for the concentration range between 14.9 and 835 ppb for chloride and between 9.66 and 542 ppb for sodium. These very low concentration solutions for the calibration were made with the syringe pump. The calibration curves for both chloride and sodium are described in Appendix C. The pipe and fittings were bought from Orion Corporation, and were made of contaminant resistant polyethylene. The inside diameter was 0.5 inch.

TABLE XIII

LIST OF EQUIPMENT

Equipment	Unit	Capacity	Manufacturer
resistivity and temperature probe (RS 1 and 2)	2		Signet Sci.
resistivity and temperature probe (RS 3)	1		Thornton Associates, Inc.
resistivity monitor	2		Signet Sci. (RS1 & 2) Thornton Associates, Inc. (RS3)
carboy	2 2 1	50 liter 30 liter 10 liter	Nalge Comp.
sampling bottle	50	110 ml	
piston pump	1	60 liter/hr	Madden Corp.
syringe pump (SAGA Model 341B)	1	min. 0.00011 μl/hr max. 20 ml/hr	Orion Research Inc.
syringe		plastipak 10 ml	Becton-Dickinson Corp.
cartridge	1		Corning Megapure
personal computer	1	AT	Assembled in PC Tech

The size of the mixed bed purification column was 3 in. inside diameter × 48 in. height and 41 in. bed depth and its size in main experimental system was 3 in. inside diameter × 42.5 in. height and 29.5 in. bed depth. Monosphere resins were used.

APPENDIX B

EXPERIMENTAL PROCEDURES

Several steps were needed before the main experiment was carried out; the preparation of deionized water, the preparation of feed solution, the separation of mixed resins and the regeneration of resins. The preparation of deionized water is showed in Figure 34. This chapter describes the resin separation, the regeneration process and the experimental procedure of the main experiments. These procedures are almost the same as those used by Harries (1986). Harries' experimental procedures were adopted because of their extensive use and simplicity. In addition, the procedures are necessary to compare the experimental results with Harries' results.

Separation of Mixed bed

Used resins samples from PSO were sent as mixed resin. Therefore, the resins had to be separated prior to regeneration. Separation was achieved by feeding deionized water upward through a column of resin. Figure 35 shows the flow diagram for resin separation. First, the appropriate amount of mixed resins was loaded into a reactor bed of 1.9 in. inside diameter × 15.7 in. height. Deionized water from a carboy was fed at the rate of about 150 ml/min to backwash. The mixed resins were separated for at most 10 minutes. Because of the density difference of cation and anion resin, anion resins were located in the upper portion of the reactor. Finally, anion resins were collected by a siphon
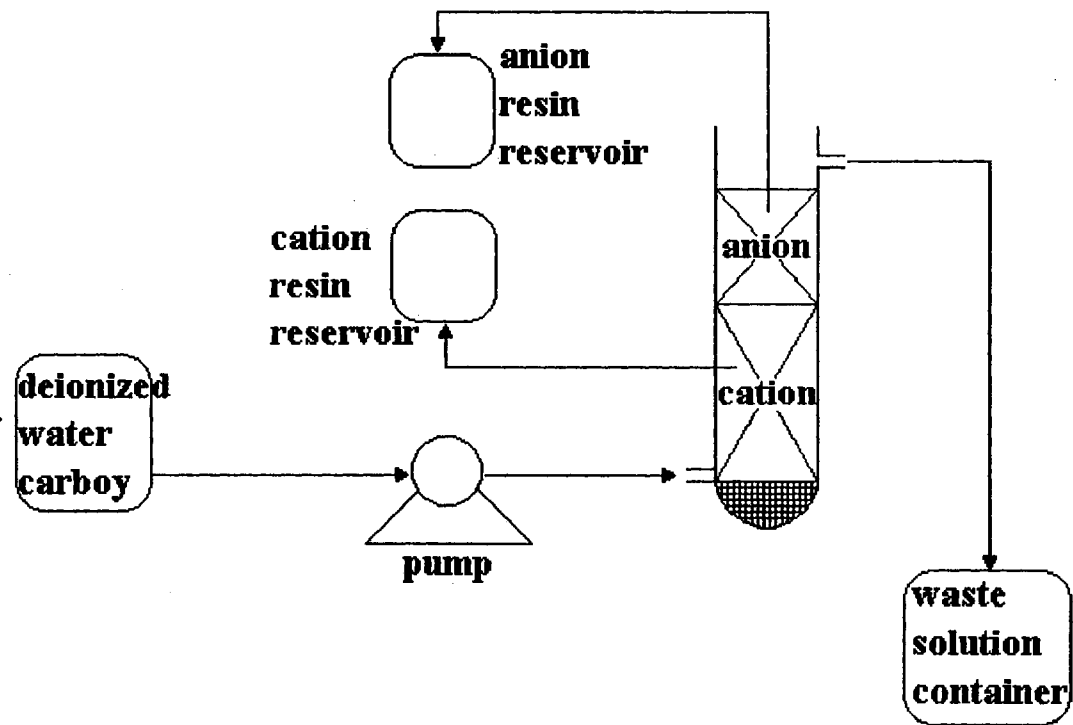
Figure 35. Flow Diagram for Resin Separation

technique with a teflon tube. The resins near the cation-anion interface were discarded. The collected resins were stored in plastic bottles before regenerating.

Regeneration Procedure

All new and used resins were put through the regeneration process to ensure a standard ionic form, and to rinse residues that can be present in new resins. All new anion resins were received in hydroxide form, and all new cation resins in hydrogen form. Figure 36 shows the regeneration system. Regenerants, HCl for cation resins and NaOH for anion resins, were dosed through port A of the reactor with a specific flow rate. The reactor was the same as that used in resin separation and all lines were made of 1/4 in. tube. After regeneration, the resins were rinsed with deionized pure water by backwash through port B until outlet conductivity from port A was lesser than 5 μScm^{-1}. The resins, whether new or used, were all regenerated in an identical manner. The following is the step by step regeneration procedure for cation and anion resins.

<u>Cation resin</u>

Step 1: 300 ml cation resin was loaded into the reactor.

Step 2: The resins were backwashed with one liter deionized water through port B of the reactor

Step 3: 0.75 liter of 1 M HCl solution was fed into the reactor through port A at 85 ml/min.

Step 4: 600 ml of deionized water was fed through port B at the same flow rate as Step 3. The amount of solution and deionized water needed in Step 3 and 4 can be changed depending on the amount of loaded resin in the reactor. The regenerant solution is needed in the ratio of 4 liter resin to 10 liter of 1

regenerant
solution
carboy

pump

deionized
water
carboy

pump

A

cation or
anion resin
bed

RS

B

---------- flow path for rinsing
RS:resistivity meter

waste
solution
container
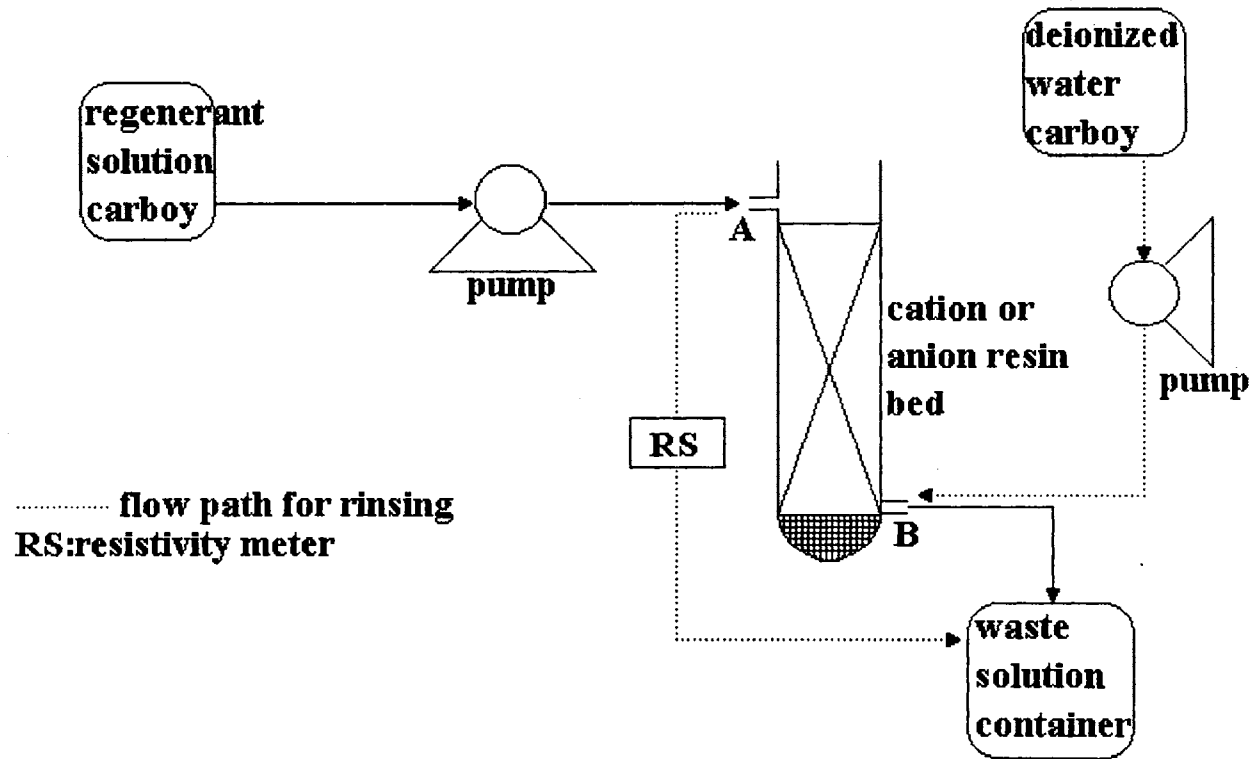
Figure 36. Flow Diagram for Regeneration Process

M HCl solution and 2 resin bed volumes of the deionized water are used to rinse.

Step 5: Deionized water was continuously fed into the reactor through portion B at 150 ml/min until the conductivity of effluent from the reactor is lesser than 5 μScm^{-1}.

Step 6: The regenerated and rinsed resins were stored in a polyethylene bottle with deionized water for future use. The resins were used within one month to avoid contamination with chemicals in the bottle, like carbon dioxide.

Anion resin

Step 1: The same as that in cation resin case.

Step 2: The same as that in cation resin case.

Step 3: 0.33 liter of 1 mole of NaOH solution was fed into the reactor at 85 ml/min. The amount of regenerant solution was calculated by Harries' procedure. Harries used 1 liter of 1 M NaOH solution per liter resin.

Step 4: The same as that in cation resin case.

Step 5: The same as that in cation resin case.

Step 6: The same as that in cation resin case.

Experimental Procedure

The feed concentrations in this study were very low (Table I), and it was difficult to make the solution under 1 ppm. In addition, minimizing water contamination was essential for accurate experimentation. These problems were solved by using a syringe pump and on-line purification as explained in Appendix A. Before starting an experimental run, a test bed and concentrated feed solution were prepared. Special attention was given to the preparation of the mixed bed, because the densities of cation and anion resins were different, and it is not easy to

mix both resins well. The following describes the experimental procedure step by step.

Step 1: About 50 liters of deionized water was prepared by passing distilled water through a mixed-bed ion exchange purification column, as in Figure 34.

Step 2: The deionized water made in Step 1 was continuously circulated until the resistivity in RS1 and 2 approached to 18.3 megaΩ-cm. The second deionization was also achieved by a mixed bed purification column. During circulation, the test column was removed to prepare the mixed bed. To make sure of water purity, the secondary deionized water was injected into the ion chromatography.

Step 3: During the preparation of make-up water, a mixed bed and concentrated feed solution were made. Resin is mixed generally by inert gas passing upward through a test column. However, the mixed bed in this study was prepared using a measuring spoon in a 100 ml beaker because the amount of resin was small. The amounts of cation and anion resins needed in a mixed bed were 40 and 20 ml, respectively. The amounts of resins were measured with a 25 ml capacity measuring cylinder, removing the resins from a reservoir by siphon, and pouring into the beaker. Deionized water coexsisting with the resins in the beaker was removed by syringe. This was necessary because the resins immersed in water could not be mixed appropriately due to density difference. The resins in the beaker were mixed slowly with a measuring spoon. The degree of mixing could be checked by color, because both resins have different colors. The mixed or single resins were poured cautiously into a test column without extra water using a measuring spoon. To pack the mixed resin uniformly and tightly in the test bed, deionized water was filled at least 20 cm past the resins and the column was tapped several times until the loaded resins were steady.

This procedure was needed to prevent channeling and remove air bubble between resins. The concentrated feed solution was prepared to match seven influent concentrations with flow rate and dosing level of the syringe pump. The concentrated feed solution was placed in the 10 ml syringe for injection.

Step 4: The single or mixed bed prepared in Step 3 was connected in the proper location in Figure 24 during temporary stop of the feed pump.

Step 5: Without dosing the concentrated solution, the test bed was rinsed again by deionized water prepared in Step 2 at the operating flow rates until resistivity in RS1 became 18.3 megaΩ-cm.

Step 6: The flow rate was measured with a 1 liter measuring cylinder between every sampling to make sure that it was steady.

Step 7: The dosing pump was turned on at a certain flow level which corresponds to the lowest influent concentration.

Step 8: When the resistivity in RS3 was constant, effluent was sampled in a polyethylene bottle . During this operation, the resistivity of pure water was checked in RS1 continuously to make sure of its purity and the uniform influent concentration was checked by RS2. The time which was needed to get uniform effluent resistivity was measured by a stop watch. It took at most 4 minutes. In addition the flow rate was measured between each effluent sampling by a measuring cylinder.

Step 9: After first sampling, the flow level of syringe pump was changed to higher level and the same procedure of step 8 was carried out. This was repeated until the runs for seven different influent concentrations were finished.

Step 10: For the experiment at different flow rates, the system was shut down and the resin was changed to another resin. Step 1 through 9 were repeated.

Step 11: The collected samples were analyzed within three days by ion

chromatograph.

APPENDIX C

ION CHROMATOGRAPH

The effluent samples from the experimental column were analyzed by a
Dionex Series 4500i Ion Chromatograph (IC). This chapter describes the IC, the
preparation of chemicals needed in IC, the operating procedure and the calibration
curves for cation and anion concentrations.

Equipments of Ion Chromatograph

Dionex Series 4500i Ion Chromatograph is designed for dual-system
operation to measure cation and anion concentrations simultaneously. IC consists
of a injection pump, a Gradient Pump, a Conductivity Detector-II, an Advanced
High-Pressure Chromatography Module, an Advanced Computer Interface and an
Eluant Degas Module for cation and anion separately. The Gradient Pump is used
to load eluant solution into a column. It is designed to load accurately up to four
different eluant solutions and mix at programmed flow rate by a microprocessor-
based eluant delivery system. The Conductivity Detector-II can automatically
offset background conductivity up to 1600 μS and compensate for conductivity
variation due to temperature. The Advanced High-Pressure Chromatography
Module consistes of a column and a micromembrane suppresser. The injection
pump is used to injecting the sample into IC.

The IC was controlled and operated by Dionex software, named as AutoIon

450 Data System (AI-450 version 3.2) and installed on an AT computer, through the Advanced Computer Interface. The software was utilized through Microsoft Window version 3.0. The IC was operated by schedule and method files which were already programmed in the software. The method file is to control all systems of the IC and the schedule file is to define the method file and data files for saving results. The software collects automatically all data and calculates peak areas. The detection level of this IC was 0.2 ppb of sodium and 0.3 ppb of chloride.

Preparation of Eluant and Regenerant

Eluant is used as the carrier of ions through a column. The mixture of 1.8 mM sodium carbonate and 1.7 mM sodium bicarbonate was used as anion eluant, and the mixture of 27.5 mM hydrochloric acid and 2.25 mM DL-2,3-diaminopropionic acid monohydrochloride as cation eluant. The flow rates of anion and cation eluants were 2.0 and 1.0 ml/min, respectively. Four plastic bottles of 1.5 liter capacity, two bottles for each ion, were used to store cation and anion eluant solution. The anion eluant was prepared by diluting 10 ml of concentrated AS4A eluant to 1 liter with deionized water. The concentrated eluant was made by dissolving 9.54 g sodium carbonate and 7.14 g sodium bicarbonate in a 500 ml volumetric flask and making up to 500 ml with deionized water. The cation eluant was prepared by diluting a mixture of 25 ml of DAP stock solution and 25 ml of 1 M HCl to 1 liter with deionized water. The DAP stock solution was made by dissolving 0.141 g DAP in 100 ml deionized water. The cation and anion eluants were stored in two bottles with the same concentration eluant, respectively, and fifty percent eluant of needed volume from one bottle was mixed with 50 % eluant from the other bottle through inert solenoid valves. The

percentages can be altered depending on eluant concentrations in each bottle. The outlets from the valves were combined in the manifold and fed to the gradient pump through the gradient mixer.

Regenerant is used to regenerate an IC column. 0.025 M sulfuric acid solution was used as anion regenerant and 70 mM tetrabutylammonium hydroxide as cation regenerant. The flow rates were 2.5 for anion and 5.0 ml/min for cation. The anion regenerant was prepared by diluting 100 ml of 0.5 N H_2SO_4 to 1 liter with deionized water. 0.5 N H_2SO_4 was made by diluting 7 ml of 36 N H_2SO_4 to 500 ml with deionized water. The cation regenerant was made by diluting 100 ml of TBAOH to 2 liter with deionized water. Two 4 liter plastic bottles were used as reservoirs of cation and anion regenerant. The used cation regenerant was collected, treated by an Auto Regeneration System provided from Dionex and reused because the price of TBAOH was expensive. The Auto Regeneration System consistes of a electric metering pump of 6 GPD maximum outlet (from PULSAtron), a Auto Regeneration Cation Cartridge and two plastic bottles which are reservoirs for used and treated regenerant. The outlet cation regenerant was stored in 1.5 liter plastic bottle, and was regenerated by the auto regeneration system connected with the bottle. The treated regenerant was poured into the reservoir of cation regenerant in IC. Table XIV shows the characteristics of chemicals used for regenerant and eluant.

Nitrogen and helium were used to degas eluant bottles and pressurize the eluant and regenerant reservoirs. The degassing procedure was necessary to prevent air bubbles from loading into the Gradient Pump and valves. If bubbles were loaded into the Gradient Module, the Gradient Pump can not work or be operated at optimum condition. This phenomenon happened sometimes, even though the Degas Module was used. It was due to shut down period, and the air

bubbles were removed by manual technique from Dionex operating manual and the discussion with an IC technician from Dionex.

TABLE XIV

CHARACTERISTIC OF CHEMICALS FOR REGENERANT AND ELUANT

name	assay	service	manufacturer
DAP*	99 %	cation eluant	Fluka Chemie
hydrochloric acid	36.5 - 38 %	cation eluant	Fisher Sci.
sodium bicarbonate	99 %	anion eluant	Fisher Sci.
sodium carbonate	99 %	anion eluant	Fisher Sci.
sulfuric acid	95 - 98 %	anion regenerant	Fisher Sci.
TBAOH*	55% aqueous solution	cation regenerant	Southwestern Analytical Chemicals Inc.

* DAP : DL-2,3-Diaminopropionic Acid Monohydrochloride
  TBAOH : Tetrabutylammonium Hydroxide

Operating Procedure of IC

The procedures of start up, software operation and shut down was carried out by the following steps.

Step 1: Screw tightly the caps of eluant and regenerant bottles to prevent gas leakage.

Step 2: Turn on the valves of helium and nitrogen gas cylinder.

Step 3: Turn on the system switch of eluant degas module.

Step 4: After 20 minutes, the two mode switches for cation and anion eluants in the are changed from sparge to pressure position.

Step 5: After 10 minutes, the gas cylinder valves are turned off and gas leakage from six reservoirs of eluants and regenerants is checked. If there is not leakage, the valves will be turned on again.

Step 6: The pressures for the eluant and regenerant bottles are checked in the pressure gauges. The pressure for eluant and regenerant bottles is fixed to between 5 and 10 psi.

Step 7: The AT computer is turned on. It is connected with the Advanced Computer Interface (ACI) and has the installed AI-450 software.

Step 8: Type "widx" in C prompt and select "run" icon.

Step 9: The main switch of ACI is turned off and on immediately. This is necessary to connect electrically between ACI and AI-450 software.

Step 10: Load schedule files for both cation and anion analyses if the dual operating system is needed.

Step 11: All numbers on front panel of the gradient pump module are assured basing on the selected method files. The operating pressure of the gradient pump is about 870 psi for anion port and 1000 psi for cation port. The minimum pump pressure is 100 psi, and the maximum is 1500 psi for cation and anion. Thus if pump pressure was below minimum or over maximum pressure, the gradient pump module stops its operation and IC does not work. This phenomenon was happened sometimes because of the penetration of air bubbles into the gradient pump module.

Step 12: IC is warmed up until the conductivities in the conductivity detectors for cation and anion are fixed to almost constant numbers, about 20.0 μScm^{-1} for anion and 7.0 μScm^{-1} for cation. It takes about 1 hour.

Step 13: In order to wash out ionic contaminants that can exist in the gradient pump, mixer and lines of IC, the pure deionized water was injected 2 or 3 times. The base line of conductivity in real-time analysis through a

computer monitor showed some fluctuation for the first injection. However it became steady for next injections. The injection is carried out by clicking on "run" in menu.

Step 14: All prepared samples are analyzed. The every resulting graphs of time to conductivity for cation and anion are saved in data files which are assigned in schedule files. The data files are used to calculate peak area in the future. The calculation of peak area in data files are carried out in "optimize" menu of AI-450 software.

Step 15: The deionized water is injected 2 or 3 times to clean out all parts of IC used after analyzing all samples.

Step 16: After finishing step 14, IC is stopped by pushing "abort" button on ACI or in a menu of AI-450.

Step 17: The two gas cylinders are turned off.

Step 18: The mode switches for cation and anion eluants in the eluant degas module are changed from pressure to sparge position.

Step 19: The system switch in eluant degas module is turned off.

Step 20: The caps of eluant and regenerant bottles are opened and then closed tightly. This is for releasing the pressure applied and preventing the penetration of contaminants in air during shut-down period.

Step 21: The main switch in ACI is turned off and on immediately.

Step 22: Close the AI-450 software.

Calibration Curves

The peak areas calculated for both cation and anion by the AI-450 were converted to actual concentrations using calibration curves. The calibration curve was made in the concentration range between 14.9 and 835 ppb for chloride, and

between 9.66 and 542 ppb for sodium. Because this concentration ranges were relatively wide, one calibration curve made for the whole range can cause large errors especially for the concentration range under 100 ppb. Therefore, the ranges were separated to low and high concentration ranges and the calibration curves for both ranges were prepared. Thus, two calibration curves were made for anion and cation, respectively. For chloride, these ranges were 14.9 and 111 ppb and 196 and 835 ppb. For sodium, the ranges were 9.66 and 72.3 ppb and 127 and 541 ppb. Table XV shows the actual concentrations used to make the calibration curves. Figure 37 through 40 show the sample curves for cation and anion which were used in the actual calculation. The curves were made for the relationship between peak area and actual concentration, and the straight lines were determined by first order least square method using a software, Grapher. Four equations for cation and anion in the above concentration ranges were determined. The equations for curves were used to convert peak areas of analyzed samples calculated in AI-450 to actual concentrations.

The solutions expressed in Table XV were made by the same procedure as the experimental procedure without a test column. The syringe pump made it possible to prepare the solutions of very low concentration under 100 ppb. The deionized water flow rate of 500 ml/min was applied to make the solutions for calibration curves dosing the appropriate amount of concentrated NaCl solution through the syringe pump. The calibration curves were newly prepared whenever the IC was started up. It was necessary because the system conditions of the IC could be changed whenever the IC was started. The different system conditions could give different calibration curves. Actually, the calibration curves which were determined at each IC start-up were a little different each time, thus the different curves could give different concentration for a certain peak area.

TABLE XV

CONCENTRATIONS USED FOR MAKING CALIBRATION CURVES

cation (ppb of sodium)	anion (ppb of chloride)
9.66	14.9
16.9	26.1
23.7	36.5
35.7	55.0
48.2	74.3
72.2	111
127	196
177	273
268	413
362	557
542	835
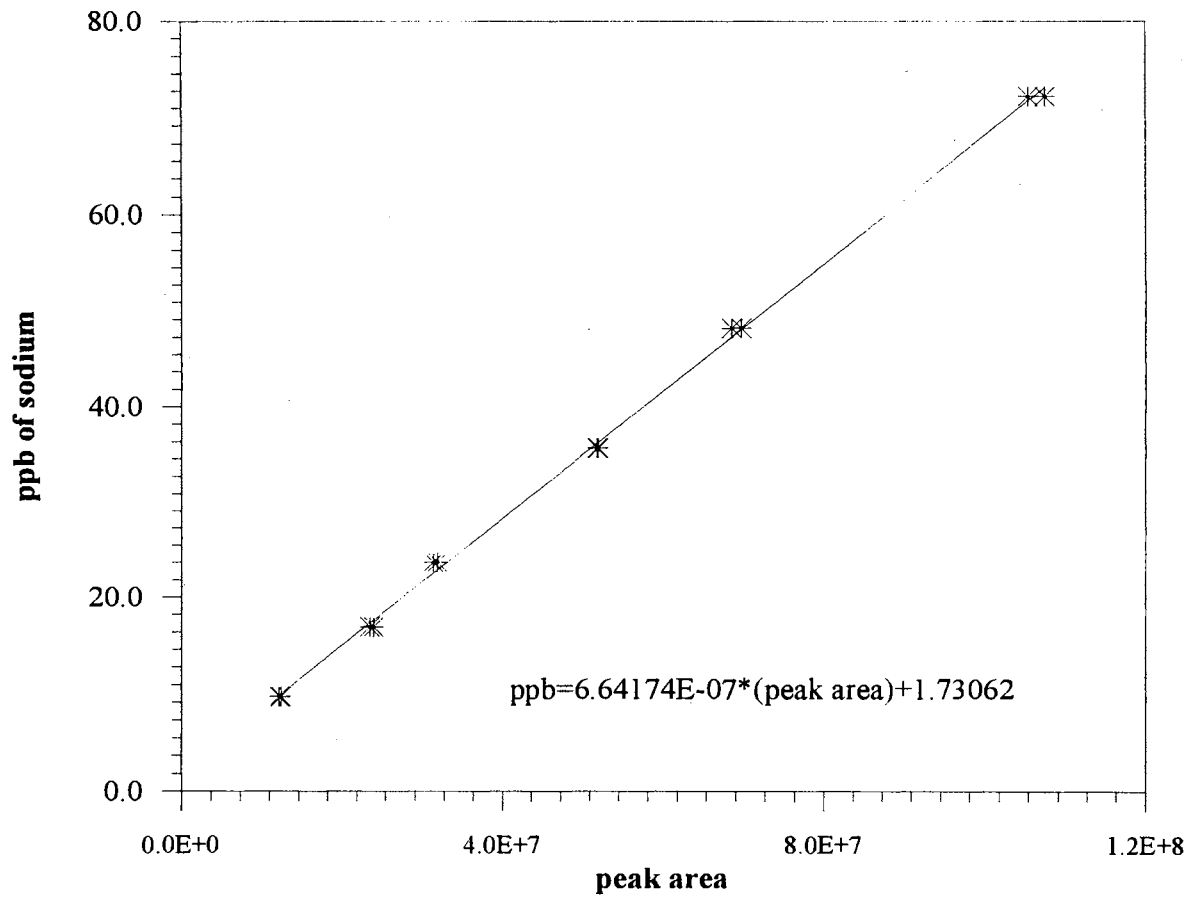
Figure 37. Calibration Curve of Sodium for Concentration Range from 9.66 to 72.3 ppb

$$ppb=5.48821E\text{-}07*(peak\ area)+27.7196$$
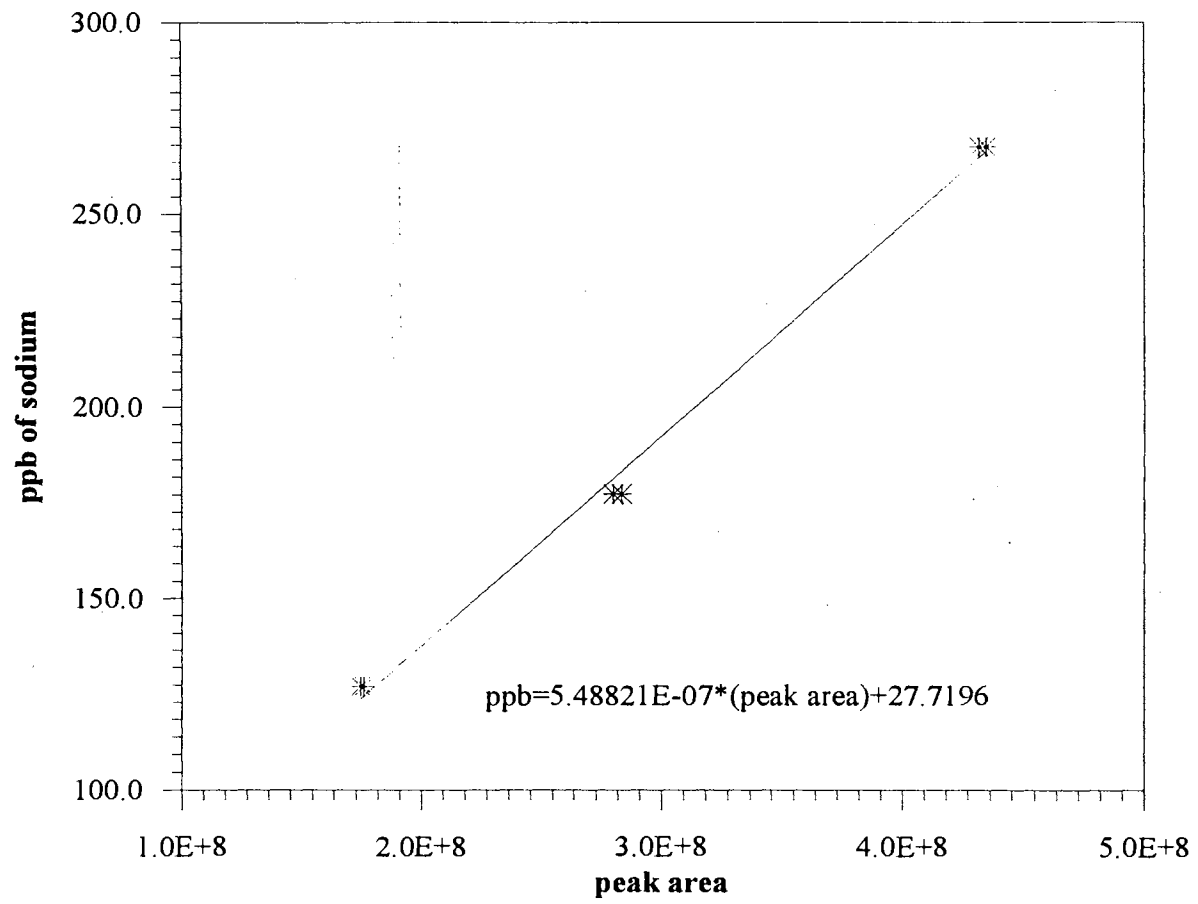
Figure 38. Calibration Curve of Sodium for Concentration Range from 127 to 541 ppb

120.0

100.0

80.0

ppb of chloride

60.0

40.0

20.0

ppb=1.28086E-06*(peak area)+10.3604

0.0

0.00E+0   4.00E+7   8.00E+7   1.20E+8

peak area
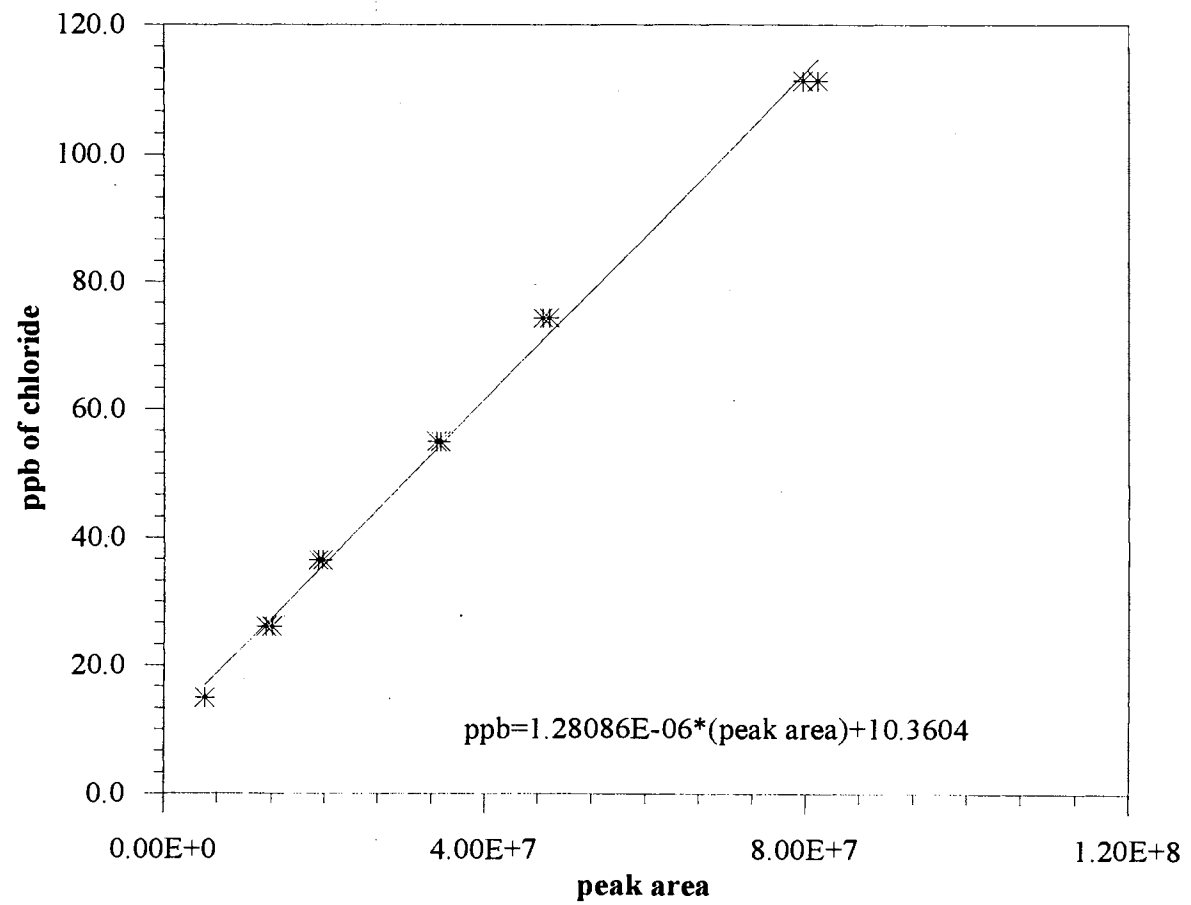
Figure 39. Calibration Curve of Chloride for Concentration Range from 14.9 to 111 ppb

$$ppb=1.24338E\text{-}06*(\text{peak area})+10.8003$$
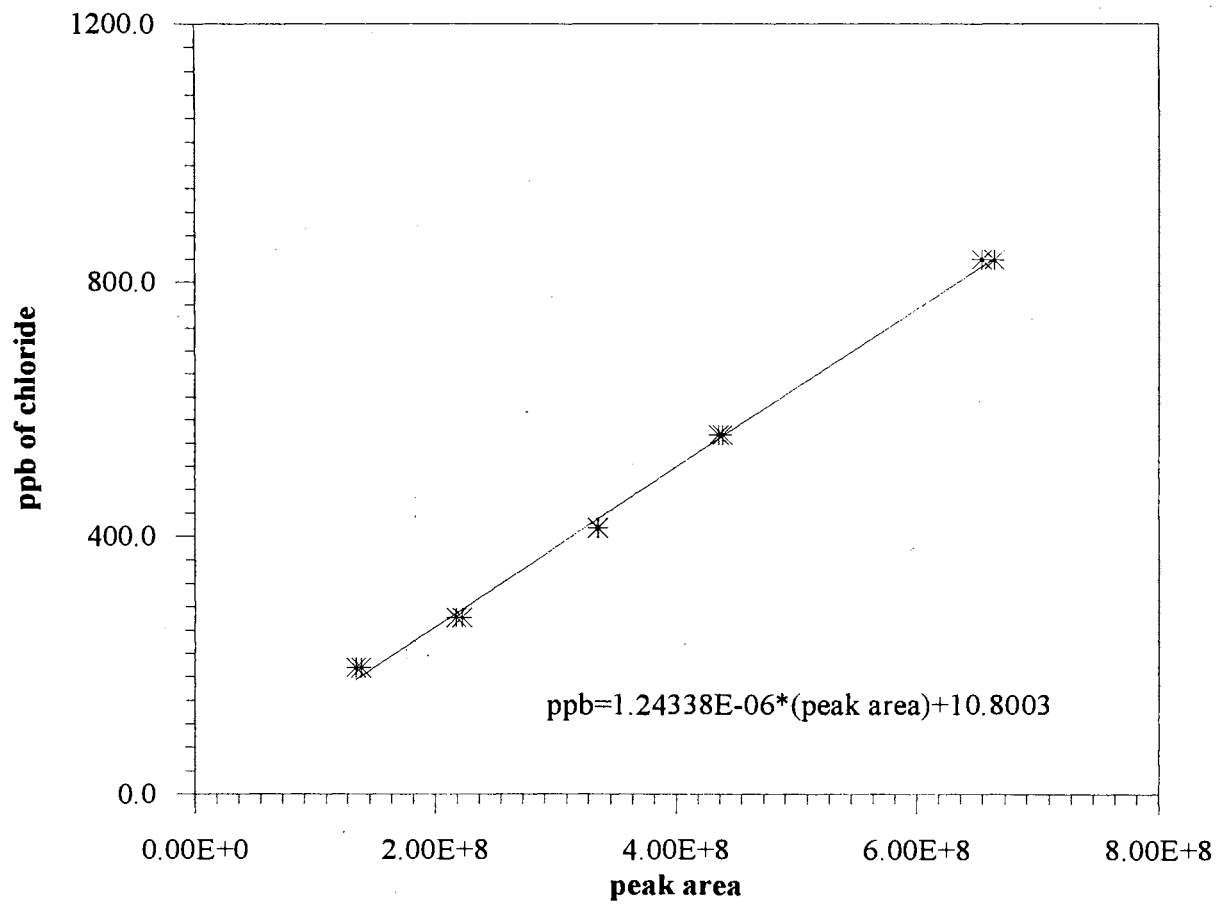
Figure 40. Calibration Curve of Chloride for Concentration Range from196 to 835 ppb

APPEDIX D

ERROR ANALYSIS

The errors in this study can be caused three ways. They are: the errors from the measurements of particular quantities, the experimental system, and the analysis of samples by IC. The sources of the measurement uncertainties are the weighing of NaCl needed to make concentrated solution and the measurements of resin volume and bed depth. The sources of the experimental system errors are the inaccuracies of flow rates from dosing and feeding pumps.

Experimental Error

The errors from measurement, experimental system and the reproducibility of data are discussed in this section. The crystal sodium chloride was weighed with a electronic digital balance, model AE 100 from Mettler. The balance could measure a weight up to four decimal points. The amount of NaCl needed in this study was usually less than 1 gram, and the error by digital reading was ± 0.0002 g for measuring a certain weight. The maximum relative error was 4.8 %.

The measurement of wet resin volume was carried out with a 25 ml measuring cylinder. The error was estimated to be half scale of the measuring cylinder. It was equivalent to ± 0.5 ml. Therefore, the maximum estimated relative error was 2.5 %. The measurement of bed depth in a test column was conducted after the procedure of removing air bubbles and making the resin

portion compact explained in Appendix B. The error was estimated to be ± 0.1 cm, and it was equal to the maximum relative error of 1.3 %.

The error from the feeding pump was estimated by the repeated measurements of effluent of test column with a 1 liter measuring cylinder and stop watch during the experimental run. The error depended on flow rate because the pump can be a little unstable at high flow rate. The errors were ± 20 ml at 900 ml/min and ± 10 ml at 500 and 700 ml/min. They were equivalent to 2.2 %, 2.0, and 1.4 %, respectively. The error from dosing pump could not be estimated practically. It was given by the manufacturer as ± 10 %. The errors from resistivity meters were not estimated because the absolute values of resistivity were not utilized in the calculation procedure of mass transfer coefficient. Bed porosity was given as a range by the manufacturer (Tables III and IV), and medium value of the range was used for calculation. The bed porosity affects specific surface area in Equation (20). Thus, in the case of Monosphere resins, the maximum and minimum relative errors in mass transfer coefficient due to boundary values of the bed porosity were ± 1.52% for both cation and anion resins, respectively. The minimum relative error was 0.75% for SBR-P-C-OH and HGR-W2-H resins. The smaller relative error for HGR-W2-H and SBR-P-C-OH resulted from smaller difference between maximum and minimum porosities than Monosphere resin.

The errors discussed above affect mass transfer coefficient. The effects of the uncertainties of pure water flow rate and bed depth to mass transfer coefficient were the same as the relative errors of each variables because the variables are linearly related with mass transfer coefficient and have constant values for a experimental run. However, the effect of the uncertainty of the dosing pump flow rate to mass transfer coefficients depends on the influent concentration, and it is related to the logarithm of the mass transfer coefficient. Therefore, the errors in

mass transfer coefficients are different with all influent concentrations. Equation (D-1) expresses the relative error of mass transfer coefficient due to the error from influent concentrations when other variables in equation (20) are constant. As a sample calculation, if the mass transfer coefficients of anion and cation are 2.518 and $1.717 \times$E-04 m/s at 1000 ppb of chloride and 1590 ppb of sodium, respectively, the errors in mass transfer coefficient will be between + 4.8 and - 4.3 % for chloride and between +3.9 and - 3.5 % for sodium. Thus, the deviations from original values were between + 0.121 and - $0.108 \times$E-04 m/s for chloride and between + 0.067 and - $0.06 \times$E-04 m/s for sodium.

$$\% \text{ Error} = \text{between } \frac{\ln 1.1}{\ln C_i^{\text{eff}} - \ln C_i^f} \times 100 \text{ and } \frac{\ln 0.9}{\ln C_i^{\text{eff}} - \ln C_i^f} \times 100 \qquad \text{(D-1)}$$

These sources of uncertainties are combined to give maximum and minimum mass transfer coefficients for each data point. The maximum and minimum values of mass transfer coefficients are expressed by following equations.

$$k_{\text{max}} = -\frac{V_{\text{max}}}{S_{\text{min}} Z_{\text{min}} AR_i} \ln \frac{C_i^{\text{eff}}}{\left(C_i^f \right)_{\text{max}}} \qquad \text{(D-2)}$$

$$k_{\text{min}} = -\frac{V_{\text{min}}}{S_{\text{max}} Z_{\text{max}} AR_i} \ln \frac{C_i^{\text{eff}}}{\left(C_i^f \right)_{\text{min}}} \qquad \text{(D-3)}$$

Maximum and minimum values of variables in Equations (D-2) and (D-3) are obtained from combining independent uncertainties of each variable. The maximum and minimum relative errors were 12.6 and -12.6 %, respectively, and

most relative errors were between ± 7 and ± 9 % in average. These errors of mass transfer coefficients were listed in Table XX (Appendix E).

Reproducibility was estimated by conducting the same run twice and conducted for mixed beds of new Monosphere resin at 700 ml/min and 900 ml/min, and used Monosphere resin from Riverside number 2 condensate polisher at 700 ml/min. Figures 41 and 42 show the sample results of the duplicated experiments for cation and anion, respectively. The maximum differences between the runs were 3.7 % at 700 ml/min and 15.4 % at 900 ml/min for new cation resin, and 4.9 % at 700 ml/min and 1.9 % at 900 ml/min for new anion. For used resin at 700 ml/min, the maximum differences were 11.1 % for cation and 6.0 % for anion. The average differences were 2.3 % at 700 ml/min and 6.5 % at 900 ml/min for new cation resin, and 2.8 % at 700 ml/min for used cation resin. For anion, the average differences were 3.0 % at 700 ml/min and 0.9 % at 900 ml/min for new anion resin, and 2.6 % at 700 ml/min for used resin.

Analytical Error of Effluent Samples

The analytical error of effluent samples was estimated by the repeated measurements of a certain sample with IC. The reproducibility of peak area was used as the criterion of analytical error. The peak area of a certain concentration depends on the method file used in the IC. The method files for cation and anion analyses used in this study were programmed to have run times of 5 minutes, and named CATIONS3.MET and ANIONS4.MET, respectively. Table XVI shows the peak areas measured repeatedly, the deviations from arithmetic mean peak area and the standard deviations for a sample. The maximum absolute deviation from arithmetic mean was 0.362 % and the percentage standard deviation were 0.332
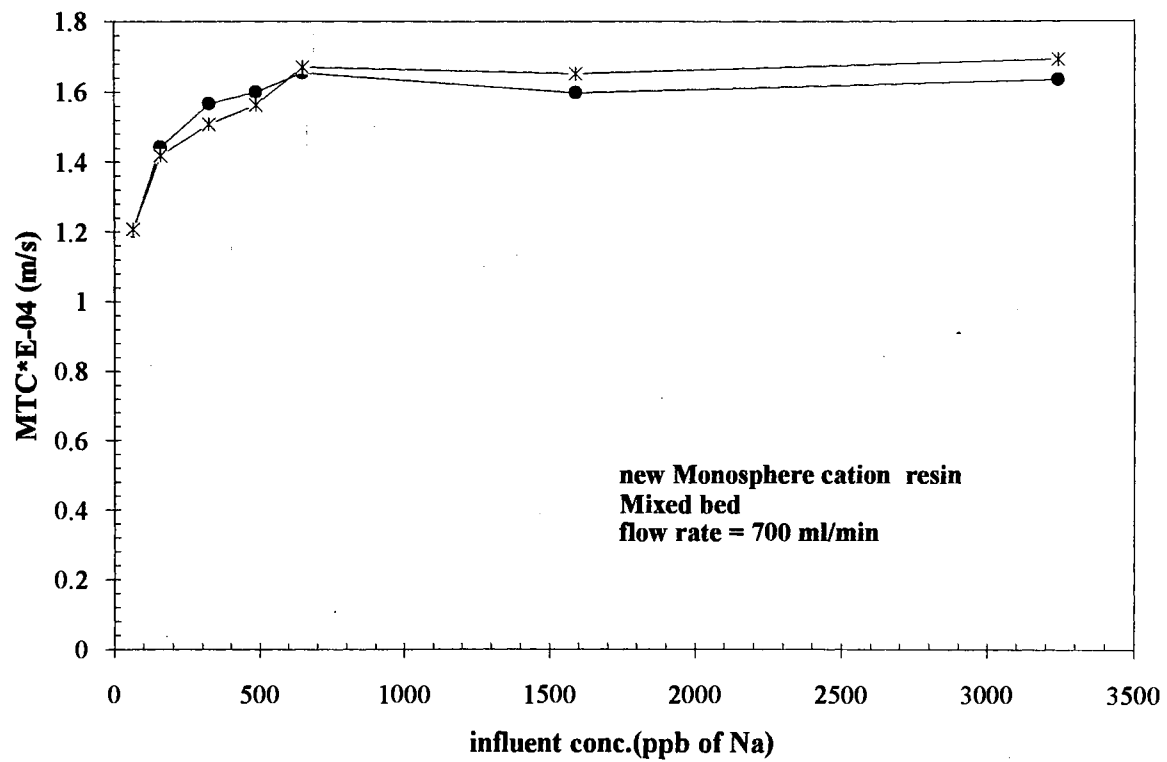
Figure 41. Reproducibility of Mass Transfer Coefficient Experiments for
Sodium
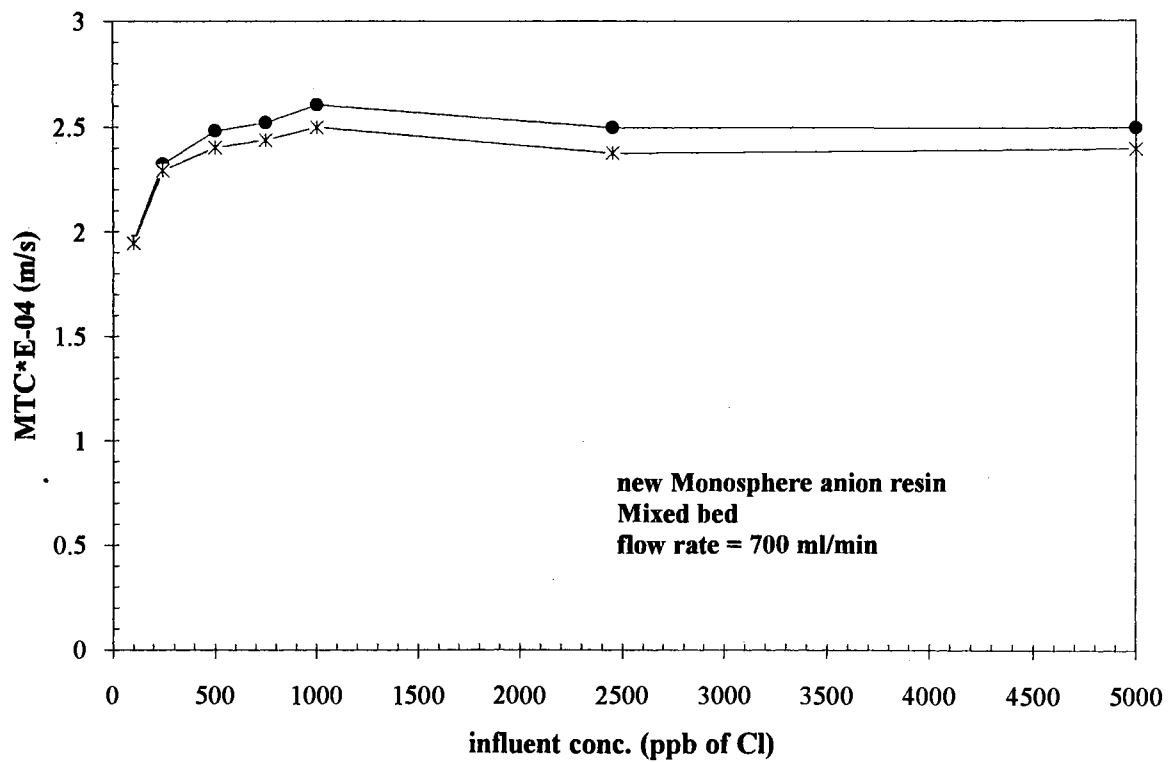
Figure 42. Reproducibility of Mass Transfer Coefficient Experiments for
Chloride

and 0.256 % for cation and anion respectively. The reproducibility of peak area was estimated whenever the IC was started up.

TABLE XVI

ANALYTICAL ERROR OF IC

ion	peak area	absolute deviation from arithmetic mean (%)	standard deviation (%)
sodium	55305588	0.362	
	55666778	0.289	
	55547282	0.073	0.332
chloride	35465629	0.190	
	35636415	0.291	
	35497169	0.101	0.256

APPENDIX E

EXPERIMENTAL DATA

Following Tables present mass transfer coefficients for sodium and chloride estimated by Equation (20) and the model.

TABLE XVII

MASS TRANSFER COEFFICIENT DATA OF HGR-W2-H AND SBR-P-C-OH RESIN ESTIMATED BY HARRIES AND RAY'S EQUATION

Influent Concentration (ppb)		Effluent Concentration (ppb)		Mass Transfer Coefficient $\times 10^{-4}$ (m/s)	
sodium	chloride	sodium	chloride	sodium	chloride
single bed					
new resin					
bed depth = 0.076 cm					
flow rate = 500 ml/min					
64.9	100	7.68	7.55	0.93	0.85
159	245	12.2	8.55	1.12	1.10
324	500	37.6	10.9	0.94	1.25
486	750	29.2	13.7	1.23	1.31
649	1000	37.8	17.1	1.24	1.33
1590	2450	98.1	35.5	1.22	1.39
3240	5000	199	63.0	1.22	1.43
flow rate = 700 ml/min					
64.9	100	7.89	7.70	1.29	1.18
159	245	14.7	11.0	1.46	1.43

TABLE XVII (Continued)

Influent Concentration (ppb)		Effluent Concentration (ppb)		Mass Transfer Coefficient $\times 10^{-4}$ (m/s)	
sodium	chloride	sodium	chloride	sodium	chloride
324	500	29.3	16.2	1.47	1.57
486	750	40.9	21.6	1.51	1.63
649	1000	50.9	27.1	1.56	1.66
1590	2450	147	64.5	1.46	1.67
3240	5000	263	114	1.54	1.74
flow rate = 900 ml/min					
64.9	100	10.2	8.20	1.46	1.48
159	245	18.6	12.6	1.69	1.75
324	500	37.9	20.9	1.69	1.87
486	750	60.4	29.4	1.64	1.91
649	1000	71.1	35.1	1.74	1.98
1590	2450	190	91.1	1.67	1.94
3240	5000	349	196	1.75	1.91

mixed bed
new resin
bed depth = 11.5 cm
flow rate = 500 ml/min

64.9	100	6.47	10.3	0.99	1.48
159	245	9.79	17.5	1.21	1.72
324	500	15.4	28.3	1.32	1.87
486	750	21.2	43.1	1.36	1.86
649	1000	25.9	52.5	1.40	1.92
1590	2450	71.6	157	1.34	1.79
3240	5000	138	291	1.37	1.85
flow rate = 700 ml/min					
64.9	100	8.06	13.9	1.27	1.80
159	245	13.2	26.3	1.51	2.03
324	500	21.6	48.3	1.64	2.13
486	750	32.4	69.9	1.64	2.16
649	1000	42.0	92.2	1.66	2.17
1590	2450	115	251	1.59	2.08
3240	5000	216	490	1.64	2.12

TABLE XVII (Continued)

Influent Concentration (ppb)		Effluent Concentration (ppb)		Mass Transfer Coefficient $\times 10^{-4}$ (m/s)	
sodium	chloride	sodium	chloride	sodium	chloride
flow rate = 900 ml/min					
64.9	100	8.65	15.2	1.57	2.21
159	245	21.1	32.8	1.57	2.35
324	500	29.6	62.4	1.87	2.44
486	750	42.4	90.8	1.90	2.47
649	1000	52.1	118	1.97	2.50
1590	2450	154	328	1.82	2.36
3240	5000	292	623	1.88	2.44
mixed bed					
used resin from Northeastern Station Number 2 Condensate Polisher					
bed depth =11.5 cm					
flow rate = 500 ml/min					
64.9	100	5.61	12.1	1.05	1.36
159	245	11.5	19.6	1.13	1.63
324	500	22.5	41.4	1.15	1.61
486	750	35.0	66.3	1.13	1.57
649	1000	44.2	85.2	1.15	1.59
1590	2450	124	233	1.10	1.52
3240	5000	232	467	1.13	1.53
flow rate = 700 ml/min					
64.9	100	7.89	13.4	1.28	1.83
159	245	14.4	26.3	1.46	2.03
324	500	23.0	47.3	1.61	2.15
486	750	41.0	75.5	1.50	2.09
649	1000	54.7	101	1.50	2.09
1590	2450	146	274	1.45	2.00
3240	5000	316	596	1.41	1.94
flow rate = 900 ml/min					
64.9	100	7.28	15.9	1.69	2.13
159	245	16.2	36.6	1.77	2.21
324	500	37.9	75.9	1.66	2.19
486	750	61.3	120	1.60	2.13
649	1000	79.5	166	1.62	2.09
1590	2450	217	431	1.54	2.02
3240	5000	448	900	1.53	1.99

TABLE XVIII

MASS TRANSFER COEFFICIENT DATA OF MONOSPHERE RESIN

ESTIMATED BY HARRIES AND RAY'S EQAUTION

Influent Concentration (ppb)		Effluent Concentration (ppb)		Mass Transfer Coefficient $\times 10^{-4}$ (m/s)	
sodium	chloride	sodium	chloride	sodium	chloride
mixed bed					
new resin					
bed depth =11.6 cm					
flow rate = 500 ml/min					
64.9	100	3.61	11.7	1.01	1.36
159	245	5.64	12.4	1.17	1.89
324	500	10.4	20.0	1.20	2.04
486	750	12.5	28.2	1.28	2.08
649 .	1000	16.0	36.6	1.29	2.10
1590	2450	42.9	108	1.26	1.98
3240	5000	87.5	206	1.26	2.02
flow rate = 700 ml/min					
64.9	100	5.54	11.1	1.20	1.95
159	245	8.29	17.9	1.44	2.32
324	500	13.1	30.7	1.57	2.48
486	750	18.4	43.9	1.60	2.52
649	1000	22.0	53.3	1.65	2.60
1590	2450	60.3	148	1.60	2.50
3240	5000	114	302	1.63	2.49
flow rate = 700 ml/min (duplicated experiment)					
64.9	100	5.49	11.2	1.21	1.95
159	245	8.70	18.5	1.42	2.29
324	500	14.8	33.5	1.51	2.40
486	750	19.8	48.1	1.56	2.44
649	1000	21.3	60.2	1.67	2.50
1590	2450	53.9	169	1.65	2.37
3240	5000	101	338	1.69	2.39
flow rate = 900 ml/min					
64.9	100	4.54	14.3	1.67	2.22
159	245	9.49	22.3	1.77	2.74
324	500	20.0	45.4	1.75	2.74

TABLE XVIII (Continued)

Influent Concentration (ppb)		Effluent Concentration (ppb)		Mass Transfer Coefficient $\times 10^{-4}$ (m/s)	
sodium	chloride	sodium	chloride	sodium	chloride
486	750	30.2	71.1	1.75	2.69
649	1000	39.6	90.8	1.76	2.74
1590	2450	98.2	250	1.75	2.61
3240	5000	230	511	1.66	2.60
flow rate = 900 ml/min (duplicated experiment)					
64.9	100	6.84	14.4	1.41	2.21
159	245	11.5	21.5	1.65	2.78
324	500	23.3	46.0	1.65	2.72
486	750	33.3	71.7	1.68	2.68
649	1000	46.0	93.6	1.66	2.71
1590	2450	108	240	1.69	2.66
3240	5000	264	517	1.58	2.59
used resin from Riverside Number 1 Condensate Polisher					
flow rate = 500 ml/min					
64.9	100	3.25	12.8	1.05	1.30
159	245	6.01	19.9	1.14	1.59
324	500	11.6	41.6	1.16	1.58
486	750	17.0	63.6	1.17	1.57
649	1000	20.5	83.3	1.21	1.58
1590	2450	60.1	225	1.14	1.52
3240	5000	123	433	1.14	1.55
flow rate = 700 ml/min					
64.9	100	5.49	22.0	1.21	1.34
159	245	6.07	40.4	1.60	1.60
324	500	14.2	72.9	1.53	1.71
486	750	24.1	109	1.47	1.71
649	1000	28.5	133	1.53	1.79
1590	2450	82.7	381	1.44	1.65
3240	5000	158	772	1.48	1.66
flow rate = 900 ml/min					
64.9	100	5.84	18.6	1.51	1.92
159	245	11.6	42.5	1.65	2.00
324	500	26.7	92.4	1.57	1.93
486	750	40.5	147	1.56	1.86
649	1000	54.6	178	1.55	1.97

TABLE XVIII (Continued)

Influent Concentration (ppb)		Effluent Concentration (ppb)		Mass Transfer Coefficient $\times 10^{-4}$ (m/s)	
sodium	chloride	sodium	chloride	sodium	chloride
1590	2450	125	493	1.60	1.83
3240	5000	265	865	1.57	2.00

used resin from Riverside Number 2 Condensate Polisher

flow rate = 500 ml/min

64.9	100	3.10	13.2	1.06	1.28
159	245	5.49	19.5	1.17	1.60
324	500	9.95	37.7	1.22	1.64
486	750	14.8	57.4	1.22	1.63
649	1000	17.8	71.5	1.25	1.67
1590	2450	47.0	192	1.23	1.61
3240	5000	88.4	363	1.26	1.66

flow rate = 700 ml/min

64.9	100	6.21	25.7	1.15	1.21
159	245	13.6	52.7	1.20	1.36
324	500	16.8	81.9	1.45	1.61
486	750	23.9	121	1.47	1.62
649	1000	27.0	145	1.55	1.72
1590	2450	84.2	379	1.44	1.66
3240	5000	161	694	1.47	1.75

flow rate = 700 ml/min (duplicated experiment)

64.9	100	6.31	27.9	1.14	1.14
159	245	10.3	52.3	1.34	1.37
324	500	16.9	88.8	1.44	1.54
486	750	24.7	123	1.46	1.60
649	1000	31.2	149	1.48	1.69
1590	2450	89.4	401	1.41	1.61
3240	5000	161	715	1.47	1.73

flow rate = 900 ml/min

64.9	100	6.04	29.8	1.49	1.39
159	245	12.4	58.2	1.60	1.64
324	500	25.1	112	1.61	1.70
486	750	37.5	164	1.61	1.74
649	1000	50.3	200	1.61	1.84
1590	2450	135	542	1.55	1.72
3240	5000	272	1010	1.56	1.83

TABLE XVIII (Continued)

Influent Concentration (ppb)		Effluent Concentration (ppb)		Mass Transfer Coefficient $\times 10^{-4}$ (m/s)	
sodium	chloride	sodium	chloride	sodium	chloride
used resin from Northeastern Station Number 3 Condensate Polisher					
flow rate = 500 ml/min					
64.9	100	3.03	11.6	1.07	1.37
159	245	4.99	13.0	1.21	1.86
324	500	9.37	20.0	1.24	2.04
486	750	15.9	33.9	1.19	1.96
649	1000	17.5	39.8	1.26	2.05
1590	2450	49.4	122	1.21	1.90
3240	5000	105	234	1.20	1.94
flow rate = 700 ml/min					
64.9	100	6.00	12.2	1.16	1.87
159	245	10.4	21.2	1.33	2.18
324	500	17.1	38.2	1.44	2.28
486	750	24.5	56.7	1.46	2.29
649	1000	30.1	69.4	1.50	2.37
1590	2450	83.6	207	1.44	2.19
3240	5000	147	429	1.51	2.18
flow rate = 900 ml/min					
64.9	100	5.30	14.8	1.57	2.18
159	245	10.9	25.5	1.68	2.58
324	500	22.5	51.7	1.67	2.59
486	750	34.2	84.5	1.67	2.49
649	1000	45.6	110	1.67	2.52
1590	2450	103	285	1.72	2.46
3240	5000	232	590	1.66	2.44
used resin from Northeastern Station Number 4 Condensate Polisher					
flow rate = 500 ml/min					
64.9	100	3.81	11.9	0.99	1.35
159	245	5.33	13.1	1.19	1.86
324	500	12.4	19.9	1.14	2.05
486	750	17.9	29.8	1.15	2.05
649	1000	23.2	39.1	1.16	2.06
1590	2450	63.2	113	1.13	1.95
3240	5000	138	233	1.10	1.95

TABLE XVIII (Continued)

Influent Concentration (ppb)		Effluent Concentration (ppb)		Mass Transfer Coefficient $\times 10^{-4}$ (m/s)	
sodium	chloride	sodium	chloride	sodium	chloride
flow rate = 700 ml/min					
64.9	100	7.05	11.7	1.08	1.91
159	245	11.3	19.1	1.29	2.27
324	500	18.8	35.5	1.39	2.35
486	750	31.2	50.9	1.34	2.39
649	1000	42.7	68.1	1.33	2.39
1590	2450	114	205	1.29	2.20
3240	5000	244	416	1.26	2.21
flow rate = 900 ml/min					
64.9	100	6.44	15.1	1.45	2.16
159	245	12.7	26.9	1.59	2.52
324	500	29.3	52.5	1.51	2.57
486	750	46.4	82.1	1.48	2.53
649	1000	57.3	109	1.52	2.53
1590	2450	155	311	1.46	2.36
3240	5000	382	628	1.34	2.37

TABEL XIX

MASS TRANSFER COEFFICIENT DATA OF MONOSPHERE RESIN IN

MIXED BED ESTIMATED BY HAUB AND FOUTCH'S MIXED

BED ION EXCHANGE MODEL

Influent Concentration (ppb)	Mass Transfer Coefficient (MTC) $\times 10^{-4}$ (m/s) and Percentage Difference (%D) by Equation (26)					
	500 ml/min		700 ml/min		900 ml/min	
new resin						
sodium	MTC	%D	MTC	%D	MTC	%D
64.9	0.91	10.0	1.05	13.0	1.47	12.0
159	1.03	12.0	1.26	13.0	1.54	13.0
324	1.03	14.0	1.36	13.0	1.52	13.0
486	1.19	6.97	1.42	11.0	1.54	12.0
649	1.08	16.0	1.46	12.0	1.53	13.0
1590	1.07	15.0	1.44	10.0	1.52	13.0
3240	1.11	12.0	1.45	11.0	1.41	15.0
chloride						
100	1.13	17.0	1.72	12.0	1.84	17.0
245	1.61	15.0	1.95	16.0	2.30	16.0
500	1.75	14.0	2.06	17.0	2.25	18.0
750	1.83	12.0	2.02	20.0	2.15	20.0
1000	1.74	17.0	2.08	20.0	2.19	20.0
2450	1.59	20.0	2.00	20.0	2.08	20.0
5000	1.62	20.0	1.94	22.0	2.08	20.0
used resin from Riverside Number 2 Condensate Polisher						
sodium	MTC	%D	MTC	%D	MTC	%D
64.9	0.98	8.00	1.08	6.02	1.37	7.98
159	1.08	8.00	1.08	9.98	1.48	7.98
324	1.11	8.96	1.33	8.02	1.48	8.03
486	1.11	9.04	1.35	8.02	1.48	8.02
649	1.17	7.02	1.43	7.99	1.48	7.97
1590	1.14	7.00	1.29	9.97	1.42	8.01
3240	1.17	7.00	1.37	7.02	1.43	7.97
chloride						
100	1.07	17.0	0.98	19.3	1.11	20.0
245	1.28	20.0	1.09	20.0	1.30	21.0
500	1.28	22.0	1.24	23.0	1.33	22.0

TABEL XIX (Continued)

Influent Concentration (ppb)	Mass Transfer Coefficient (MTC) $\times 10^{-4}$ (m/s) and Percentage Difference (%D) by Equation (26)					
	500 ml/min		700 ml/min		900 ml/min	
chloride	MTC	%D	MTC	%D	MTC	%D
750	1.27	22.0	1.27	22.0	1.36	22.0
1000	1.31	22.0	1.32	23.0	1.43	22.0
2450	1.26	22.0	1.28	23.0	1.34	22.0
5000	1.27	24.0	1.37	22.0	1.42	22.0
used resin from Northeastern Station Number 3 Condensate Polisher						
sodium	MTC	%D	MTC	%D	MTC	%D
64.9	0.95	11.0	1.01	13.0	1.39	12.0
159	1.06	12.0	1.16	13.0	1.46	13.0
324	1.09	12.0	1.25	13.0	1.46	13.0
486	1.03	14.0	1.27	13.0	1.49	11.0
649	1.11	12.0	1.31	13.0	1.49	11.0
1590	1.07	11.9	1.27	12.0	1.53	11.0
3240	1.05	12.0	1.33	12.0	1.44	13.0
chloride						
100	1.14	17.0	1.63	13.0	1.83	16.0
245	1.55	17.0	1.87	14.0	2.12	18.0
500	1.72	16.0	1.96	14.0	2.15	17.0
750	1.63	17.0	1.88	18.0	1.99	20.0
1000	1.66	19.0	1.94	18.0	1.99	21.0
2450	1.52	20.0	1.73	21.0	1.94	21.0
5000	1.55	20.0	1.70	22.0	1.95	20.0

TABEL XX

MAXIMUM AND MINIMUM RELATIVE ERRORS OF MASS TRANSFER
COEFFICIENTS DUE TO EXPERIMENTAL UNCERTAINTIES

Influent Concentration (ppb)	Mass Transfer Coefficient (k) $\times 10^{-4}$ (m/s)			Relative Error (%)	
	k	k_{max}	k_{min}	maximum	minimum
HGR-W2-H and SBR-P-C-OH Resins					
new resin, single bed, 500 ml/min					
sodium					
64.9	0.93	1.01	0.85	7.98	-8.72
159	1.12	1.20	1.03	7.21	-7.93
324	0.94	1.02	0.86	7.94	-8.68
486	1.23	1.31	1.14	6.87	-7.58
649	1.24	1.33	1.15	6.83	-7.54
1590	1.22	1.30	1.12	6.90	-7.61
3240	1.22	1.31	1.13	6.89	-7.60
chloride					
100	0.85	0.91	0.78	7.18	-7.91
245	1.10	1.17	1.02	6.30	-7.01
500	1.25	1.33	1.17	5.94	-6.64
750	1.31	1.39	1.23	5.83	-6.52
1000	1.33	1.41	1.25	5.78	-6.48
2450	1.39	1.47	1.30	5.69	-6.38
5000	1.43	1.51	1.34	5.62	-6.30
new resin, single bed, 700 ml/min					
sodium					
64.9	1.29	1.39	1.18	7.43	-8.26
159	1.46	1.56	1.34	6.89	-7.71
324	1.47	1.57	1.36	6.85	-7.66
486	1.51	1.62	1.40	6.73	-7.54
649	1.56	1.66	1.44	6.62	-7.43
1590	1.46	1.56	1.35	6.88	-7.70
3240	1.54	1.64	1.42	6.68	-7.49
chloride					
100	1.18	1.26	1.09	6.59	-7.41
245	1.43	1.51	1.33	5.93	-6.72
500	1.57	1.66	1.47	5.63	-6.41

TABLE XX (Continued)

Influent Concentration (ppb)	Mass Transfer Coefficient (k) $\times 10^{-4}$ (m/s)			Relative Error (%)	
	k	k_{max}	k_{min}	maximum	minimum
chloride					
750	1.63	1.72	1.52	5.54	-6.31
1000	1.66	1.75	1.55	5.49	-6.26
2450	1.67	1.76	1.57	5.47	-6.24
5000	1.74	1.83	1.63	5.37	-6.13
new resin, single bed, 900 ml/min					
sodium					
64.9	1.46	1.59	1.32	8.89	-9.63
159	1.69	1.83	1.54	8.16	-8.89
324	1.69	1.83	1.54	8.16	-8.89
486	1.64	1.78	1.49	8.30	-9.03
649	1.74	1.88	1.59	8.03	-8.75
1590	1.67	1.81	1.52	8.21	-8.94
3240	1.75	1.89	1.60	7.99	-8.72
chloride					
100	1.48	1.59	1.36	7.51	-8.23
245	1.75	1.87	1.62	6.89	-7.60
500	1.87	2.00	1.73	6.67	-7.37
750	1.91	2.04	1.77	6.61	-7.31
1000	1.98	2.11	1.83	6.51	-7.21
2450	1.94	2.07	1.80	6.56	-7.26
5000	1.91	2.04	1.77	6.61	-7.31
new resin, mixed bed, 500 ml/min					
sodium					
64.9	0.99	1.07	0.92	7.15	-7.96
159	1.21	1.28	1.12	6.42	-7.20
324	1.32	1.40	1.23	6.12	-6.89
486	1.36	1.44	1.26	6.03	-6.80
649	1.40	1.48	1.30	5.94	-6.71
1590	1.34	1.42	1.25	6.06	-6.83
3240	1.37	1.45	1.28	6.00	-6.77

TABLE XX (Continued)

Influent Concentration (ppb)	Mass Transfer Coefficient (k) $\times 10^{-4}$ (m/s)			Relative Error (%)	
	k	k_{max}	k_{min}	maximum	minimum
chloride					
100	1.48	1.59	1.36	7.21	-8.04
245	1.72	1.83	1.59	6.62	-7.42
500	1.87	1.99	1.74	6.31	-7.11
750	1.86	1.98	1.73	6.33	-7.12
1000	1.92	2.04	1.78	6.22	-7.01
2450	1.79	1.90	1.66	6.47	-7.27
5000	1.85	1.97	1.72	6.34	-7.14
new resin, mixed bed, 700 ml/min					
sodium					
64.9	1.27	1.35	1.17	6.99	-7.90
159	1.51	1.60	1.40	6.23	-7.11
324	1.64	1.74	1.53	5.91	-6.78
486	1.64	1.74	1.53	5.91	-6.78
649	1.66	1.76	1.55	5.88	-6.74
1590	1.59	1.69	1.48	6.03	-6.90
3240	1.64	1.74	1.53	5.91	-6.78
chloride					
100	1.80	1.93	1.65	7.25	-8.19
245	2.03	2.17	1.88	6.68	-7.60
500	2.13	2.27	1.97	6.48	-7.39
750	2.16	2.30	2.00	6.42	-7.32
1000	2.17	2.31	2.01	6.40	-7.30
2450	2.08	2.21	1.92	6.59	-7.50
5000	2.12	2.25	1.96	6.51	-7.41
new resin, mixed bed, 900 ml/min					
sodium					
64.9	1.57	1.70	1.43	7.97	-8.79
159	1.57	1.70	1.44	7.97	-8.79
324	1.87	2.00	1.72	7.20	-8.00
486	1.90	2.04	1.75	7.12	-7.92
649	1.97	2.10	1.81	6.99	-7.78
1590	1.82	1.95	1.67	7.31	-8.11
3240	1.88	2.01	1.73	7.18	-7.98

TABLE XX (Continued)

Influent Concentration (ppb)	Mass Transfer Coefficient (k) $\times 10^{-4}$ (m/s)			Relative Error (%)	
	k	k_{max}	k_{min}	maximum	minimum
chloride					
100	2.21	2.39	2.01	8.31	-9.15
245	2.35	2.54	2.15	7.98	-8.82
500	2.44	2.63	2.23	7.82	-8.64
750	2.47	2.66	2.26	7.75	-8.57
1000	2.50	2.69	2.29	7.70	-8.52
2450	2.36	2.54	2.15	7.98	-8.81
5000	2.44	2.63	2.23	7.81	-8.64

used resin from Northeastern Station Number 2 condensate polisher mixed bed, 500 ml/min

chloride					
100	1.37	1.48	1.26	7.54	-8.38
245	1.64	1.75	1.52	6.78	-7.59
500	1.62	1.73	1.50	6.84	-7.65
750	1.58	1.69	1.46	6.94	-7.76
1000	1.60	1.71	1.48	6.88	-7.69
2450	1.53	1.64	1.41	7.06	-7.88
5000	1.54	1.65	1.42	7.04	-7.85
sodium					
64.9	1.06	1.13	0.98	6.90	-7.71
159	1.14	1.21	1.05	6.63	-7.43
324	1.15	1.23	1.07	6.58	-7.37
486	1.14	1.22	1.06	6.63	-7.42
649	1.16	1.24	1.08	6.55	-7.34
1590	1.10	1.18	1.02	6.74	-7.54
3240	1.14	1.22	1.06	6.62	-7.41

flow rate = 700 ml/min

chloride					
100	1.83	1.96	1.68	7.16	-8.10
245	2.03	2.17	1.88	6.68	-7.59
500	2.15	2.29	1.99	6.45	-7.35
750	2.09	2.23	1.93	6.56	-7.47
1000	2.09	2.23	1.93	6.56	-7.47
2450	2.00	2.13	1.84	6.76	-7.68
5000	1.94	2.07	1.79	6.90	-7.82

TABLE XX (Continued)

Influent Concentration (ppb)	Mass Transfer Coefficient (k) $\times 10^{-4}$ (m/s)			Relative Error (%)	
	k	k_{max}	k_{min}	maximum	minimum
sodium					
64.9	1.28	1.37	1.18	6.94	-7.86
159	1.46	1.55	1.35	6.37	-7.26
324	1.60	1.70	1.49	6.00	-6.87
486	1.50	.1.59	1.39	6.26	-7.14
649	1.50	1.59	1.39	6.26	-7.14
1590	1.45	1.54	1.34	6.40	-7.29
3240	1.41	1.50	1.31	6.50	-7.40
flow rate = 900 ml/min					
chloride					
100	2.14	2.31	1.94	8.27	-9.15
245	2.23	2.41	2.03	8.06	-8.92
500	2.21	2.39	2.01	8.10	-8.96
750	2.15	2.32	1.95	8.25	-9.12
1000	2.10	2.28	1.91	8.35	-9.23
2450	2.03	2.21	1.84	8.54	-9.42
5000	2.01	2.18	1.82	8.61	-9.50
sodium					
64.9	1.71	1.83	1.57	7.38	-8.21
159	1.78	1.91	1.64	7.19	-8.01
324	1.67	1.80	1.53	7.46	-8.30
486	1.61	1.74	1.48	7.63	-8.47
649	1.64	1.76	1.50	7.56	-8.40
1590	1.55	1.67	1.42	7.82	-8.67
3240	1.54	1.66	1.41	7.85	-8.70

TABEL XX (Continued)

Influent Concentration (ppb)	Mass Transfer Coefficient (k) $\times 10^{-4}$ (m/s)			Relative Error (%)	
	k	k_{max}	k_{min}	maximum	minimum
650C-H and 550A-OH Resins (mixed bed)					
new resin					
flow rate = 500 ml/min					
chloride					
100	1.36	1.49	1.24	9.11	-8.97
245	1.89	2.04	1.75	7.81	-7.66
500	2.04	2.19	1.89	7.57	-7.42
750	2.08	2.24	1.93	7.51	-7.36
1000	2.10	2.26	1.94	7.48	-7.33
2450	1.98	2.13	1.83	7.66	-7.51
5000	2.02	2.18	1.87	7.60	-7.44
sodium					
64.9	1.01	1.09	0.93	7.92	-7.77
159	1.16	1.25	1.08	7.46	-7.30
324	1.20	1.29	1.11	7.37	-7.21
486	1.28	1.37	1.19	7.20	-7.04
649	1.29	1.38	1.20	7.16	-7.01
1590	1.26	1.35	1.17	7.23	-7.07
3240	1.26	1.35	1.17	7.23	-7.07
flow rate = 700 ml/min					
chloride					
100	1.95	2.12	1.79	8.38	-8.35
245	2.32	2.50	2.15	7.67	-7.61
500	2.48	2.66	2.30	7.43	-7.37
750	2.52	2.71	2.34	7.37	-7.31
1000	2.60	2.79	2.42	7.25	-7.19
2450	2.50	2.68	2.31	7.40	-7.34
5000	2.49	2.68	2.31	7.41	-7.35
sodium					
64.9	1.20	1.30	1.11	7.90	-7.85
159	1.44	1.55	1.34	7.23	-7.17
324	1.57	1.68	1.46	6.97	-6.90
486	1.60	1.71	1.49	6.90	-6.83
649	1.65	1.77	1.54	6.80	-6.73

TABLE XX (Continued)

Influent Concentration (ppb)	Mass Transfer Coefficient (k) $\times 10^{-4}$ (m/s)			Relative Error (%)	
	k	k_{max}	k_{min}	maximum	minimum
sodium					
1590	1.60	1.71	1.49	6.91	-6.83
3240	1.63	1.75	1.52	6.84	-6.77
flow rate = 700 ml/min (duplicated experiment)					
chloride					
100	1.95	2.11	1.78	8.39	-8.36
245	2.29	2.47	2.12	7.71	-7.66
500	2.40	2.58	2.22	7.54	-7.48
750	2.44	2.62	2.26	7.48	-7.43
1000	2.50	2.68	2.31	7.40	-7.34
2450	2.37	2.55	2.20	7.58	-7.53
5000	2.39	2.57	2.21	7.55	-7.50
sodium					
64.9	1.21	1.30	1.11	7.88	-7.84
159	1.42	1.52	1.32	7.29	-7.22
324	1.51	1.61	1.40	7.09	-7.02
486	1.56	1.67	1.46	6.97	-6.90
649	1.67	1.78	1.56	6.77	-6.70
1590	1.65	1.77	1.54	6.80	-6.73
3240	1.69	1.81	1.58	6.74	-6.66
flow rate = 900 ml/min					
chloride					
100	2.22	2.43	2.01	9.59	-9.47
245	2.74	2.97	2.51	8.62	-8.49
500	2.74	2.97	2.51	8.62	-8.49
750	2.69	2.92	2.46	8.70	-8.57
1000	2.74	2.98	2.51	8.62	-8.49
2450	2.61	2.84	2.38	8.83	-8.71
5000	2.60	2.83	2.38	8.84	-8.71
sodium					
64.9	1.67	1.81	1.54	8.21	-8.08
159	1.77	1.91	1.63	8.00	-7.87
324	1.75	1.89	1.61	8.05	-7.91
486	1.74	1.89	1.61	8.05	-7.92
649	1.76	1.90	1.62	8.03	-7.89

TABLE XX (Continued)

Influent Concentration (ppb)	Mass Transfer Coefficient (k) $\times 10^{-4}$ (m/s)			Relative Error (%)	
	k	k_{max}	k_{min}	maximum	minimum
sodium					
1590	1.75	1.89	1.61	8.05	-7.91
3240	1.66	1.80	1.53	8.23	-8.10
flow rate = 900 ml/min (duplicated experiment)					
chloride					
100	2.21	2.42	2.00	9.61	-9.50
245	2.78	3.02	2.55	8.56	-8.43
500	2.72	2.96	2.49	8.64	-8.52
750	2.68	2.91	2.45	8.71	-8.58
1000	2.71	2.94	2.47	8.67	-8.54
2450	2.66	2.89	2.43	8.75	-8.62
5000	2.59	2.82	2.36	8.86	-8.73
sodium					
64.9	1.41	1.54	1.29	8.90	-8.77
159	1.65	1.79	1.52	8.26	-8.13
324	1.65	1.79	1.52	8.25	-8.12
486	1.68	1.82	1.55	8.18	-8.05
649	1.66	1.80	1.53	8.23	-8.10
1590	1.69	1.83	1.55	8.17	-8.04
3240	1.58	1.71	1.44	8.44	-8.31
used resin from Riverside Number 1 condensate polisher					
flow rate = 500 ml/min					
chloride					
100	1.30	1.42	1.18	9.32	-9.19
245	1.59	1.73	1.46	8.44	-8.29
500	1.58	1.71	1.45	8.48	-8.34
750	1.56	1.70	1.43	8.51	-8.37
1000	1.58	1.71	1.45	8.48	-8.34
2450	1.51	1.65	1.39	8.64	-8.50
5000	1.55	1.68	1.42	8.55	-8.40
sodium					
64.9	1.05	1.13	0.97	7.80	-7.65
159	1.14	1.23	1.06	7.51	-7.36
324	1.16	1.25	1.08	7.46	-7.31
486	1.17	1.26	1.09	7.44	-7.29

TABLE XX (Continued)

Influent Concentration (ppb)	Mass Transfer Coefficient (k) $\times 10^{-4}$ (m/s)			Relative Error (%)	
	k	k_{max}	k_{min}	maximum	minimum
sodium					
649	1.21	1.29	1.12	7.35	-7.20
1590	1.14	1.23	1.06	7.51	-7.36
3240	1.14	1.23	1.06	7.52	-7.36
flow rate = 700 ml/min					
chloride					
100	1.36	1.48	1.20	9.47	-11.21
245	1.62	1.75	1.45	8.42	-10.14
500	1.72	1.86	1.56	8.08	-9.79
750	1.73	1.87	1.56	8.07	-9.77
1000	1.81	1.95	1.64	7.84	-9.54
2450	1.67	1.80	1.50	8.26	-9.97
5000	1.67	1.81	1.51	8.24	-9.95
sodium					
64.9	1.22	1.30	1.11	6.96	-8.63
159	1.61	1.71	1.49	5.99	-7.64
324	1.54	1.64	1.42	6.12	-7.77
486	1.48	1.57	1.36	6.25	-7.91
649	1.54	1.64	1.42	6.12	-7.78
1590	1.46	1.55	1.34	6.30	-7.96
3240	1.49	1.58	1.37	6.23	-7.89
flow rate = 900 ml/min					
chloride					
100	1.92	2.12	1.72	10.39	-10.28
245	2.00	2.20	1.80	10.15	-10.04
500	1.93	2.13	1.73	10.37	-10.26
750	1.86	2.06	1.66	10.58	-10.48
1000	1.97	2.17	1.77	10.24	-10.13
2450	1.83	2.03	1.64	10.68	-10.57
5000	2.00	2.21	1.80	10.15	-10.04
sodium					
64.9	1.51	1.64	1.38	8.61	-8.48
159	1.65	1.78	1.51	8.27	-8.13
324	1.57	1.70	1.44	8.46	-8.33
486	1.56	1.69	1.43	8.47	-8.34
649	1.55	1.69	1.42	8.49	-8.36

TABLE XX (Continued)

Influent Concentration (ppb)	Mass Transfer Coefficient (k) $\times 10^{-4}$ (m/s)			Relative Error (%)	
	k	k_{max}	k_{min}	maximum	minimum
sodium					
1590	1.60	1.73	1.47	8.38	-8.25
3240	1.57	1.71	1.44	8.45	-8.31
used resin from Riverside Number 2 condensate polisher					
flow rate = 500 ml/min					
chloride					
100	1.28	1.40	1.17	9.39	-9.26
245	1.60	1.74	1.47	8.41	-8.27
500	1.64	1.78	1.51	8.32	-8.18
750	1.63	1.77	1.50	8.35	-8.21
1000	1.67	1.81	1.54	8.25	-8.10
2450	1.61	1.75	1.48	8.39	-8.24
5000	1.66	1.80	1.53	8.27	-8.12
sodium					
64.9	1.06	1.14	0.98	7.75	-7.59
159	1.17	1.26	1.09	7.43	-7.28
324	1.22	1.30	1.13	7.33	-7.17
486	1.22	1.31	1.13	7.33	-7.17
649	1.25	1.34	1.17	7.24	-7.09
1590	1.23	1.32	1.14	7.30	-7.14
3240	1.26	1.35	1.17	7.24	-7.08
flow rate = 700 ml/min					
chloride					
100	1.13	1.27	1.00	11.63	-11.67
245	1.37	1.51	1.23	10.29	-10.30
500	1.54	1.68	1.39	9.61	-9.60
750	1.60	1.75	1.45	9.37	-9.36
1000	1.69	1.84	1.54	9.08	-9.06
2450	1.61	1.76	1.46	9.35	-9.34
5000	1.73	1.88	1.57	8.97	-8.95
sodium					
64.9	1.14	1.23	1.05	8.13	-8.08
159	1.33	1.43	1.24	7.50	-7.44
324	1.44	1.55	1.34	7.23	-7.17
486	1.46	1.56	1.35	7.20	-7.13
649	1.48	1.59	1.38	7.14	-7.07

TABLE XX (Continued)

Influent Concentration (ppb)	Mass Transfer Coefficient (k) $\times 10^{-4}$ (m/s)			Relative Error (%)	
	k	k_{max}	k_{min}	maximum	minimum
sodium					
1590	1.41	1.51	1.30	7.32	-7.26
3240	1.47	1.57	1.36	7.17	-7.11
flow rate = 700 ml/min (duplicated experiment)					
chloride					
100	1.21	1.34	1.07	11.16	-11.19
245	1.36	1.51	1.22	10.32	-10.33
500	1.61	1.76	1.46	9.35	-9.34
750	1.62	1.77	1.47	9.30	-9.29
1000	1.72	1.87	1.56	9.00	-8.98
2450	1.66	1.81	1.51	9.18	-9.16
5000	1.75	1.91	1.60	8.89	-8.87
sodium					
64.9	1.15	1.24	1.05	8.10	-8.05
159	1.20	1.30	1.11	7.90	-7.85
324	1.45	1.55	1.34	7.22	-7.16
486	1.47	1.58	1.37	7.17	-7.10
649	1.55	1.66	1.44	6.99	-6.92
1590	1.43	1.54	1.33	7.25	-7.18
3240	1.47	1.57	1.36	7.17	-7.11
flow rate = 900 ml/min					
chloride					
100	1.38	1.56	1.21	12.68	-12.60
245	1.64	1.83	1.46	11.39	-11.30
500	1.70	1.89	1.52	11.14	-11.05
750	1.74	1.93	1.55	11.01	-10.92
1000	1.84	2.03	1.64	10.65	-10.55
2450	1.72	1.91	1.53	11.07	-10.97
5000	1.83	2.02	1.63	10.70	-10.59
sodium					
64.9	1.49	1.62	1.36	8.66	-8.53
159	1.60	1.74	1.47	8.37	-8.24
324	1.61	1.74	1.47	8.36	-8.23
486	1.61	1.74	1.48	8.36	-8.22
649	1.61	1.74	1.47	8.36	-8.23

TABLE XX (Continued)

Influent Concentration (ppb)	Mass Transfer Coefficient (k) $\times 10^{-4}$ (m/s)			Relative Error (%)	
	k	k_{max}	k_{min}	maximum	minimum
sodium					
1590	1.55	1.68	1.42	8.51	-8.38
3240	1.56	1.69	1.43	8.49	-8.36

used resin from Northeastern Station Number 3 condensate polisher
flow rate = 500 ml/min

Influent Concentration (ppb)	k	k_{max}	k_{min}	maximum	minimum
chloride					
100	1.37	1.49	1.25	9.09	-8.95
245	1.86	2.01	1.72	7.87	-7.72
500	2.04	2.20	1.89	7.57	-7.41
750	1.96	2.12	1.82	7.69	-7.54
1000	2.05	2.20	1.89	7.56	-7.41
2450	1.90	2.05	1.76	7.79	-7.64
5000	1.94	2.09	1.79	7.73	-7.57
sodium					
64.9	1.07	1.15	0.99	7.72	-7.57
159	1.21	1.30	1.12	7.35	-7.19
324	1.24	1.33	1.15	7.28	-7.13
486	1.19	1.28	1.11	7.38	-7.23
649	1.26	1.35	1.17	7.23	-7.07
1590	1.21	1.30	1.12	7.34	-7.18
3240	1.20	1.28	1.11	7.38	-7.22

flow rate = 700 ml/min

Influent Concentration (ppb)	k	k_{max}	k_{min}	maximum	minimum
chloride					
100	1.87	2.03	1.71	8.58	-8.55
245	2.18	2.35	2.00	7.92	-7.87
500	2.28	2.46	2.11	7.73	-7.68
750	2.29	2.47	2.12	7.71	-7.66
1000	2.37	2.55	2.19	7.59	-7.53
2450	2.19	2.37	2.02	7.89	-7.84
5000	2.18	2.35	2.01	7.91	-7.86
sodium					
64.9	1.16	1.26	1.07	8.04	-7.99
159	1.33	1.43	1.23	7.51	-7.46
324	1.44	1.54	1.33	7.24	-7.18
486	1.46	1.56	1.36	7.19	-7.13
649	1.50	1.61	1.39	7.10	-7.04

TABEL XX (Continued)

Influent Concentration (ppb)	Mass Transfer Coefficient (k) $\times 10^{-4}$ (m/s)			Relative Error (%)	
	k	k_{max}	k_{min}	maximum	minimum
sodium					
1590	1.44	1.54	1.34	7.24	-7.18
3240	1.51	1.62	1.40	7.08	-7.01
flow rate = 900 ml/min					
chloride					
100	2.18	2.39	1.97	9.68	-9.57
245	2.58	2.81	2.36	8.87	-8.75
500	2.59	2.82	2.36	8.86	-8.73
750	2.49	2.72	2.27	9.03	-8.91
1000	2.52	2.74	2.29	8.98	-8.86
2450	2.46	2.68	2.23	9.10	-8.98
5000	2.44	2.66	2.22	9.13	-9.01
sodium					
64.9	1.57	1.71	1.44	8.44	-8.31
159	1.68	1.82	1.55	8.19	-8.05
324	1.67	1.81	1.54	8.20	-8.07
486	1.67	1.80	1.53	8.22	-8.09
649	1.67	1.81	1.53	8.22	-8.08
1590	1.72	1.86	1.58	8.11	-7.98
3240	1.66	1.79	1.52	8.24	-8.11

used resin from Northeastern Station Number 4 condensate polisher
flow rate = 500 ml/min

chloride	MTC	kmax	kmin	%dev(max)	%dev(min)
100	1.35	1.47	1.23	9.15	-9.02
245	1.86	2.01	1.72	7.87	-7.72
500	2.05	2.20	1.89	7.56	-7.41
750	2.05	2.20	1.89	7.56	-7.41
1000	2.06	2.21	1.91	7.54	-7.39
2450	1.95	2.10	1.80	7.71	-7.56
5000	1.95	2.10	1.80	7.72	-7.57
sodium					
64.9	0.99	1.07	0.91	7.99	-7.84
159	1.18	1.27	1.10	7.41	-7.25
324	1.14	1.22	1.05	7.52	-7.37
486	1.15	1.24	1.07	7.49	-7.34
649	1.16	1.25	1.08	7.46	-7.31

TABLE XX (Continued)

Influent Concentration (ppb)	Mass Transfer Coefficient (k) $\times 10^{-4}$ (m/s)			Relative Error (%)	
	k	k_{max}	k_{min}	maximum	minimum
sodium					
1590	1.12	1.21	1.04	7.56	-7.41
3240	1.10	1.19	1.02	7.63	-7.47
flow rate = 700 ml/min					
chloride					
100	1.91	2.07	1.75	8.49	-8.46
245	2.27	2.44	2.09	7.76	-7.71
500	2.35	2.53	2.17	7.62	-7.57
750	2.39	2.57	2.21	7.56	-7.50
1000	2.39	2.57	2.21	7.56	-7.51
2450	2.20	2.38	2.03	7.87	-7.82
5000	2.21	2.38	2.04	7.86	-7.81
sodium					
64.9	1.08	1.17	0.99	8.34	-8.30
159	1.29	1.39	1.19	7.62	-7.57
324	1.39	1.49	1.29	7.35	-7.29
486	1.34	1.44	1.24	7.48	-7.43
649	1.33	1.43	1.23	7.52	-7.46
1590	1.29	1.39	1.19	7.63	-7.58
3240	1.26	1.36	1.17	7.71	-7.65
flow rate = 900 ml/min					
chloride					
100	2.16	2.37	1.95	9.74	-9.63
245	2.52	2.75	2.30	8.97	-8.85
500	2.57	2.80	2.35	8.89	-8.76
750	2.53	2.75	2.30	8.97	-8.85
1000	2.53	2.76	2.31	8.96	-8.84
2450	2.36	2.58	2.14	9.30	-9.17
5000	2.37	2.59	2.15	9.27	-9.15

TABLE XX (Continued

Influent Concentration (ppb)	Mass Transfer Coefficient (k) $\times 10^{-4}$ (m/s)			Relative Error (%)	
	k	k_{max}	k_{min}	maximum	minimum
sodium					
64.9	1.45	1.58	1.33	8.78	-8.65
159	1.59	1.72	1.45	8.41	-8.28
324	1.51	1.64	1.38	8.61	-8.48
486	1.48	1.60	1.35	8.71	-8.58
649	1.52	1.65	1.40	8.57	-8.44
1590	1.46	1.59	1.33	8.75	-8.62
3240	1.34	1.47	1.22	9.12	-9.00

VITA

Gang-Choon Lee

Candidate for the Degree of

Doctor of Philosophy

Thesis: THE IONIC MASS TRANSFER COEFFICIENTS OF CATION AND ANION EXCHANGE RESINS AT VARIOUS FLOW RATES AND INFLUENT CONCENTRATIONS IN SINGLE AND MIXED BEDS

Major Field: Chemical Engineering

Biographical:

Personal Data: Born in Gangwon-Do, Korea, November 24, 1963, the son of Ki-Tak Lee and In-Young Yang.

Education: Graduated from Sangmoon High School, Seoul, Korea in February 1982; received Bachelor of Science and Master of Science Degrees in Chemical Engineering from Sungkyunkwan University at Seoul in February 1986 and February 1988, respectively; completed requirements for the Doctor of Philosophy Degree at Oklahoma State University in May, 1994

Professional Experience: Graduate Teaching and Research Assistant at the School of Chemical Engineering, Oklahoma State University, Jan., 1990, to May, 1994.

Professional Societies: The Korean Scientists and Engineers Association in America.

Name: Gang-Choon Lee

Date of Degree: May. 1994

Institution: Oklahoma State University

Location: Stillwater, Oklahoma

Title of Study: THE IONIC MASS TRANSFER COEFFICIENTS OF CATION AND ANION EXCHANGE RESINS AT VARIOUS FLOW RATES AND INFLUENT CONCENTRATIONS IN SINGLE AND MIXED BEDS

Pages in Study: 157

Candidate for the Degree of Doctor of Philosophy

Major Field: Chemical Engineering

Scope and Method of Study: Kinetics of ion exchange resin were estimated by mass transfer coefficient. Experiments were carried out in various operating conditions, and mass transfer coefficients were estimated from operating parameter and inlet and outlet concentrations by Harries and Ray's equation and Haub and Foutch's mixed bed ion exchange model. The effects of flow rate, influent concentration, bed types (single and mixed beds), and resin types to mass transfer coefficient were investigated. In addition, particle mass transfer resistance were considered for used resins.

Findings and Conclusions: Ionic mass transfer coefficients strongly depended on flow rate. As flow rate increased, the mass transfer coefficients increased. This verified liquid film control. Also, mass transfer coefficient depends on influent concentration in low influent concentration range. The mass transfer coefficients in mixed bed were higher than those in single bed. This could be explained theoretically by bulk phase and film neutralizations. Further, resin type affected mass transfer coefficient mainly due to diameter difference. Haub and Foutch's mixed bed ion exchange model estimated lower mass transfer coefficients than Harries and Ray's equation. Harries and Ray's equation cannot explain the effects of bulk and interface concentration changes, coion existence, and single ionic diffusivity to mass transfer. The effective diffusivity in Haub and Foutch's mixed bed ion exchange model accounts for these effects. Particle mass transfer coefficients estimated by series resistance model helped to qualitative analysis for used resin kinetics.

ADVISER'S APPROVAL _____